BEARING CAPACITY OF DRIVEN PILES IN SAND

A Dissertation

by

RENO REINE CASTELLO

Submitted to the Graduate College of
Texas A&M University
in partial fulfillment of the requirement for the degree of

DOCTOR OF PHILOSOPHY

August 1979

Major Subject: Civil Engineering

BEARING CAPACITY OF DRIVEN PILES IN SAND

A Dissertation

by

RENO REINE CASTELLO

Approved as to style and content by:

Harry M. Coyle
(Chairman of Committee)

Charles H. Lawson, Jr.
(Head of Department)

Wayne A. Dunlap
(Member)

C C Mathewson
(Member)

Lee Lowery Jr
(Member)

August 1979

ABSTRACT

Bearing Capacity of Driven Piles in Sand (August 1979)

Reno Reine Castello, Civil Engineer, Universidade Federal do Espírito Santo, Brazil;

M.Sc., Pontifícia Universidade Católica do Rio de Janeiro, Brazil

Chairman of Advisory Committee: Dr. Harry M. Coyle

A thorough review of the literature regarding bearing capacity theories and experimental studies for piles driven in sand has been made. Experimental studies indicate that the theories currently used to predict pile bearing capacity fail to consider all significant parameters. As a result of the literature review, qualitative hypotheses regarding the mechanism of pile-soil interaction are formulated and all significant parameters are identified.

The unit point and side resistances obtained from thirty-four field pile load tests are used to determine which of the pile geometry and soil parameters are most significant. Bearing capacity factors are calculated and correlated with the most significant pile-soil system parameters. Three types of load test data are used: compression test data adjusted for residual stresses, unadjusted compression test data and compression/tension test data.

The best and simplest correlations are developed by plotting the bearing capacity factors versus the relative depth, i.e., the depth of penetration to diameter ratio. A family of curves is obtained when the sand friction angle is included in the correlations. A gradual increase

in unit point and side resistances is indicated for increasing relative depth. An error analysis of these correlations provides the basis for the conclusion that both unadjusted compression and compression/tension test correlations yield fairly accurate predictions (usually within $\pm$ 20%) for total bearing capacity. However, the compression/tension test correlations give the best predictions for point and side bearing capacity. Recommendations are made concerning the use of the correlations developed in this study for prediction of pile bearing capacity in sand.

ACKNOWLEDGEMENTS

The financial support of the author's graduate studies at Texas A&M University, provided jointly by Universidade Federal do Espirito Santo (Brazil) and CAPES (Brazilian Ministry of Education), is gratefully acknowledged.

To name every person who helped in the achievement of the proposed goal would be too lengthy; however two persons can not be omitted. Special thanks are expressed to Robinson Leão Castello, the author's father, for his moral and material support, and to the Chairman of the Advisory Committee, Dr. Harry M. Coyle, for his enthusiasm and encouragement. Thanks are also expressed to Mrs. Joy Taylor for her patience and efficiency in typing this dissertation.

DEDICATION

To:

Robinson Leão Castello and Anna Borge Miguel Castello, my parents,

Helena Maria, my wife, and

Liege, my daughter.

TABLE OF CONTENTS

Page

LIST OF TABLES

LIST OF FIGURES

Page

Page

INTRODUCTION

Piles have been used by man since prehistoric times (46). This long experience has generated numerous pile design "rules of thumb" for certain geographic regions and certain types of piles (primarily short wooden piles). However, in recent years new pile types and larger pile sizes have been designed for massive use in new geographic regions and the piles penetrate to depths never before imagined. These uses have caused new problems to arise and have shown that the earlier "rules of thumb" are no longer valid.

Since direct observation of the interaction between a pile and the soil is impossible, the development of theories has been based primarily on experience and simplified models. These models were based upon the observed behavior of shallow foundations, and did not consider the higher confining stresses which exist in a deep foundation. Because of different assumptions the results obtained from the different theories vary widely.

Despite inherent scaling limitations, laboratory observations provide the only practical means of obtaining indirect examination of the poorly understood phenomenon of pile-soil interaction. The results of those laboratory observations have identified new parameters which influence the pile-soil interaction. Also, in many instances the results of the experimental studies strongly refute the traditional theoretical (model) assumptions.

The style and format of this dissertation follows that used by the Journal of the Geotechnical Engineering Division, American Society of Civil Engineers

As a consequence of those observations it was recognized that there is an imperative need to update the current design practice with the recent findings. For larger and more important projects it is customary practice to base foundation design on pile load tests performed at the proposed site. The results of those tests have shown that the lack of agreement between theory and experimental values is applicable to all types of soils. However, the lack of agreement is particularly bad in the case of sandy soils. Consequently, in engineering practice, it is customary to use the lowest estimated values of bearing capacity for piles in sand and this may result in overconservative designs.

The present study is an effort to improve the actual "state-of-the-art" for the design of piles driven in cohesionless soils. Results obtained from full-scale field load tests were used to evaluate bearing capacity factors. These factors were then correlated with parameters identified from laboratory experiments. Those parameters include depth of pile penetration, pile diameter, effective overburden pressure, and friction angle or relative density of the sand. Data from about 30 pile load tests were collected from the published literature. Those data permitted the evaluation of bearing capacity factors and the other important parameters.

Special attention was devoted to the problem of "residual stresses" for piles in sands. A hypothesis was developed that the failure load in a tension test represents the compression side load adjusted for residual stresses. The use of this hypothesis consistently led to accurate predictions of both total load and unit resistances.

In developing correlations for use in predicting failure loads on piles bearing in sand, all commonly accepted factors from existing theories were used. A total of six factors were correlated for three types of field test data (unadjusted compression test, adjusted compression test, and compression/tension test). Then, using these correlations the total load of each pile was estimated, and the estimated load was compared with the actual field load.

THEORETICAL INVESTIGATIONS

The static formula method is used to determine the ultimate axial bearing capacity of a pile, Q_u, as shown in Fig. 1. The ultimate bearing capacity is separated into two components as follows:

$$Q_u = Q_p + Q_s \quad \ldots\ldots\ldots\ldots\ldots\ldots\ldots \quad (1)$$

where Q_p = ultimate load carried by the point, and

Q_s = ultimate load carried by the side.

Point Load

The theoretical determination of the point resistance has received extensive attention through the years. According to Vesić (55) the theoretical approach to solve this problem was initiated by Caquot and Buisman in the mid-1930's. Caquot and Buisman extended the classical work on punching failure done by Prandtl and Reissner approximately 15 years earlier. Following the same basic approach several different solutions were subsequently presented with different assumptions concerning the failure pattern and/or new empirical corrections were introduced. Among the many contributors in this area of study were: Terzaghi, De Beer, and Jáky in the 1940's; Meyerhof, Caquot and Kérisel in the 1950's; Brinch Hansen, Berezantsev and Yaroshenko, and Vesić in the 1960's. A somewhat different approach was taken by Skempton, Yassin and Gibson in the early 1950's when they dealt with the soil failure

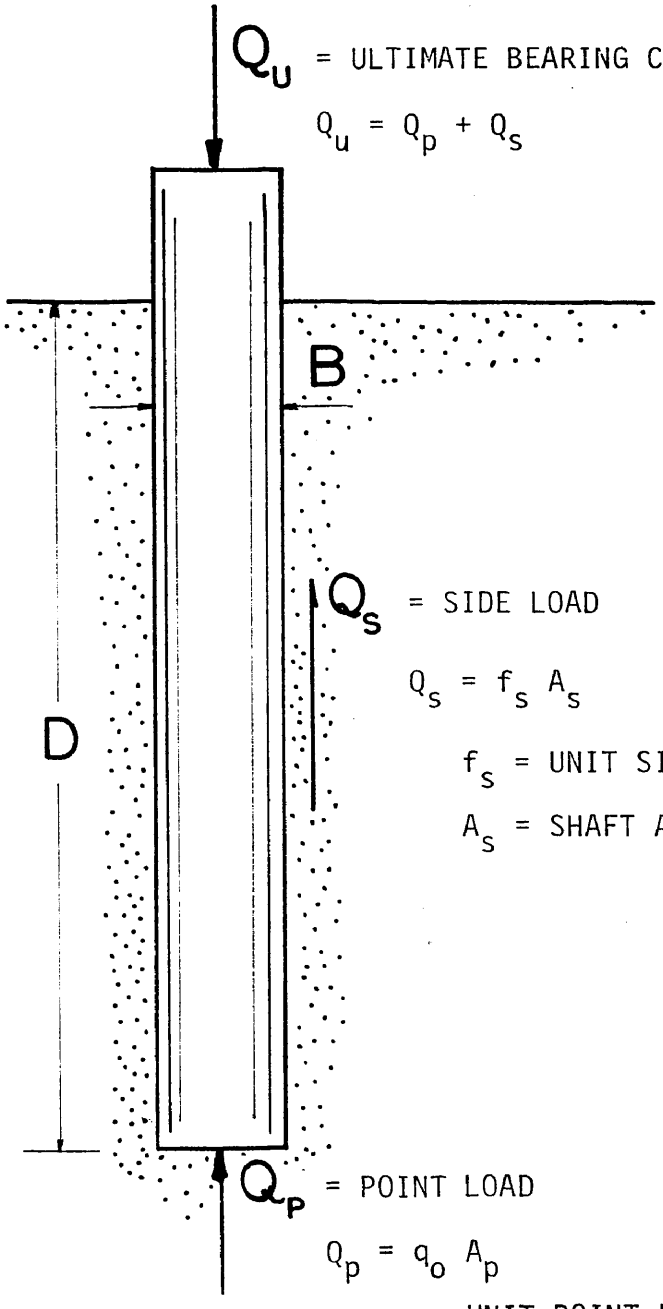

FIG. 1 - ULTIMATE BEARING CAPACITY - STATIC METHOD

induced by the pile point as a special case of the expansion of a cavity inside a solid. This same idea was used again by Vesić in 1977 (58). Vesić's latest approach involves the use of complex soil parameters.

In all of these theoretical solutions the ultimate point load, Q_p, is given by:

$$Q_p = q_o A_p \quad \ldots\ldots\ldots\ldots\ldots\ldots\ldots \quad (2)$$

where q_o = ultimate unit point resistance, and

A_p = area of the pile point.

The ultimate unit point resistance, q_o, is given as follows:

$$q_o = \gamma b N^*_\gamma s_\gamma + c N^*_c s_c + p_o N^*_q s_q \quad \ldots\ldots\ldots \quad (3)$$

where: γ = effective unit weight of the soil at the pile point.

b = smallest foundation dimension,

p_o = effective overburden pressure at the pile point level,

c = cohesion of the soil,

s_γ, s_c, s_q = shape factors, and

N^*_γ, N^*_q, N^*_c = bearing capacity factors usually depending on the soil friction angle, ϕ', and the assumed pattern or mechanism of failure.

In engineering practice this equation can and usually is simplified. In the first place, since the study is restricted to sands (cohesionless soils), the second term of the equation can be eliminated. Secondly, when comparing the two remaining terms, it is seen that the first term is relatively small and can be neglected. Finally, the last simplification concerns the form of the remaining term. Since most piles have circular or square cross sections and the shape factor is the same (26, 54) it is reasonable to use a new bearing factor, N_q, which incorporates this constant shape factor. Therefore, the commonly used form (11) of Eq. 3 becomes:

$$q_o = p_o N_q \quad \ldots\ldots\ldots\ldots\ldots\ldots\ldots \quad (3a)$$

In most of the theories the basic parameters, in addition to the pile geometry, are: the friction angle, ϕ', which is used to determine the bearing capacity factor N_q, and the effective confining pressure of the soil. None of the theories consider the side resistance of the soil along the pile shaft, or a possible interdependence between side and point resistances. Some of the theories consider the soil to be a rigid-plastic body and the failure patterns are shown in Fig. 2. Others consider the soil to be compressible, and the failure patterns are shown in Fig. 3.

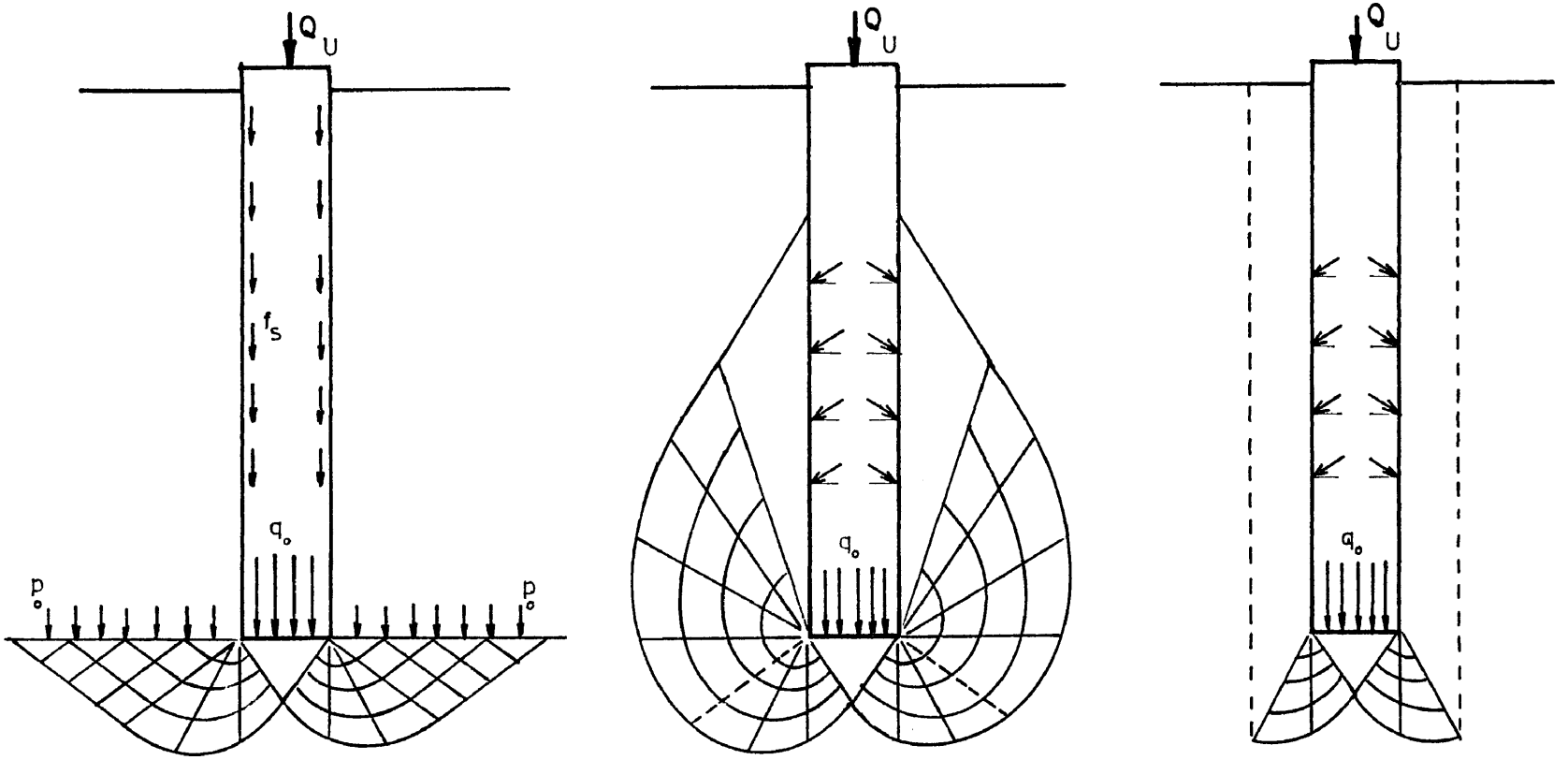

Prandtl (1921)
Reissner (1924)
Caquot (1934)
Buisman (1935)
Terzaghi (1943)

DeBeer (1945)
Jáky (1948)
Meyerhof (1951)

Berezantsev & Yaroshenko (1962)
Vesić (1963)

FIG. 2 - ASSUMED FAILURE PATTERNS - RIGID-PLASTIC SOIL (54)

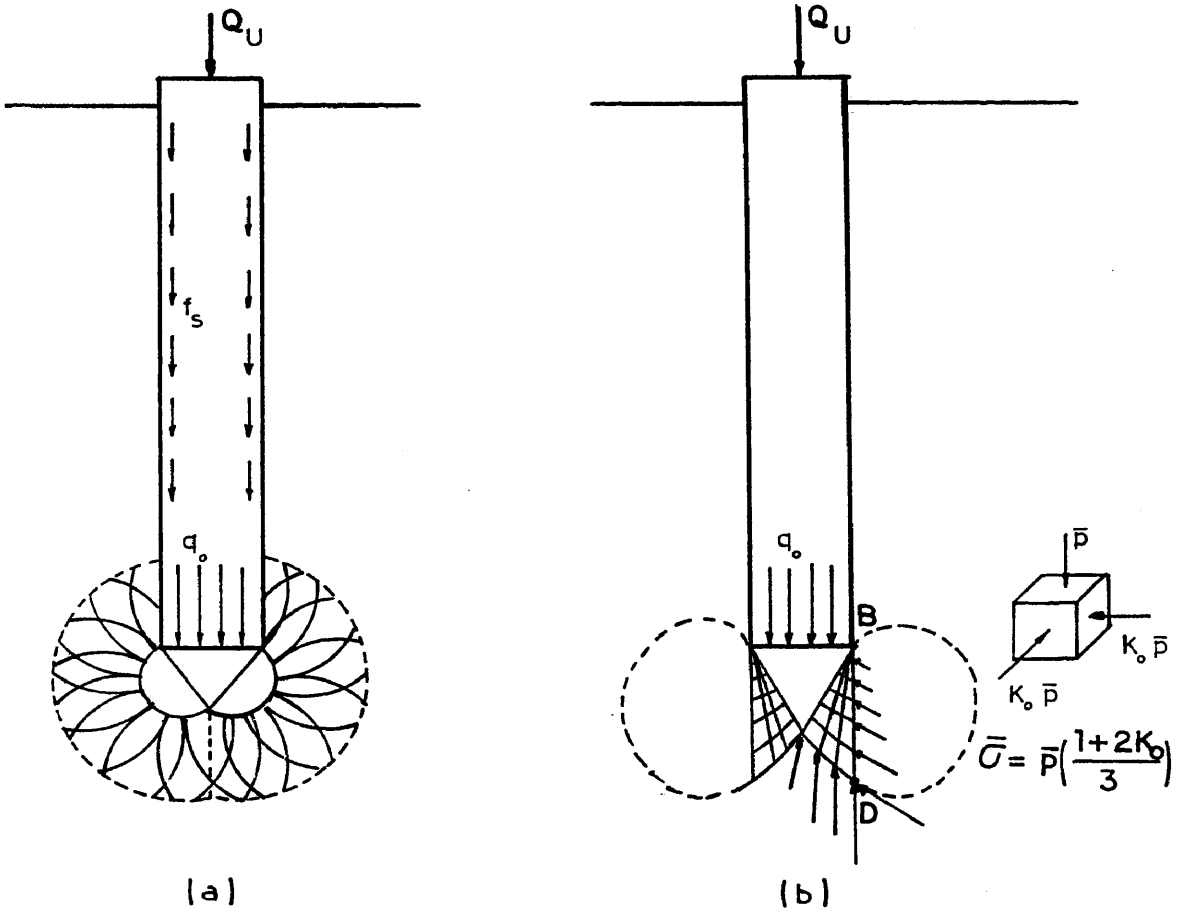

Bishop, Hill & Mott (1945)

Skempton, Yassin & Gibson (1953)

Vesić (1977)

FIG. 3 - ASSUMED FAILURE PATTERNS - COMPRESSIBLE SOIL (54, 58)

Vesic (56, 58) in 1972, realizing that soil is compressible, developed a different failure mechanism for pile penetration. As shown in Fig. 3b along the circular ring (BD) there would be lateral displacement of the soil below the pile point creating a space for penetration. In addition, Vesic defined the average confining pressure as follows:

$$\bar{\sigma} = \left(\frac{1 + 2K_o}{3}\right) p_o \quad \ldots\ldots\ldots\ldots\ldots\ldots \quad (4)$$

where: K_o = the coefficient of lateral earth pressure at rest. Also, the expression for q_o, the unit point resistance, is redefined as:

$$q_o = \bar{\sigma} N_\sigma \quad \ldots\ldots\ldots\ldots\ldots\ldots \quad (5)$$

where N_σ is now a bearing capacity factor, which is a function of the rigidity index, I_r. The rigidity index for cohesionless soils is defined as:

$$I_r = \frac{E}{2\,(1 + \nu)\, p_o \tan \phi'} \quad \ldots\ldots\ldots\ldots\ldots\ldots \quad (6)$$

where: E = modulus of deformation of the soil,

ν = Poisson's ratio for the soil,

p_o = initial effective vertical ground stress, and

ϕ' = friction angle based on effective stresses.

It is important to note that this theory allows for a variation in the bearing capacity factor N_σ for the same friction angle.

Because of the fact that the parameters used in this theory are difficult to evaluate, it is not recommended for application in ordinary situations. However the theory seems to be more realistic because it recognizes the compressibility of the soil. If it is desirable to use the more common relationship for q_o, as given in Eq. 3a (page 7), the following equation can be used to evaluate N_q if N_σ is known:

$$N_q = \left(\frac{1 + 2K_o}{3}\right) N_\sigma \quad \ldots\ldots\ldots\ldots\ldots\ldots\ldots \quad (7)$$

All of the bearing capacity theories require the evaluation of N_q for use in Eq. 3a. A summary of the range of values of N_q according to the different theories is presented in Table 1. The values for Vesić's 1972 theory were calculated using Eq. 7. The value of N_σ, for a given friction angle, varies according to the rigidity index, I_r. According to Vesić (56), the range of I_r, for sands is from 70 to 150. The coefficient of earth pressure at-rest, K_o, was evaluated by using the empirical relationship developed by Jáky (28). This empirical relationship for normally consolidated sands is:

$$K_o = 1 - \sin \phi' \quad \ldots\ldots\ldots\ldots\ldots\ldots\ldots \quad (8)$$

It is evident that there are major deviations from one theory to another, leading to the conclusion that the true failure mechanism is not, generally, well understood. Vesić in 1977 (58) stated: "Computation of the ultimate load is quite difficult and a general solution is

TABLE 1. - BEARING CAPACITY FACTORS FOR DEEP FOUNDATIONS (56, 58)

Theories	Approximate N_q Values ϕ' - Friction Angle				
	25^o	30^o	35^o	40^o	45^o
De Beer (1945)	59	155	380	1150	4000
Meyerhof (1953) - Driven Piles	38	89	255	880	4000
Caquot-Kerisel (1956)	26	55	140	350	1050
Brinch Hansen (1961)	23	46	115	350	1650
Skempton-Yassin-Gibson (1953)	46	66	110	220	570
Brinch Hansen (1951)	32	54	97	190	400
Berezantsev (1961)	16	33	75	186	-
Vesić (1963)	15	28	58	130	315
Vesić (1972) - $I_r = 60$	36	46	57	70	84
$I_r = 200$	60	79	103	131	164
Terzaghi (1943) - General shear	12.7	22.5	41.4	81.3	173.3
Localized shear	5.6	8.3	12.6	20.5	35.1

not yet available", and added: "In view of the many uncertainties involved in analysis of pile foundations, it has become customary, and in many cases mandatory, to perform a certain number of full scale pile load tests at the site of more important projects".

Side Load

The theoretical determination of side resistance for piles in sand has received very little attention in the literature and only a few methods (35, 40) have been published. The interaction between the soil and the pile is very complex and poorly understood. The friction between the pile shaft and the soil develops a resistive force, Q_s, which has been illustrated in Fig. 1 (page 5). This side load, Q_s, is given in equation form as:

$$Q_s = f_s A_s \quad \ldots\ldots\ldots\ldots\ldots\ldots\ldots\ldots \quad (9)$$

where: f_s = ultimate unit side resistance, and

A_s = area of pile shaft.

The determination of the ultimate unit side resistance, f_s, is based on the laws of mechanics considering friction between solid surfaces. Fig. 4 shows the system of forces considered. The magnitude of f_s is determined using the following equation:

$$f_s = K \bar{p} \tan \delta \quad \ldots\ldots\ldots\ldots\ldots\ldots\ldots \quad (10)$$

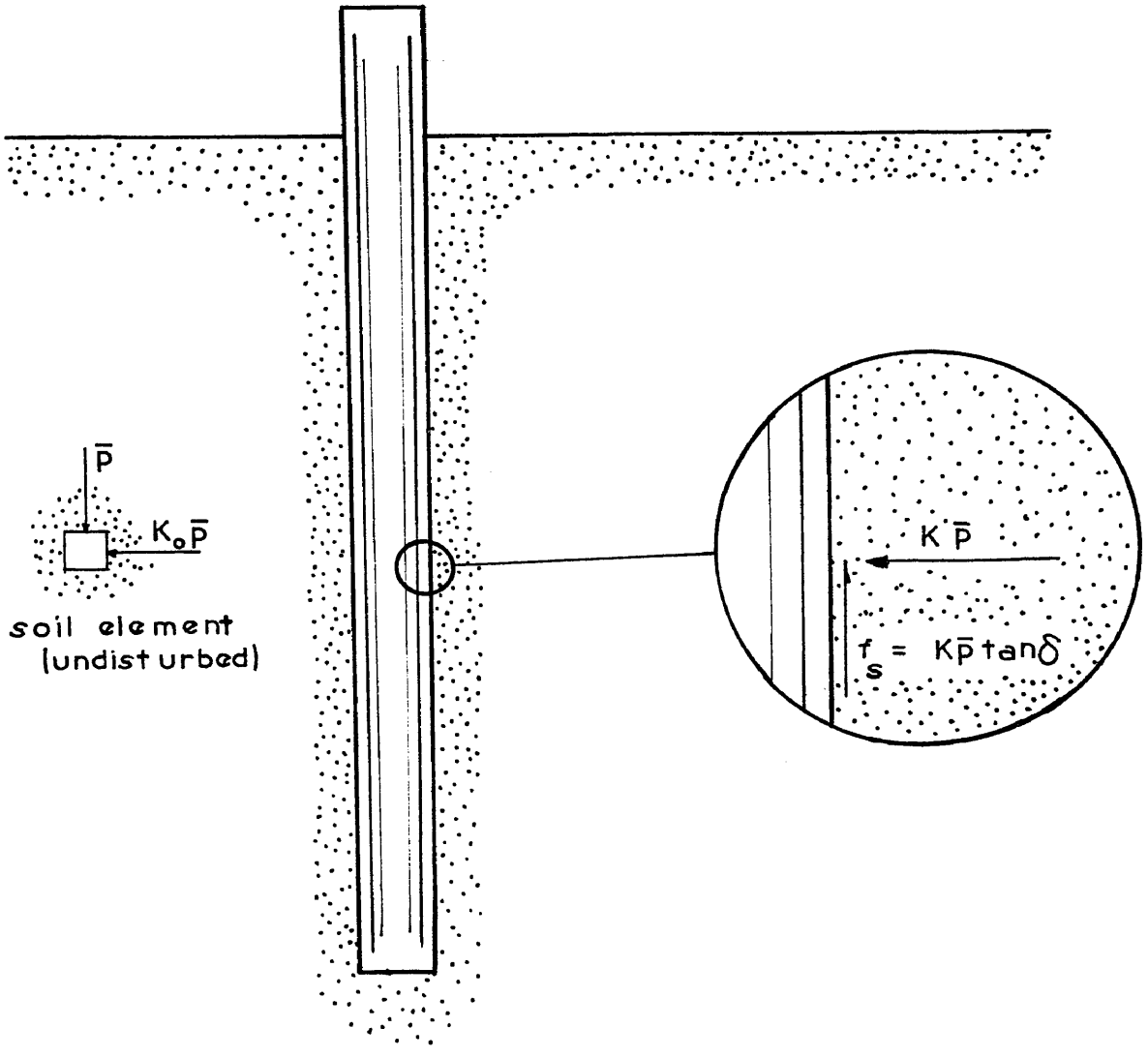

FIG. 4 - SIDE RESISTANCE ALONG SHAFT

where: K = a lateral earth pressure coefficient,

$\bar{p}$ = average effective overburden pressure along the segment of pile being analysed, and

$\tan \delta$ = a coefficient of friction between the pile and the soil.

The average effective overburden pressure, $\bar{p}$, is calculated from the knowledge of the location of the ground water level (usually static) and the magnitude of the unit weight of the sand. The factors K and $\tan \delta$ are the ones that need to be determined.

Potyondy (41) determined in laboratory the coefficient of friction between various construction materials and cohesionless soils at different densities. This determination was made using direct shear tests. In addition to the determination of the coefficient of friction, $\tan \delta$, between the soil and the pile material, the angle of friction of the sand, ϕ', was also determined. Consequently, it was possible to develop a relationship between δ and ϕ'.

Vesić (58) proposed a different approach for the determination of $\tan \delta$. The sand located at the interface between the soil and the pile is considered to be at a state of ultimate failure for determination of side resistance. Consequently the angle of friction between the pile and the soil, δ, is independent of the initial soil density and pile material. Therefore it can be considered equal to the residual friction angle of the sand, ϕ'_{res}. The difference between the values determined by Potyondy (41) and those suggested by Vesić (58) do not seem to be significant.

Meyerhof in 1959 (35), and Nordlund in 1963 (40) dealt theoretically with the problem of the determination of the lateral earth pressure

coefficient, K. The basic assumption in both studies is illustrated in Fig. 5. It is assumed that the pile displaces the sand in a horizontal direction, without any vertical deformation. This displacement induces compaction in the surrounding soil which is maximum at the pile-soil interface. Since the wall pushes against the sand and the horizontal movement is large (equal to the pile radius), it is theorectically possible for the magnitude of the lateral earth pressure coefficient, K, to be as high as the passive earth pressure coefficient.

A list of typical values of lateral earth pressure coefficients for pile foundations compiled by Kézdi (26) is presented in Table 2. It should be noted that, with the exception of Ireland who presents a range of values, only one value is suggested by each author. And no consideration is given to parameters defining the soil-pile system such as pile penetration.

A brief review has been given of the state-of-the-art for the prediction of both point and side resistances for piles in sand. The problem is not new and has received much attention through the years. However, in spite of this effort, Tavenas indicated in 1971 (48): "The determination of the bearing capacity of piles driven into granular materials, when both skin-friction and end-bearing resistances are acting simultaneously, is one of the geotechnical problems for which no valid theoretical solution has yet been proposed".

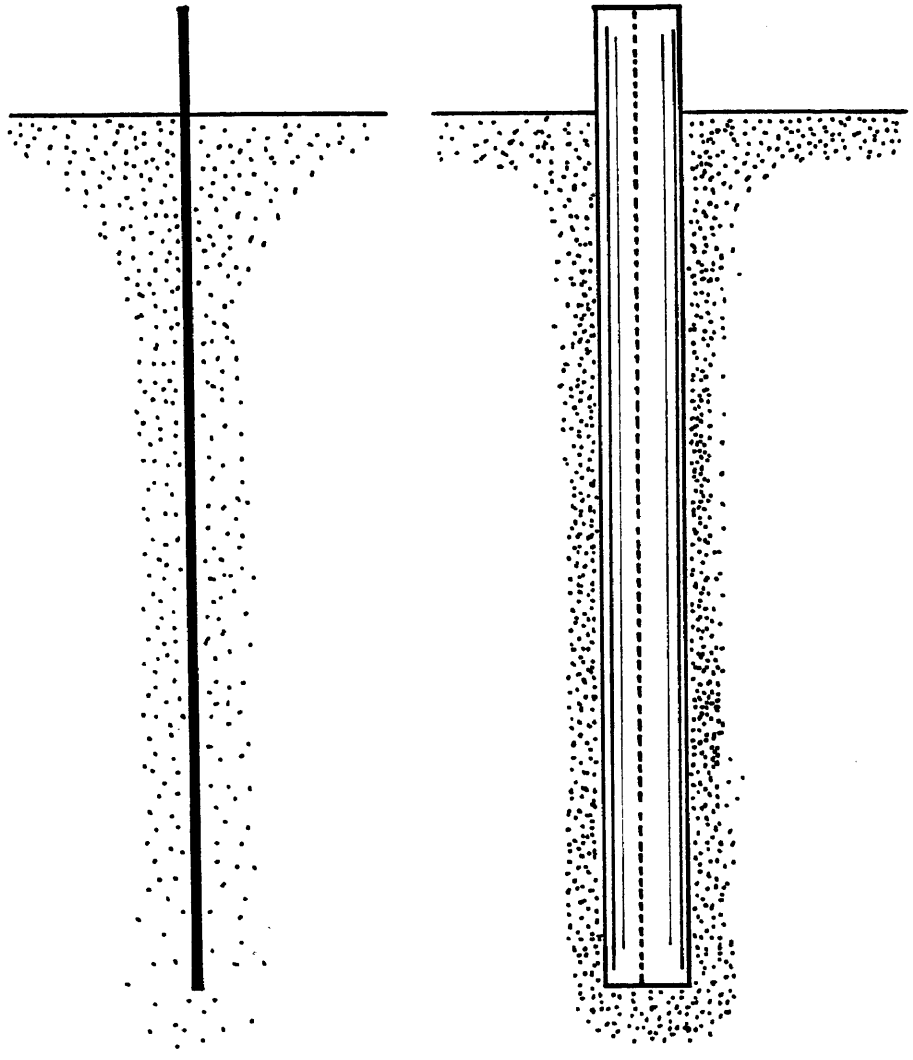

FIG. 5 - IDEALIZATION OF PILE PLACEMENT (40)

TABLE 2. - TYPICAL VALUES OF EARTH PRESSURE COEFFICIENTS (26)

Author	Basis of Relationship	Soil Type	K
Brinch Hansen	Theory	Sand	$\cos^2 \phi$
Lundgren, 1960	Pile Test	Sand	0.8
Henry	Theory	Sand	K_p
Ireland, 1957	Pulling Tests	Sand	1.75 to 3
Meyerhof, 1951	Analysis of field data	Loose sand	0.5
		Dense sand	1.0
Mansur-Kaufman, 1958	Analysis of field data	Silt	0.3 (Compression)
			0.6 (Tension)
Lambe-Whitman, 1969	Guess		2
Kezdi, 1958	Theory	Granular	K_p

EXPERIMENTAL INVESTIGATIONS

A general outline of the method for dealing with physical problems was presented by Morgan (39) as follows:

1st) recognition of the existence of the problem;

2nd) observation of the phenomenon;

3rd) analysis of the data;

4th) formulation of a hypothesis;

5th) experimentation with the purpose of testing the accuracy of the hypothesis. With these results the hypothesis is adjusted or changed until a reasonable explanation of known experimental facts is obtained. Then the hypothesis becomes a theory:

6th) formulation of a law or principle. In this final step the theory has been verified and acknowledged as the universal explanation of the phenomenon.

The 5th step of this outline describes the actual state-of-the-art in the case of pile foundations in sand. Many theories or pseudo-theories (hypotheses, according to the previous outline) have been developed with a limited amount of experimental data, and do not present a generally satisfactory explanation of the phenomenon. Adjustments need to be made on the actual hypotheses and theories. More experimentation and observation of the phenomenon need to be made before a law emerges. Vesić, in 1977 (58) commented: "The theories seeking to relate the unit resistances (q_o and f_s) to known pile and soil characteristics are still under development."

Also, it has been shown previously that the variation of predicted

values of N_q and K is so wide that the choice of one theory in lieu of another is a very difficult exercise in engineering judgement. The differences in calculated allowable ultimate loads for a pile is so large that even adjustment in the factors of safety will not yield general agreement. The need for a better understanding of the failure mechanisms and the development of a general theory resulted in a number of laboratory investigations. Also laboratory investigators hoped to identify important new pile parameters and soil properties.

Mayer and L'Herminier in 1953 (31) reported on work done by others and recognized three distinct patterns for sand failure according to depth of penetration. These patterns are shown in Fig. 6 as a general shear failure for very shallow foundations, a localized shear failure for deep foundations, and a Meyerhof type failure for intermediate penetrations. In 1957 Tomlinson (51) noted that these failure patterns, with soil being displaced upwards and away from the pile, indicated a tendency to form a gap between the pile shaft and the soil. Consequently, the active case of lateral earth pressure could develop.

In 1959 Meyerhof (35) indicated that, in cohesionless soils, the effect of pile driving is general compaction resulting from permanent rearrangement and some crushing of the soil particles. In addition, the driving of the pile in the soil mass alters its state of stress. Subsequently, in 1966, Broms (8) reported on the zones which undergo general compaction and alteration from the original state of stress as those depicted in Fig. 7.

Measurements made by Szechy in 1961 (47), using laboratory model tests, indicated that the idea of general sand compaction is not valid.

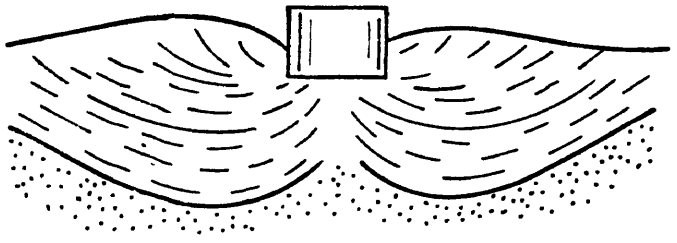

a) SURFACE FOUNDATION - GENERAL SHEAR

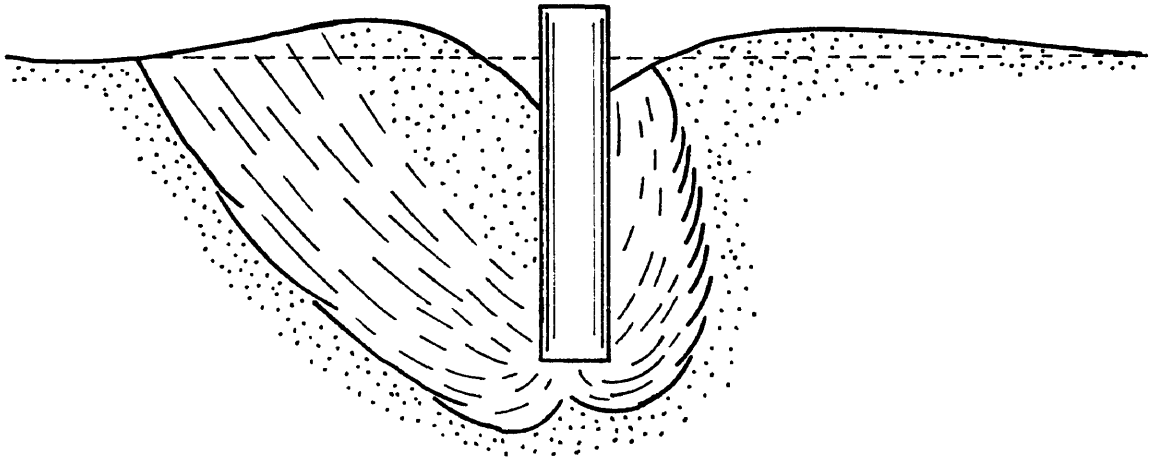

b) INTERMEDIATE DEPTH - MEYERHOF TYPE

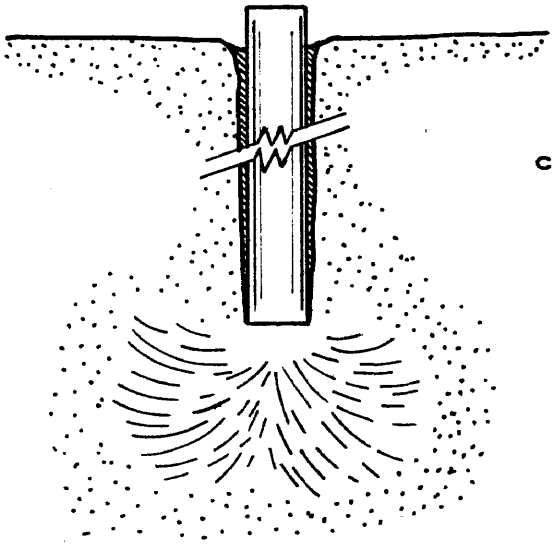

c) DEEP FOUNDATION - LOCAL SHEAR

FIG. 6 - FAILURE PATTERNS ACCORDING TO DEPTH (31)

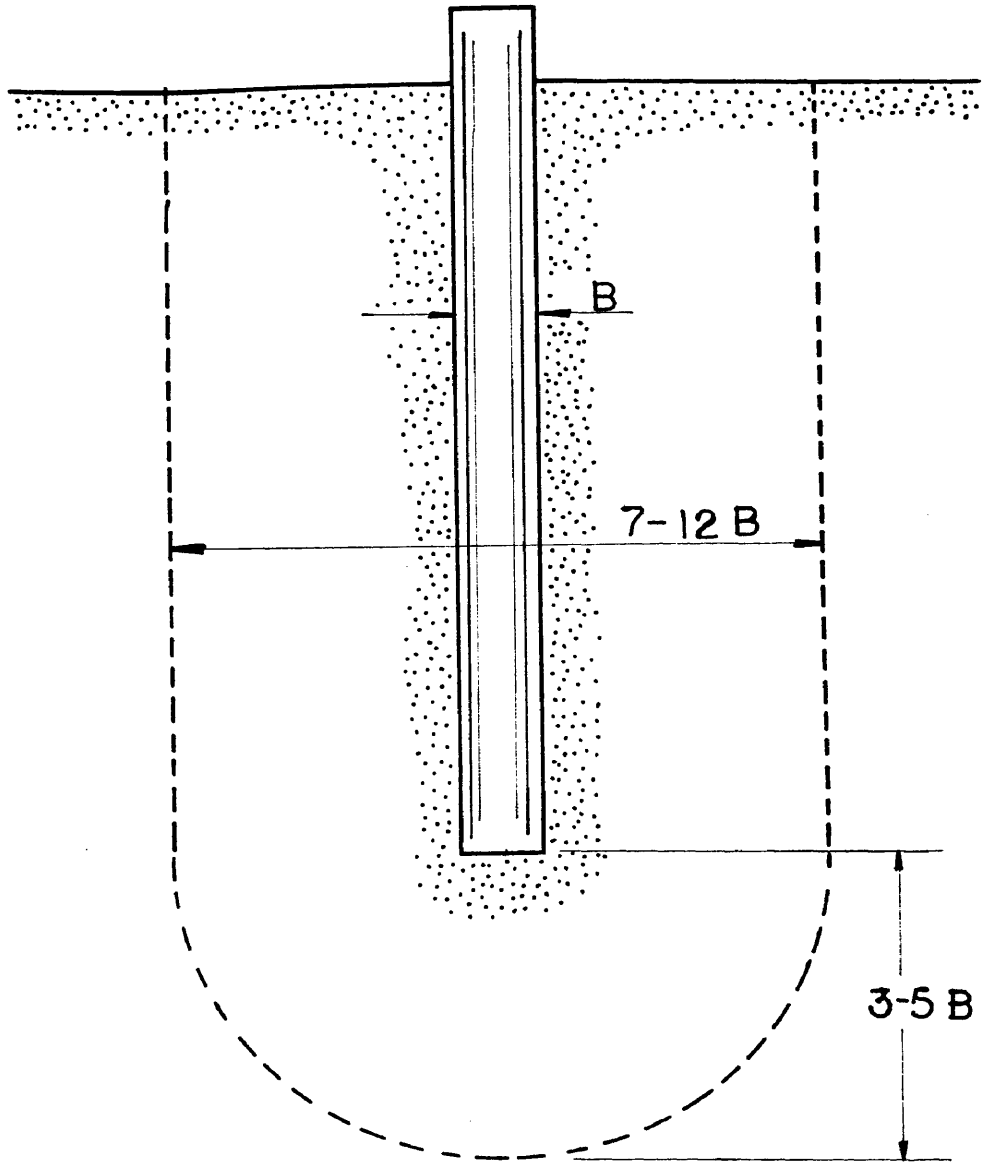

FIG. 7 - PILE COMPACTION OF SANDS (8)

Szechy found that "the highly compressed stress concentration areas are surrounded with areas of stress-relief below the pile toe as well as around the pile shaft". In 1964 Robinsky and Morrison (42) with more sophisticated measurements made on loose and medium dense sands in the laboratory confirmed the earlier findings. According to Robinsky and Morrison the overall process of sand compaction results in a seemingly erratic accumulation of high and low density areas. A thin sleeve of loose sand is created around the pile wall, which is encircled by a cylinder of dense sand. This cylinder, by arching, prevents the development of full lateral earth pressure on the pile. Also, in 1964, Robinsky and others (43) reported on additional experimentation. These results indicated that with pile penetration the "arches" around areas of loosened sand would be built-up and broken-down inducing continuous changes in mobilized side resistance. This could explain a "wavy" distribution of side resistance along the pile shaft. The arching system would be very delicate and quite easily disrupted by a change in the loading conditions.

Confirming that the densification of sand around the pile is not steadily increasing or decreasing was a report by Kérisel, L'Herminier and Tcheng in 1965 (25). For a sand with a dry density of 98.6 pcf (1.58 t/m^3) it was found that at depths greater than 3.3 ft (1 m), for a pile 12.6 in. (320 mm) in diameter, there was densification of sand at the pile point level. However, dilation occurred along the side of the pile. Fig. 8 presents the measurements made with equipment which evaluates the volumetric deformation by absorption or expulsion of water. Fig. 8a shows the volumetric variation given by the four devices

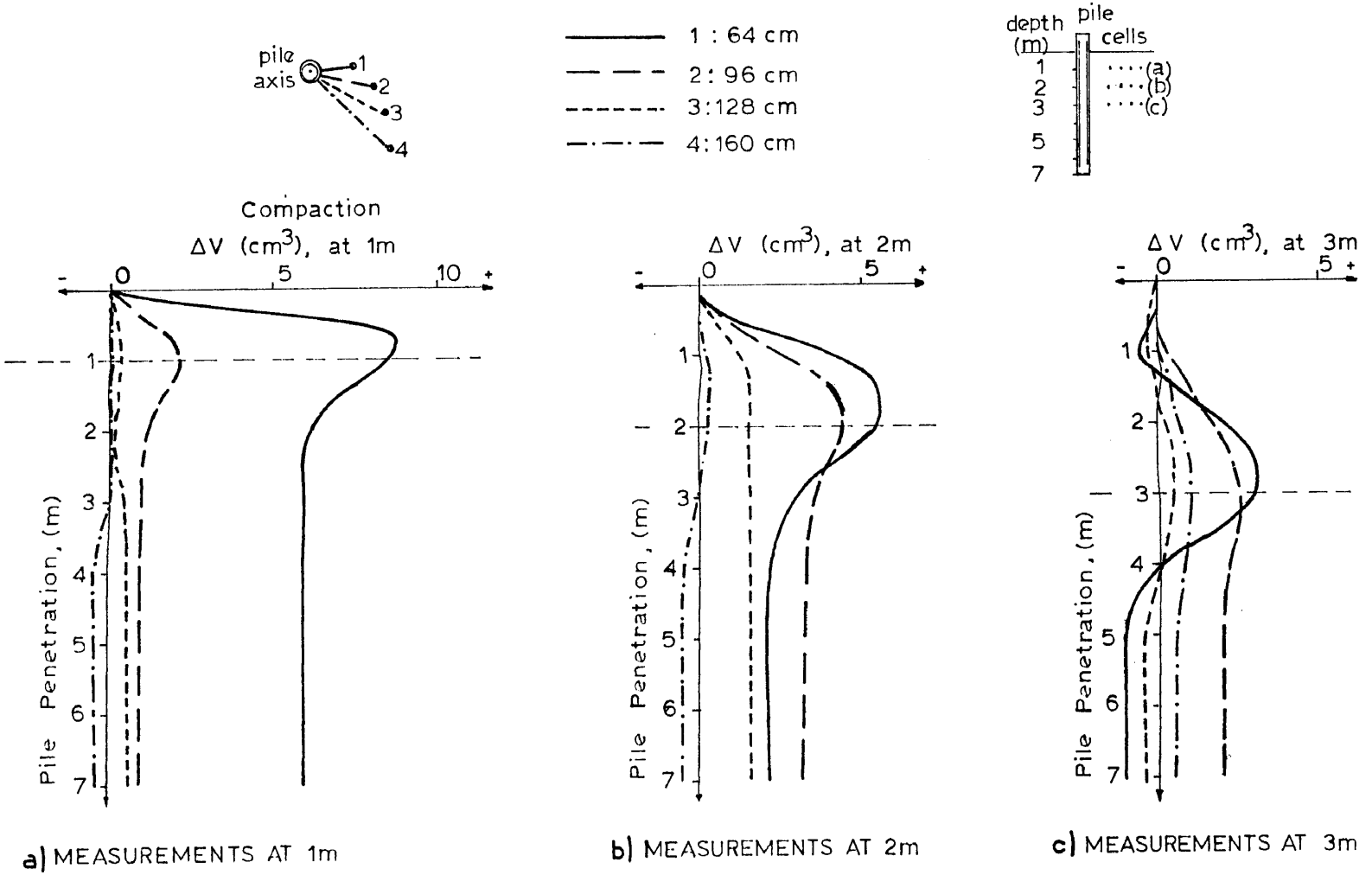

FIG. 8 - SAND DENSITY VARIATION WITH PILE PENETRATION (25)

installed at a depth of 1 m, as the pile penetrated from the 0 to the 7 m depth. Figs. 8b and 8c show the same measurements when the devices were located at depths of 2 m and 3 m, respectively.

Kérisel in 1961 (24) published a noteworthy paper concerning laboratory experiments in sand. It was observed that different size piles in the same sand attained a maximum value of unit load resistance which remained constant with increasing penetration. The depth where the constant value was attained would vary with the pile diameter. The larger the pile diameter the deeper the required penetration. This phenomenon is illustrated qualitatively in Fig. 9.

Vesić (57) in 1970 confirmed, with field tests, the tendency for unit resistances to increase with depth to some limiting value. Vesić noted that even though the rate of increase sharply decreases at some "critical" depth, there was an additional increase with further penetration. This "critical" depth was defined as being between ten pile diameters for loose sands and twenty for denser sands. In 1977, Meyerhof and Valsankgar (37) obtained additional laboratory evidence of a limiting value for unit point resistance. The study also showed that the "critical" depth for submerged sands is 1.6 times greater than that for dry sands. This increased "critical" depth is probably caused by buoyancy effects.

Biarez and Gresillon (3) in 1972 reported on laboratory experiments performed at Grenoble, France. Pile models of various diameters were penetrated into metallic rollers (a bi-dimensional problem), into glass spheres of same diameter, and into sand. The sand was tested at various densities and with different surcharges applied by means of air pressure

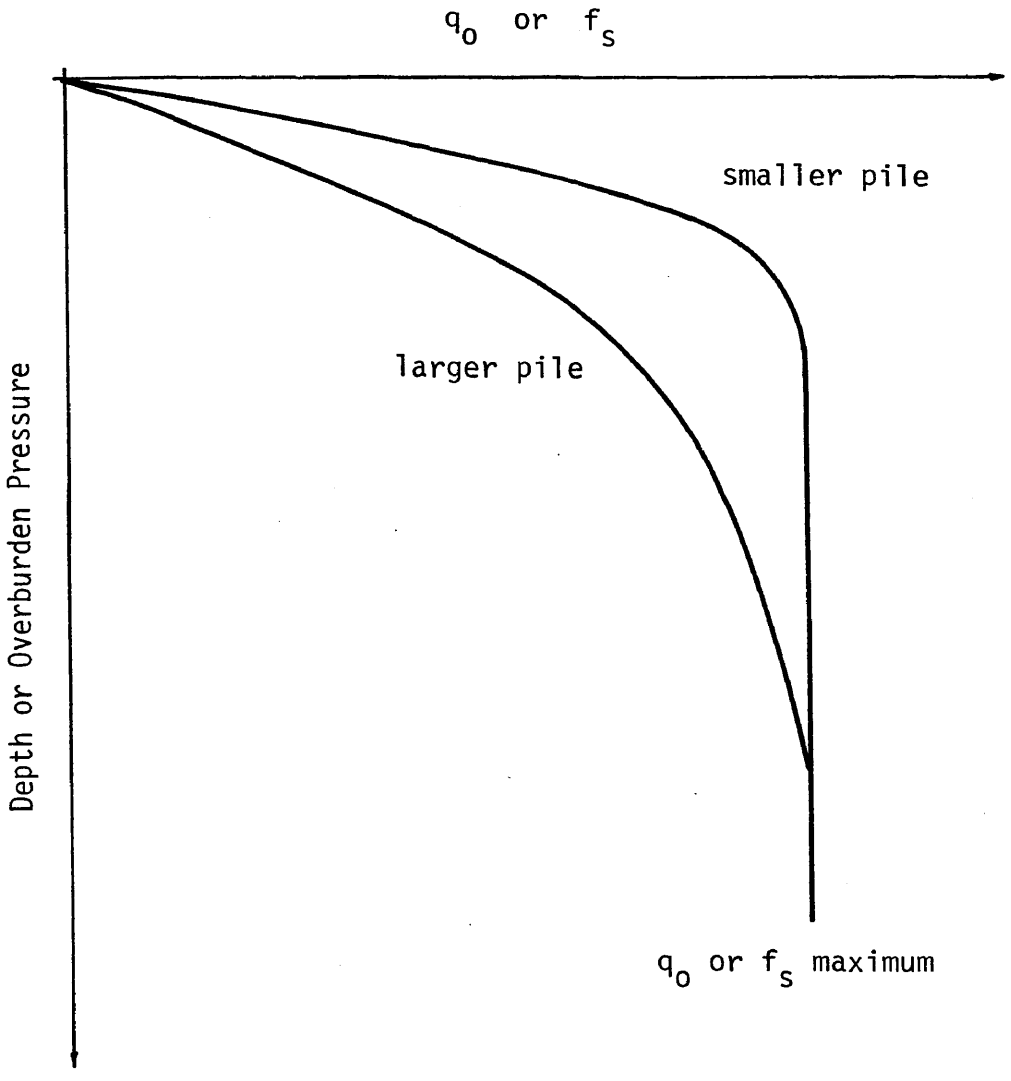

FIG. 9 - UNIT RESISTANCES VARIATION WITH DEPTH OR PRESSURE

(with membranes covering the sand). Once again limiting unit resistances were obtained. One conclusion of this study was that the compressibility of the soil is a very important property in the determination of the bearing capacity of deep foundations. It was also hypothesized that the sand around the pile shaft would expand in order to compensate for the compression of the soil mass under the pile point. Consequently the vertical pressure at the pile point would be less than the initial overburden pressure. With respect to soil compressibility it is important to note that the critical void ratio of sand is pressure dependent. For deeper foundations (greater confining pressures) the critical void ratio would be smaller, which would facilitate soil compression. Another important factor in relation to compressibility is the crushing of the soil grains as noted by DeBeer (14).

IMPROVED HYPOTHESES

As a result of the theoretical and experimental investigations, it is possible to formulate qualitative hypotheses regarding the mechanism of pile-soil interaction. These hypotheses will be helpful later on in the formulation of the proposed correlations.

There are three types of point failure patterns for foundations according to depth of penetration or confining pressure, as shown by Fig. 6 (page 21). An explanation of the process would be that at shallow and intermediate penetrations the stress needed to compress the soil and accomodate the pile would be greater than its shear strength. Consequently, the soil mass would be sheared and displaced upward towards the surface. At deeper penetration only a localized shear failure would occur, directly beneath the pile tip. The surrounding soil mass would be strong enough to resist a general shear failure and large enough to accomodate the soil displaced by the pile point. In this case the compressibility of the soil would play a fundamental role. Consequently, the penetration required for determination of the type of failure must depend on the pile volume, i.e., the larger the pile diameter the larger the volume of soil displaced per foot of penetration.

The results of experimental studies have indicated that certain parameters control the pile-soil behavior at the pile tip. These parameters are: effective overburden pressure (related to depth); soil displacement (related to pile diameter); and sand relative density or friction angle (a soil property). In addition, the compressibility of the soil as related to the field state of stress influences the

pile-soil behavior. In this study, the compressibility of the soil is to be taken in account empirically through a combination of the aforementioned parameters.

These parameters may be independent or they may be interrelated. Depth of pile penetration and effective overburden pressure are very closely related, especially when the soils are grouped according to relative density or friction angle. A method of trying to determine the particular influence of each would be by means of surcharges. When using surcharges the pressure would vary but not the depth of pile penetration. Another method would be the use of submerged and non-submerged soils. In this case, the effective pressure would be reduced by buoyancy effects for submerged soils but the depth of penetration would not be changed.

A second pair of strongly interrelated parameters are the sand relative density and friction angle. Normally these parameters are extrapolated from the Standard Penetration Tests. In order to determine these parameters more accurately, it would be necessary to obtain undisturbed sand samples. Also, it should be noted that these parameters are influenced by different physical soil characteristics. For example, it is possible to have a dense (high relative density) fine sand with the same friction angle as a loose (low relative density) coarse sand depending on the degree of particle roundness.

The visualization of the interaction between the pile point and the sand is relatively simple. However, the interaction between the pile shaft and the soil is more complex. The state of stress and overall properties of the adjacent soil mass can be substantially changed

by the penetration of the pile. The pile point would compress the sand mass leaving behind, through arching effects, a cylinder of highly compacted material which has a diameter greater than the pile itself. The anulus between this compressed cylinder and the pile surface would be filled with loose sand. With further pile penetration, parts of the compressed cylinder would fail and be pushed against the pile surface. This type of failure would be less frequent for deeper pile penetrations due to higher confining stresses. At zones of failure dilation would occur in the soil mass.

The mechanism of side load transfer is very complicated because of the erratic and unpredictable occurrence of delicate arching. How the arching occurs is not known, but it has been recognized that arching is associated with the distribution of the total load between the pile point and side. Robinsky and others (43) report that piles driven dynamically carried about 10% to 20% more side load than statically pushed piles, but in both cases the total load was about the same. Therefore, it was concluded that side and point loads are interdependent. For a given set of conditions, when the point resistance varies between a maximum and minimum the side resistance would vary between a minimum and maximum. The minimum side resistance would occur when the delicate arching system is not destroyed.

It has been shown that the point and side resistances are interrelated. Consequently the parameters which affect the pile-soil interaction for both point and side resistances are the same. In summary the significant parameters for the pile-soil system are:

a) effective overburden pressure (related to depth);

b) soil displacement (related to pile diameter or the diameter of a circle with the same area as the pile cross section); and

c) sand relative density or friction angle (a soil property.

Finally, it should be noted that the experimental results are based primarily on model tests in the laboratory. Since the laboratory results are qualitative, there is a need for verification through full scale field tests. Field tests can be used to investigate the significance of the parameters by means of appropriate correlations. These correlations would permit a more accurate evaluation of the ultimate bearing capacity of piles in sand which is the main objective of this study. The achievement of this objective may permit the eventual formulation of a general theory.

INTERPRETATION OF FIELD LOAD TESTS

Load Distribution and Compression Test

As a consequence of the present state-of-the-art the safest way to deal with design problems has been to use conservative values for bearing capacity factors in preliminary analysis and then if feasible, to proceed with field load tests at the site. For larger and more important projects load tests on preliminary piles are widely recommended.

In this study data from load test reports are used for the determination of actual bearing capacity factors. For correlation purposes, it is necessary that the load tests in sands be conducted on instrumented piles allowing measurement and separation of the total load into its components: side load —— distributed along the pile shaft, and point load —— concentrated at the pile point.

The total force at the top of the pile is usually applied by means of a jack. This force can be accurately measured by means of a load cell. The force and the corresponding measured settlement at the top of the pile permit the development of a load-settlement curve as illustrated in Fig. 10a.

The distribution of the total force between the pile point and the shaft can be obtained by means of strain gages or a load cell placed close to the pile tip. If additional strain gages are placed along the pile shaft the side load distribution can be calculated also, as shown in Fig. 10b. The difference in load determinations between two strain gages or any pair of measuring devices gives the load being transmitted

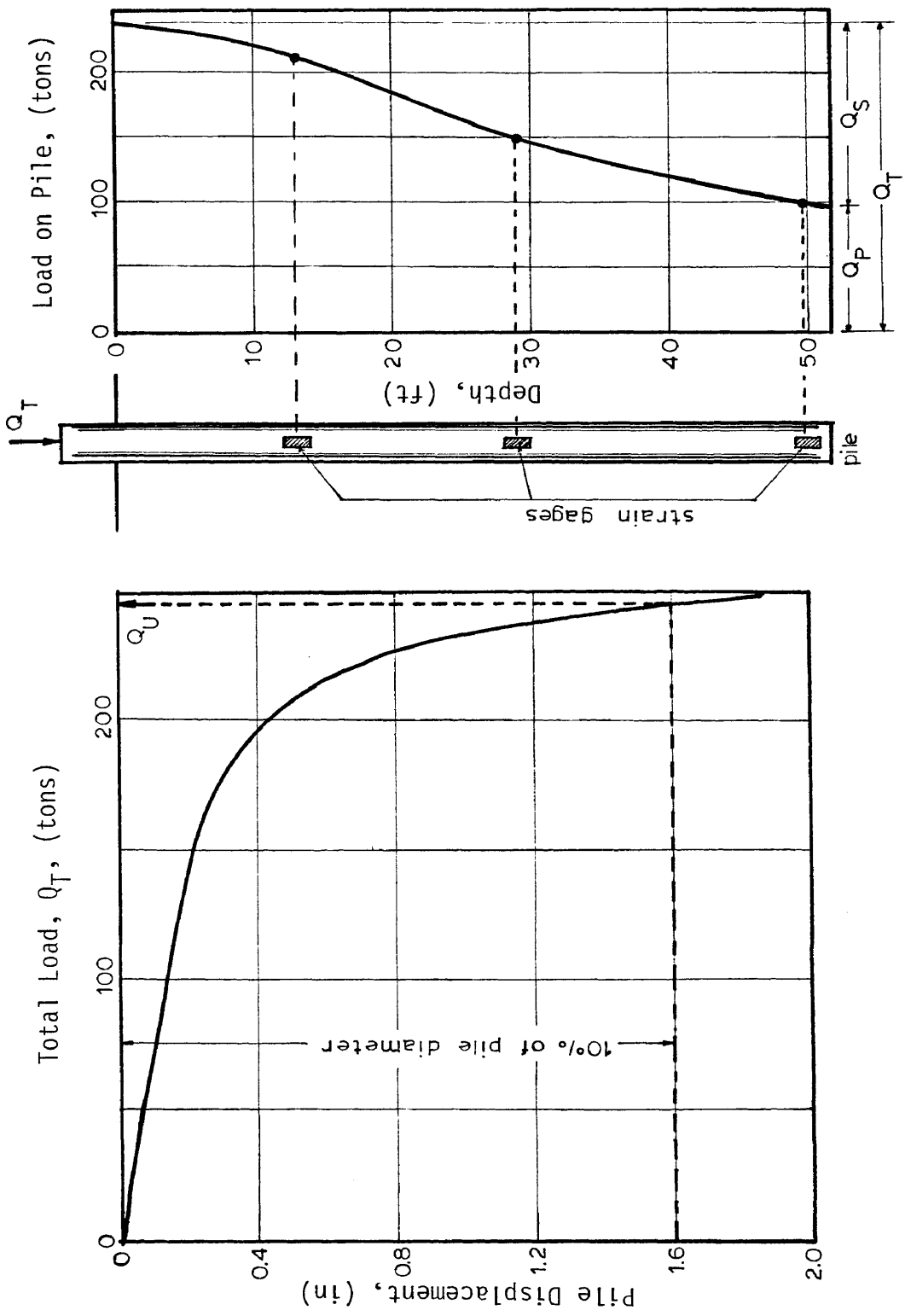

FIG. 10 - TYPICAL INSTRUMENTED PILE LOAD TEST RESULTS (1 in = 2.54 cm; 1 ft = 0.305 m; 1 ton = 8.90 kN)

by friction from the pile to the surrounding soil in that pile section. From the strain gage, or other measuring device, placed close to the tip it is possible to obtain both total side load and total point load. Then using Eqs. 2 (page 6) and 9 (page 13) and knowing the pile geometry, it is possible to determine both the unit side and point resistances.

When analysing field load tests in sand conducted at different sites an important problem that arises is the definition of failure load. Vesić (58) lists fifteen different criteria for definition of failure load. For this study the Vesić (58) suggestion of taking the failure load as being the one which induces a total settlement (see Fig. 10a) equal to 10% of the point diameter was used. In cases where load transfer curves (see Fig. 10b) were not given for the established failure load, it was necessary to extrapolate and develop a load transfer curve corresponding to the failure load.

Residual Stresses and Tension Tests

Instrumented tension tests performed as part of the Arkansas River Navigation Project (21) have shown, consistently, that a resistive concentrated load exists at the pile point. Also, when measurements of load distribution along the pile were made after the compression loads in a test pile were released, it was shown that the stresses along the pile were not zero. These observations confirm the existence of residual stresses in hammer driven piles, which can mask the real distribution of the total load between side and point. Hunter and Davisson (21) concluded that measurements of these load components (side and point) are "likely to be seriously in error" if residual loads are not

considered. However, the total loads in both compression and tension are not changed.

Even though the presence of residual stresses in hammer driven piles is widely recognized (18, 20, 21, 45, 48 and 59), a method of correcting for residual stresses has not been generally adopted. A rational method for this purpose was presented as early as 1964 (15). Hunter and Davisson (21) advocated the use of the same method in 1969. Also, Vesić (59) in 1978 emphasized the significance of the use of this method of correcting for residual stresses. Vesić added the information that driving of subsequent piles in a group changes the distribution of residual loads in the group system. The application of this method of correcting for residual stresses is illustrated in Fig. 11. In addition to the measurements taken during an ordinary compression test, it is necessary to conduct a tension test. The explanation of the procedure used in applying the method is as follows:

a) Curve (1) represents the measured compression load distribution, assuming no stresses in the pile at start of test;

b) Curve (2) represents the measured compression load distribution after complete release of the compressive loads, assuming no stresses in the pile at start of test;

c) Curve (3) represents measured tension load distribution assuming no stresses in the pile at start of this test;

d) Curve (4) represents the measured tension load distribution after complete release of tensile loads, assuming no stresses in the pile at start of test;

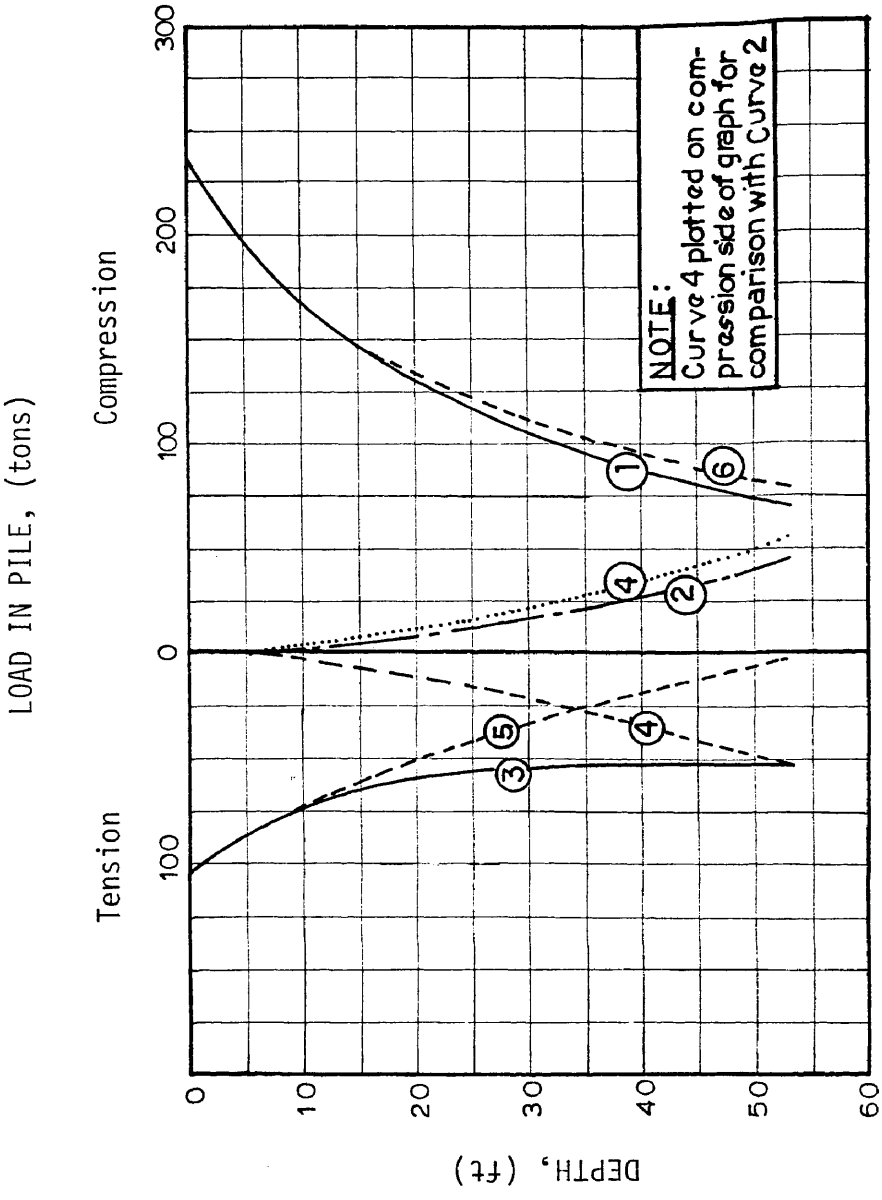

FIG. 11 - CORRECTION FOR RESIDUAL STRESSES (1 ft = 0.305 m; 1 ton = 8.90 kN); (15)

e) It is assumed that no residual stresses should be present at the end of the tension test, so curve (4) represents the residual compressive stresses for this test and should be subtracted from curve (3) in order to give curve (5), the adjusted tension load distribution; and

f) Curve (4) includes the original compressive residual stresses in the pile, before the compression test, plus the residual stresses induced by the compression test. The subtraction of curve (2) from curve (4) gives the original compressive residual stresses which are then added to curve (1) resulting in the adjusted compression load distribution as represented by curve (6).

Gregersen, Aas and DiBiagio in 1973 (18) explained the presence of residual stresses as being caused by cracks in a concrete pile due to tensile stress waves which occur during driving. However, since the first measurements of residual stresses, published in 1964 by Fruco and Associates (15), were on metalic pipe piles this explanation could not be applicable to all cases. A better explanation of the cause of residual stresses was presented by Sherman and others (45) in 1974. This explanation received experimental support from the work done by Hanna and Tan (19), in 1973. According to Sherman and others the origin of residual stresses could be explained by the fact that when piles are hammer driven they penetrate the soil in a compressed state. When the driving forces are released, friction would prevent the complete rebound of the pile to its original length, and the pile would remain compressed. The fact that piles driven by vibration or jetting do not cause residual loads lend support to this explanation. Fig. 12 presents the idealization

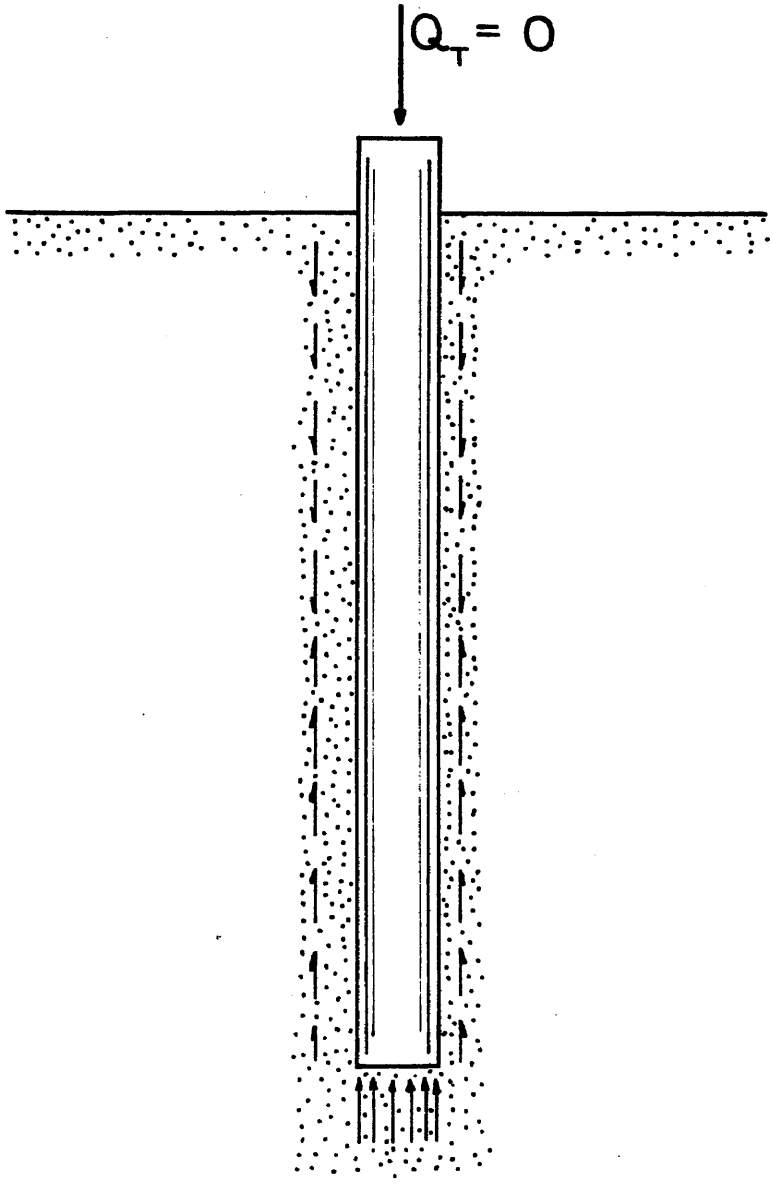

FIG. 12 - RESIDUAL STRESSES IN SAND (58, 19)

by Vesić (58) and Hanna and Tan (19) concerning the residual load distribution on a pile. In the upper portions of the pile the upward movement due to rebounding would be large enough to induce a downward sand resistance. This downward resistance would then react to the rebounding forces below and maintain the pile in a compressed state.

A very important consequence of the adjustment of loads for residual stresses, as suggested by Holloway, Clough and Vesić (20), is that the adjusted compressive side load should be equal to the tensile load obtained in a pull-out test. Robinsky and others (42, 43) pointed out that the residual stresses caused in the soil by the pile driving induce instability in the arching system which surrounds the pile wall. Since a pull-out test reverses the direction of applied stresses in the soil it is very likely that the most unstable part of the delicate arching system is destroyed and a more permanent side resistance is attained.

ANALYSIS OF FIELD LOAD TEST DATA

Test Pile Data and Bearing Capacity Factors

The purpose of this study is to investigate possible relationships between bearing capacity factors and pile-soil system parameters. In order to develop correlations, field data must be obtained which includes the required pile and soil data. Other useful information includes a description of the pile and the method of driving (jetted, pre-drilled, and cast-in-place piles were not used in this study).

The evaluation of the bearing factors, N_q and K, as used in Eqs. 3a (page 7) and 10 (page 13) requires knowledge of the unit resistances, the coefficient of friction between pile and soil, and the effective soil pressure along the pile. In addition, for correlation purposes it is necessary to know the friction angle and the relative density of the sand.

The average unit resistances, q_o and f_s, can be calculated as explained previously from instrumented pile test data. Another way of obtaining the side and point loads and corresponding resistances is to use the tension test load as the adjusted compressive side load (20). The point load is obtained by subtracting the tension test load from the total compression test load. For purposes of data analysis, loads and unit resistances obtained in this manner will be referred to as "compression/tension" data.

In most cases the evaluation of the sand parameters was based on Standard Penetration Test data in conjunction with soil descriptions. Similar procedures were used to obtain the unit weight of the sand

which is needed for evaluation of the effective overburden pressure. Also, information regarding the ground water had to be known.

In order to evaluate the lateral earth pressure coefficient, K, it was necessary to determine the soil-pile angle of friction, "δ". As noted previously, there is disagreement (41, 58) concerning the evaluation of "δ". Consequently, for purposes of data analysis two methods of evaluation will be used. One method will be to use the residual friction angle of the sand, and the other method will be to use 0.8 times the peak friction angle. For comparison purpose the combined effect of "K tan δ" will be investigated.

Table 3 presents a summary of the data obtained from field tests in sand and Table 4 presents the calculated bearing capacity factors and earth pressure coefficients based on the field test data. In Table 3 "B" represents the pile diameter or, in the case of piles with non-circular cross sections, "B" represents the diameter of a circle with the same cross-sectional area. It is interesting to note that all tests were made at sites where the ground water table level was very close to the ground surface. The deepest water table occurred at the "Jonesville" test site at a depth of 8 ft (2.4 m).

In dealing with soil investigation a lot of engineering judgment has to be used in extrapolating soil properties from bore holes at the test location. This becomes particularly difficult for soils of varying composition and sometimes the tested pile itself acts as a probe uncovering the influence of minor occurrences in the soil strata. That was the case for the "Jonesville" piles, where longer piles had less load capacity. It was deduced that "clay laminations" at greater depths were

TABLE 3 - TEST PILE AND SOIL DATA

Pile Test		Pile Description		Pile Penetration (ft)	Soil Description	Sand Friction Angle, ϕ', (^{0})	Sand Relative Density, D_R, (%)	Eff. Ov. Pressure, p, (tsf)	FAILURE LOADS (tons) Total Q_u	Point Q_p	Side Q_s	References
ARKANSAS	# 1	Closed steel pipe pile of diameter, B (ft):	1.20	0	Fine sand,SP	32	40	0.475		48[a]	124[a]	(15); (21); and (30)
				33	Fine sand w/ silt &	35	70	1.265	172	85[b]	87[b]	
				53.1	clay, SP & SM	35	70	1.580		79[c]	93[c]	
				Aver.		33	50	0.774				
	# 2		1.50	0	Fine sand,SP	32	40	0.302		75[a]	167[a]	
				21	Fine sand w/ silt &	33	60	1.073	242	120[b]	122[b]	
				52.8	clay, SP & SM	34	60	1.540		130[c]	112[c]	
				Aver.		33	50	0.766				
	# 3		1.70	0	Fine Sand,SP	32	40	0.506		110[a]	162[a]	
				35	Fine sand w/ silt &	35	70	1.294	272	160[b]	112[b]	
				53	clay, SP & SM	35	70	1.575		152[c]	120[c]	
				Aver.		33	50	0.774				
	# 10[+]		1.42	0	Fine sand, SP	32	40	0.300		71[a]	171[a]	
				21	Fine sand w/ silt &	33	60	1.071	242	80[b]	162[b]	
				53	clay, SP & SM	34	60	1.543		135[c]	107[c]	
				Aver.		33	50	0.765				

TABLE 3 - Continued

Pile Test		Pile Description		Pile Penetration (ft)	Soil Description	Sand Friction Angle, ϕ', (^{o})	Sand Relative Density, D_R, (%)	Eff. Ov. Pressure, p, (tsf)	FAILURE LOADS (tons) Total Q_u	Point Q_p	Side Q_s	References
ARKANSAS	# 4	Precast sq. concrete (16"x16") B = 1.5 ft		0	Fine sand w/ silt or clay laminations, SP & SM	32	45	0.593	200	104[c]	96[c]	(15); (21); and (30)
				40.2		35	70	1.184				
	# 6	"H" piles "14BP73" of equivalent diameter, B (ft):	1.34	0	Fine sand, SP	32	40	0.475	183	46[a]	137[a]	
				33	Fine sand w/ silt &	35	70	1.060				
				40	clay, SP & SM	35	70	1.170				
				Aver.		33	45	0.578				
	# 7		1.34	0	Fine sand, SP	31	40	0.300	243	59[a]	184[a]	
				21	Fine sand w/ silt &	33	65	1.065		90[b]	153[b]	
				52.1	clay, SP & SM	34	65	1.532		175[c]	68[c]	
				Aver.		32	55	0.757				
	# 9		1.34	0	Fine sand, SP	33	40	0.508	250	38[a]	212[a]	
				35	Fine sand w/ silt &	35	70	1.302				
				53.2	clay, SP & SM	35	70	1.589				
				Aver.		34	50	0.780				

TABLE 3 - Continued

Pile Test		Pile Description		Pile Penetration (ft)	Soil Description	Sand Friction Angle, ϕ', (^{o})	Sand Relative Density, D_R, (%)	Eff. Ov. Pressure, p, (tsf)	FAILURE LOADS (tons) Total Q_u	Point Q_p	Side Q_s	References
JONESVILLE	# 1	Precast sq.concrete, 18" x 18" : B = 1.70 ft		0 38	Fine & medium silty sand with lenses of silt and clay, SP - SM	38 38	80 > 100	0.745 1.483	410	280[c]	130[c]	(16); and (45)
	# 2			0 45		38 38	80 > 100	0.855 1.703	340	190[c]	150[c]	
	# 3			0 54		38 38	80 > 100	1.000 1.995	390	260[c]	130[c]	
LOW - SILL	# 2	Closed steel pipe pile of diameter B (ft) :	1.75	0 48 65	Silt Fine & medium sand	— 36 36	— 100 100	1.25* 1.615 1.980		166[c]	90[c1]	(29); and (45)
	# 4		1.42	0 48 66	Silt Fine & medium sand w/ pocket of gravel	— 36 36	— 100 100	1.25* 1.632 2.013		196[c]	130[c1]	
	# 6		1.52	0 50 65	Silt Fine & medium sand	— 36 36	— 100 100	1.25* 1.610 1.969		151[c]	180[c1]	
	# 3	"H" pile w/ bottom plate (~14"x10") B = 1.7 ft		0 52 71	Silt Fine & medium sand	— 36 36	— 100 100	1.25* 1.670 2.090		105[c]	—	

TABLE 3 - Continued

Pile Test		Pile Description	Pile Penetration (ft)	Soil Description	Sand Friction Angle, ϕ', (^{o})	Sand Relative Density, D_R, (%)	Eff. Ov. Pressure, p, (tsf)	FAILURE LOADS (tons) Total Q_u	Point Q_p	Side Q_s	References
VESIĆ	H-11	Closed end steel pipe pile of diameter B = 1.50 ft	0 9.92	Silty sand until 12 ft. Below 12 ft: fine & medium sand, SW - SP.	33 33	50 50	0.230 0.424	76	61[a]	15[a]	(53); and (57)
	H-12		0 20.08		35 38	60 85	0.410 0.755	232	173[a]	59[a]	
	H-13		0 29.08		35 38	70 85	0.560 1.048	297	212[a]	85[a]	
	H-14		0 39.33		36 39	70 90	0.725 1.396	347	214[a]	133[a]	
	H-15		0 49.25		37 40	75 90	0.891 1.715	421	258[a] 248[c]	163[a] 173[c]	
	H-2	Precast sq. concrete, (16"x16"), B = 1.50 ft	0 50		33 39	60 80	0.891 1.715	303	172[a]	131[a]	
GREGERSEN	# A	Precast cylindrical concrete, B = 0.92 ft	0 26.2	Sandy fill until 5.6 ft. From 5.6 ft to 9.8 ft: fine sand, SP. Below 9.8 ft: medium to coarse sand, SP.	30 30	10 5	0.492 0.983	27	21[a] 17[c]	6[a] 10[c]	(18)
	# D/A		0 52.5		30 31	5 10	0.911 1.822	49	38[a] 22[c]	11[a] 27[c]	

TABLE 3 - Continued

Pile Test		Pile Description	Pile Penetration (ft)	Soil Description	Sand Friction Angle, ϕ', (^{o})	Sand Relative Density, D_R, (%)	Eff. Ov. Pressure, p, (tsf)	FAILURE LOADS (tons) Total Q_u	Point Q_p	Side Q_s	References
TAVENAS	H-1	"H" pile "12BP73" of equivalent diameter B = 1.14 ft	0	Loose crushed stone until 16 ft. Below 16 ft: medium to fine uniform sand, SP.	32	45	0.340	76	16[a]	19[a]	(48)
			19		34	60	0.582				
	H-2		0		33	50	0.477	68	38[a]	30[a]	
			29		34	60	0.895				
	H-3		0		33	50	0.624	112	60[a]	52[a]	
			39		34	60	1.208				
	H-4		0		33	55	0.775	125	65[a]	60[a]	
			49		34	60	1.521				
	H-5		0		33	55	0.928	150	74[a]	76[a]	
			59		34	60	1.834				
	J-1	Precast hexagonal concrete pile (Hercules H-800), of eq.diam. B=1.05 ft	0		32	40	0.327	50	41[a]	9[a]	
			18		34	60	0.551				
	J-2		0		33	50	0.463	75	42[a]	33[a]	
			28		34	60	0.864				
	J-3		0		33	50	0.609	100	55[a]	45[a]	
			38		34	60	1.177				

TABLE 3 - Continued

Pile Test		Pile Description	Pile Penetration (ft)	Soil Description	Sand Friction Angle, ϕ', (^{o})	Sand Relative Density, D_R, (%)	Eff. Ov. Pressure, p, (tsf)	FAILURE LOADS (tons) Total Q_u	Point Q_p	Side Q_s	References
TAVENAS	J-4	Precast hex. concrete pile, (Herc. H-800), eq. diameter: B = 1.05 ft	0	Loose crushed stone until 16 ft. Below 16 ft: medium to fine uniform sand, SP.	33	55	0.760	125	57[a]	68[a]	(48)
			48		34	60	1.490				
	J-5		0		33	55	0.944	150	62[a]	88[a]	
			60		34	60	1.865				
COYLE	C. CHRISTI	Precast sq. concrete (16"x16") B = 1.5 ft	0	Fine sand, SP	27	15	0.285	168	123[a]	45[a]	(12)
			8	Fine silty sand, SP & SM	31	50	0.645				
			28.5		37	75	0.940				
			Aver.		30	45	0.554				

* Pressure at bottom of silt layer.

[a] Unadjusted compression test.

[b] Adjusted compression test.

[c] Compression/tension test

[c1] Tension in sand layer.

† Driven by vibratory hammer.

B = Pile diameter or diameter of the circle of same pile area.

Note: 1 in = 2.54 cm; 1 ft = 0.305 m; 1 tsf = 95.76 kN/m^2; 1 ton = 8.90 kN.

TABLE 4 - BEARING CAPACITY FACTORS FROM FIELD TESTS

Pile Test		$\frac{D}{B}$	$\frac{p\ D^{\dagger}}{\gamma_w B^2}$	UNADJUSTED COMPRESSION TESTS						COMPRESSION/TENSION TESTS					
				q_o (tsf)	N_q	f_s (tsf)	Ktanδ	K ($\delta=\phi'_{res}$)	K ($\delta=0.8\phi'$)	q_o (tsf)	N_q	f_s (tsf)	Ktanδ	K ($\delta=\phi'_{res}$)	K ($\delta=0.8\phi'$)
ARKANSAS	# 1 O	22.2	915			0.590	0.762	1.50	1.54			0.442 .414[a]	0.571 .535[a]	1.12 1.05[a]	1.15 1.08[a]
		44.3	1,867	49.0	31.0					80.6 86.7[a]	51.0 54.9[a]				
	# 2 O	17.6	288			0.627	0.819	1.61	1.65			0.399 .466[a]	0.521 .608[a]	1.02 1.19[a]	1.05 1.22[a]
		35.2	1,158	47.2	30.6					81.8 75.5[a]	53.1 49.0[a]				
	# 3 O	15.6	228			0.473	0.611	1.20	1.23			0.388 .317[a]	0.501 .410[a]	0.98 0.80[a]	1.01 0.83[a]
		31.2	926	49.3	31.3					67.0 70.5[a]	42.5 44.8[a]				
	# 10 ●	18.5	322			0.479	0.626	1.23	1.26			0.390 .489[a]	0.510 .457[a]	1.00 0.90[a]	1.03 0.92[a]
		37	1,300	44.7	28.9					83.0 50.3[a]	53.8 32.6[a]				
	# 4 □	13	170									0.445	0.750	1.41	1.57
		27	678							58.5	49.4				
	# 6 ⊞	15	206			0.721	1.25	2.35	2.52						
		30	835	32.9	28.1										

TABLE 4 - Continued

Pile Test		B/D	$\frac{p\,D^{\dagger}}{\gamma_w B^2}$	UNADJUSTED COMPRESSION TESTS						COMPRESSION/TENSION TESTS					
				q_o (tsf)	N_q	f_s (tsf)	Ktanδ	K ($\delta=\phi'_{res}$)	K ($\delta=0.8\phi'$)	q_o (tsf)	N_q	f_s (tsf)	Ktanδ	K ($\delta=\phi'_{res}$)	K ($\delta=0.8\phi'$)
ARKANSAS	# 7 ⊞	19.5	352			0.628	0.830	1.63	1.73			0.275	0.363	0.71	0.76
												.526[a]	.695[a]	1.36	1.45
		39	1,425	47.1	30.7					127.0	82.8				
										65.2[a]	42.6[a]				
	# 9 ⊞	20	370			0.842	1.080	2.12	2.10						
		40	1,509	27.1	17.1										
JONESVILLE	# 1 ◧	11	157									0.570	0.765	1.44	1.30
		22	625							124.0	83.9				
	# 2 ◧	13	213									0.556	0.650	1.22	1.11
		26	850							84.4	49.6				
	# 3 ◧	16	299									0.401	0.401	0.75	0.68
		32	1,195							116.0	57.9				
LOW - SILL	# 2 ◑	32	955									0.963	0.596	1.08	1.08
		37	1,347							69.0	34.9				
	# 4 ◑	40	1,479									1.620	0.993	1.79	1.81
		47	2,112							124.0	61.5				
	# 6 ◑	36	1,189									1.070	0.665	1.20	1.21
		41	1,643							77.0	39.1				
	# 3 ■	53	2,405												
		61	3,474							105.0	50.0				

TABLE 4 - Continued

Pile Test		$\frac{D}{B}$	$\frac{p\,D^{\dagger}}{\gamma_w B^2}$	UNADJUSTED COMPRESSION TESTS						COMPRESSION/TENSION TESTS					
				q_o (tsf)	N_q	f_s (tsf)	Ktanδ	K ($\delta=\phi'_{res}$)	K ($\delta=0.8\phi'$)	q_o (tsf)	N_q	f_s (tsf)	Ktanδ	K ($\delta=\phi'_{res}$)	K ($\delta=0.8\phi'$)
VESIĆ	H-11 ●	3.3 6.6	16.3 59.9	34.5	81.4	0.321	1.400	2.86	2.81						
	H-12 ●	6.7 13.4	58.6 216	97.9	130.0	0.624	1.520	2.99	2.86						
	H-13 ●	9.7 19.4	116 434	120.0	115.0	0.620	1.110	2.00	2.08						
	H-14 ●	13.0 26.0	203 782	121	86.7	0.718	0.990	1.79	1.80			0.745	0.836	1.51	1.47
	H-15 ●	16.5 33.0	313 1,203	146	85.1	0.702	0.788	1.42	1.39	140	81.6	0.745	0.836	1.51	1.47
	H-2 ■	16.5 33	313 1,269	97	54.5	0.491	0.551	0.99	1.11						
GREGERSEN	# A ●	14 28	244 975	10	10.2	0.306	0.622	1.10	1.40	28	28.5	0.145	0.295	0.52	0.66
	#D/A ●	28.5 57	906 3,622	18	9.9	0.277	0.304	0.49	0.68	37	20.3	0.197	0.216	0.35	0.49
TAVENAS	H-1 ⊠	8.5 17	80 272	16	27.5	0.247	0.726	1.28	1.52						
	H-2 ⊠	12.5 25	171 640	37	41.3	0.255	0.535	0.89	1.08						

TABLE 4 - Continued

Pile Test		D/B	$\frac{p\ D^{\dagger}}{\gamma_w B^2}$	UNADJUSTED COMPRESSION TESTS						COMPRESSION/TENSION TESTS					
				q_o (tsf)	N_q	f_s (tsf)	Ktanδ	K ($\delta=\phi'_{res}$)	K ($\delta=0.8\phi'$)	q_o (tsf)	N_q	f_s (tsf)	Ktanδ	K ($\delta=\phi'_{res}$)	K ($\delta=0.8\phi'$)
TAVENAS	H-3 ■	17.0	300			0.329	0.527	0.91	1.06						
		34.0	1,162	58	48.0										
	H-4 ■	21.5	468			0.302	0.390	0.68	0.79						
		43	1,838	63	41.4										
	H-5 ■	26	675			0.318	0.343	0.59	0.69						
		52	2,669	72	39.3										
	J-1 ○	8.5	86			0.143	0.437	0.70	0.91						
		17	288	48	87.1										
	J-2 ○	13.5	188			0.337	0.728	1.21	1.47						
		27	703	49	56.7										
	J-3 ○	18	336			0.338	0.555	0.96	1.12						
		36	1,300	64	54.4										
	J-4 ○	23	530			0.405	0.533	0.92	1.07						
		46	2,079	66	44.3										
	J-5 ○	28.5	823			0.419	0.444	0.77	0.89						
		57	3,253	72	38.6										
COYLE ◪		11.2	112			0.297	0.536	1.05	1.20						
C.Christi		22.3	382	69.2	73.6										

† See Appendix I for explanation of terms.

[a] Adjusted compression test data.

Note: 1 tsf = 95.76 kN/m^2.

creating planes of weakness which could explain the reduction in capacity. For this reason only the shortest pile, "Jonesville #1" was used for correlation purposes.

The "Vesic" piles H-11 to H-15 were actually only one pile which was tested in increments of approximately 10 ft (3 m). The shortest penetration test was designated H-11 and so on until the maximum penetration of approximately 50 ft (15 m) which was designated H-15. The erratic nature of upper soil deposits (down to 12 ft (3.5 m) approximately) at the site, with occasional presence of very soft highly plastic clay and denser spots of sand did not warrant confidence in evaluating the soil properties. Only the deepest penetration, H-15, along with pile H-2 were used for correlation purposes.

The "Low-Sill" piles were tested on a site overlayed by a silt stratum of about 50 ft (15 m) in thickness. All measurements given refer to the underlying sand stratum, with silt influencing only the effective overburden pressure and depth of penetration. Meyerhof (37) suggests that, in layered soils, a penetration of about ten pile diameters in one stratum is enough to mask the influence of the thickness and strength of the upper layer.

The "Tavenas" test pile included two pile types, each type tested at five different penetrations. The "H" piles carried less load than the concrete pile down to a depth of about 15 ft (4.5 m). Below 15 ft (4.5 m) the load carried by both piles was about the same. Therefore, the use of the outer perimeter of the H-pile in defining its cross section was warranted. In addition, the work of Klos and Tejchman (27), with model pipe piles in the laboratory, showed that the ultimate

capacity of open pipes tends to be the same as closed pipes particularly at penetrations greater than about 20 pile diameters.

The "Gregersen" piles also represent tests made on the same pile, at different penetrations. The driving residual stresses were analysed and the measured loads adjusted (18). However the method of adjustment was different from that presented by Hunter and Davisson (21). This last method would yield larger adjusted point load.

Comparison Between Field Data and Theory

Before an attempt is made to develop improved correlations for calculating bearing capacity it is important to show that there is a need for improved correlations. To do this bearing capacity factors and parameters obtained from field pile test data will be compared with corresponding values obtained using existing theories.

In order to verify the suggestion presented previously (20) that the pull-out resistance of a pile is equal to the adjusted compressive side resistance, the K-values presented in Table 5 were evaluated. For these "Arkansas" piles (15) the average values of the lateral earth pressure coefficient, K (with δ taken as 0.8 ϕ') were evaluated for the unadjusted compression tests, the adjusted compression tests, and the tension tests. A fourth set of K-values was determined by arbitrarily multiplying the unadjusted values by 0.7. This fourth set of K-values represents a suggested empirical determination of side resistance (33) for tension tests. As shown in Table 5 these values compare well with field measured tension values and even better with the adjusted values. This reinforces the idea that the side resistance obtained in a tension

TABLE 5. - COMPARISON OF "K" FROM PILE TESTS

Test		K				K Deviation* from 0.7 Unadj. (%)	
		Unadj.	Adjust.	Tension	0.7 of Unadj.	Adjust.	Tension
Arkansas	#1	1.54	1.08	1.15	1.08	0.0	+ 6.5
	#2	1.65	1.22	1.05	1.16	+ 5.2	- 9.5
	#3	1.23	0.83	1.01	0.86	- 3.5	+ 17.4
	#10	1.26	0.92	1.03	0.88	+ 4.5	+ 17.0
					Average, $\overline{D}$	+ 1.6	+ 7.9
					Std. Deviation	4.1	12.6

* Deviation = $D_i = \frac{K - K_{0.7}}{K_{0.7}} \times 100$

Std. Deviation = $\sqrt{\frac{\sum_{1}^{n} (D_i - \overline{D})^2}{n - 1}}$

test is equal to the side resistance obtained from an adjusted compression test.

The comparison of N_q-values obtained from field test data and theories are given in Fig. 13. Curves are plotted for the better known theories, covering a wide range of possible N_q-values. Also, the N_q-values obtained from field test data are plotted for each type of field test (unadjusted compression, adjusted compression, and compression/tension).

Fig. 13a, for the unadjusted compression tests, shows clearly that none of the theories is able to present consistently a fair prediction of the N_q-values. The "Tavenas" hexagonal pile results prove that the influence of depth is very important in the sense that as D/B increases the N_q-value decreases. Even though the Terzaghi General Shear Theory is favored the measured N_q-values deviate from the theory by as much as $\pm$ 100%.

Fig. 13b, for the compression/tension tests, shows a marked reduction in scatter for the favored Terzaghi General Shear Theory. Even though this better fit leaves considerable margin for improvement, a clear advantage of this method over the unadjusted method is indicated. In Fig. 13c the amount and range of data for the adjusted compression tests is not enough for a reasonable evaluation. The limited data favors, but not conclusively the Terzaghi General Shear Theory.

As a result of the evaluation of the data presented in Fig. 13, it can be concluded that when theoretical predictions are compared with actual field measurements, clear disagreements arise. Also, it appears that the depth to diameter ratio has a marked influence on the magnitude

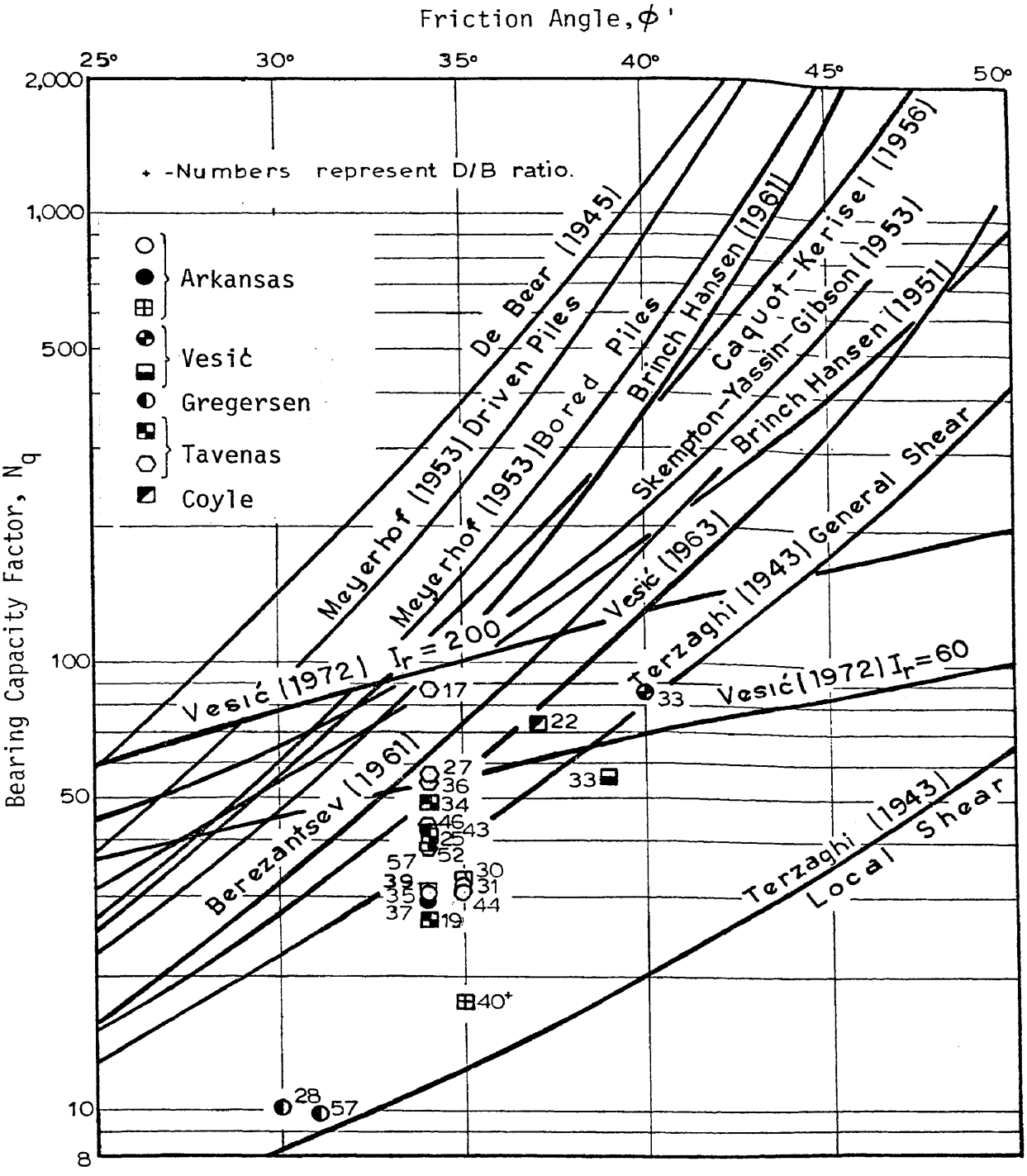

(a) Unadjusted Compression Tests

FIG. 13 - BEARING CAPACITY FACTOR, N_q (54, 58)

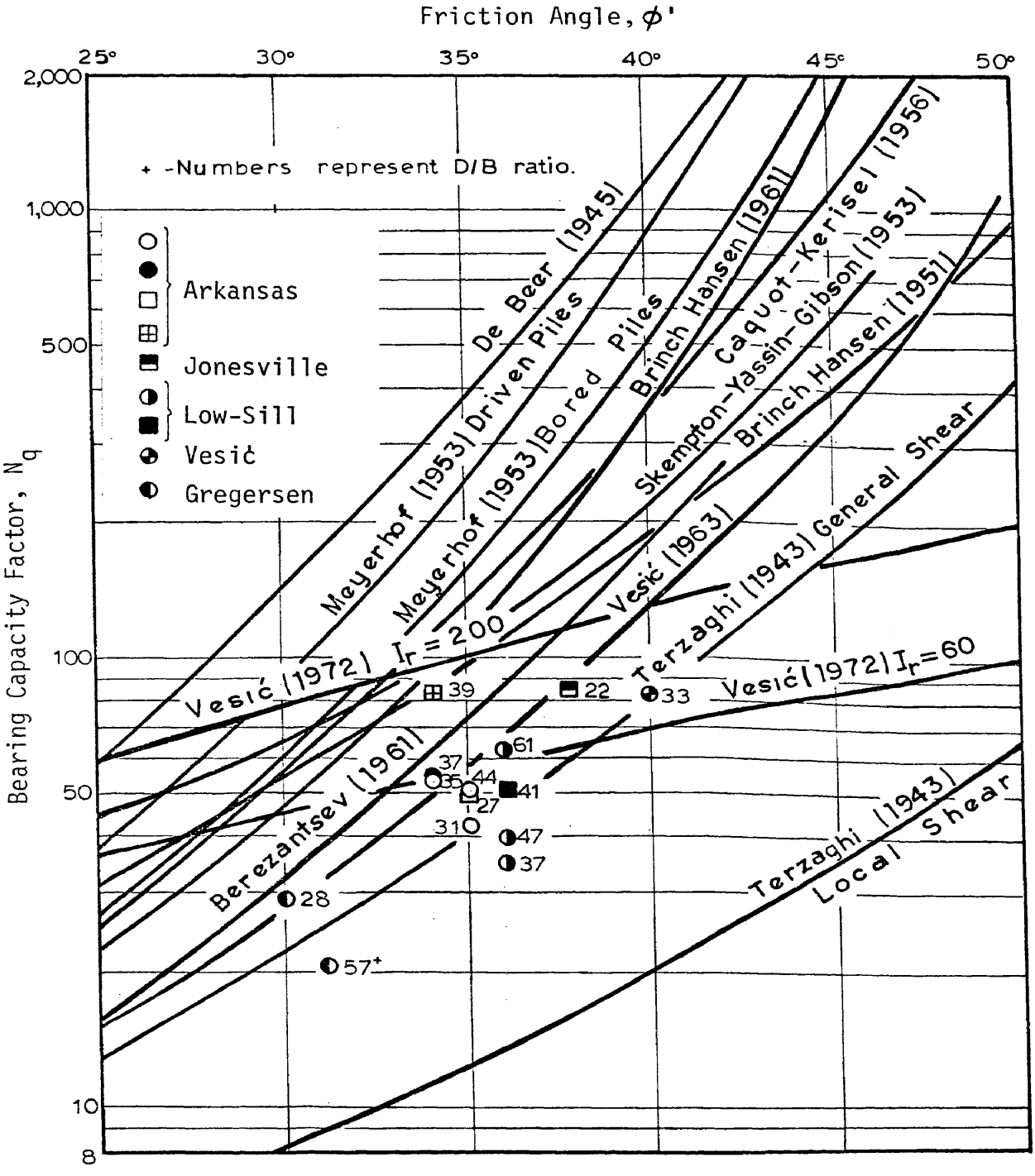

(b) Compression/Tension Tests

FIG. 13 - Continued

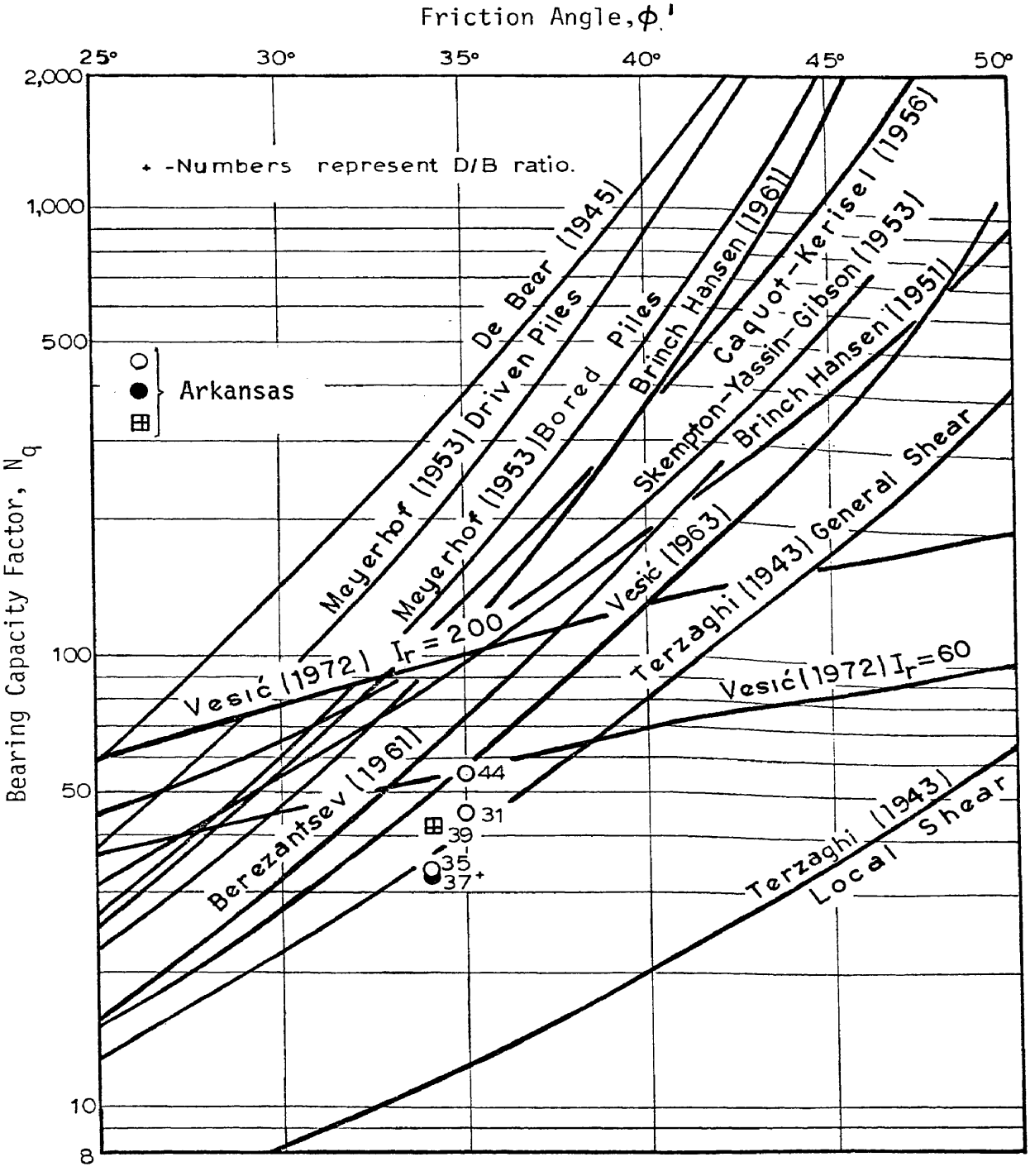

(c) Adjusted Compression Tests

FIG. 13 - Continued

of N_q.

For the past several years at Texas A&M University (13) pile load test data have been used to evaluate the earth pressure coefficient, K. It has been found that the magnitude of K varies with depth. Fig. 14 shows the typical variation of K with depth. Indications are that the magnitude of K near the surface approaches the passive earth pressure coefficient, and near the pile point the magnitude of K approaches the active earth pressure coefficient. When this distribution is compared with proposed values found in the literature, as presented in Table 2 (page 18), it is concluded that all values are possible, depending on the depth of pile penetration. A correlation of the type illustrated in Fig. 14 could be extended to include the appropriate soil parameters such as friction angle and relative density.

This brief comparison between field data and theories or factors currently used in the determination of pile bearing capacity, shows that all significant parameters are not considered. Despite the wide variation of suggested and theoretical values of N_q and K all values may be correct depending on the depth of pile penetration. It is no wonder that well known authorities in pile design (36, 58) are unanimous in suggesting pile load tests as the only reliable method of determining bearing capacity.

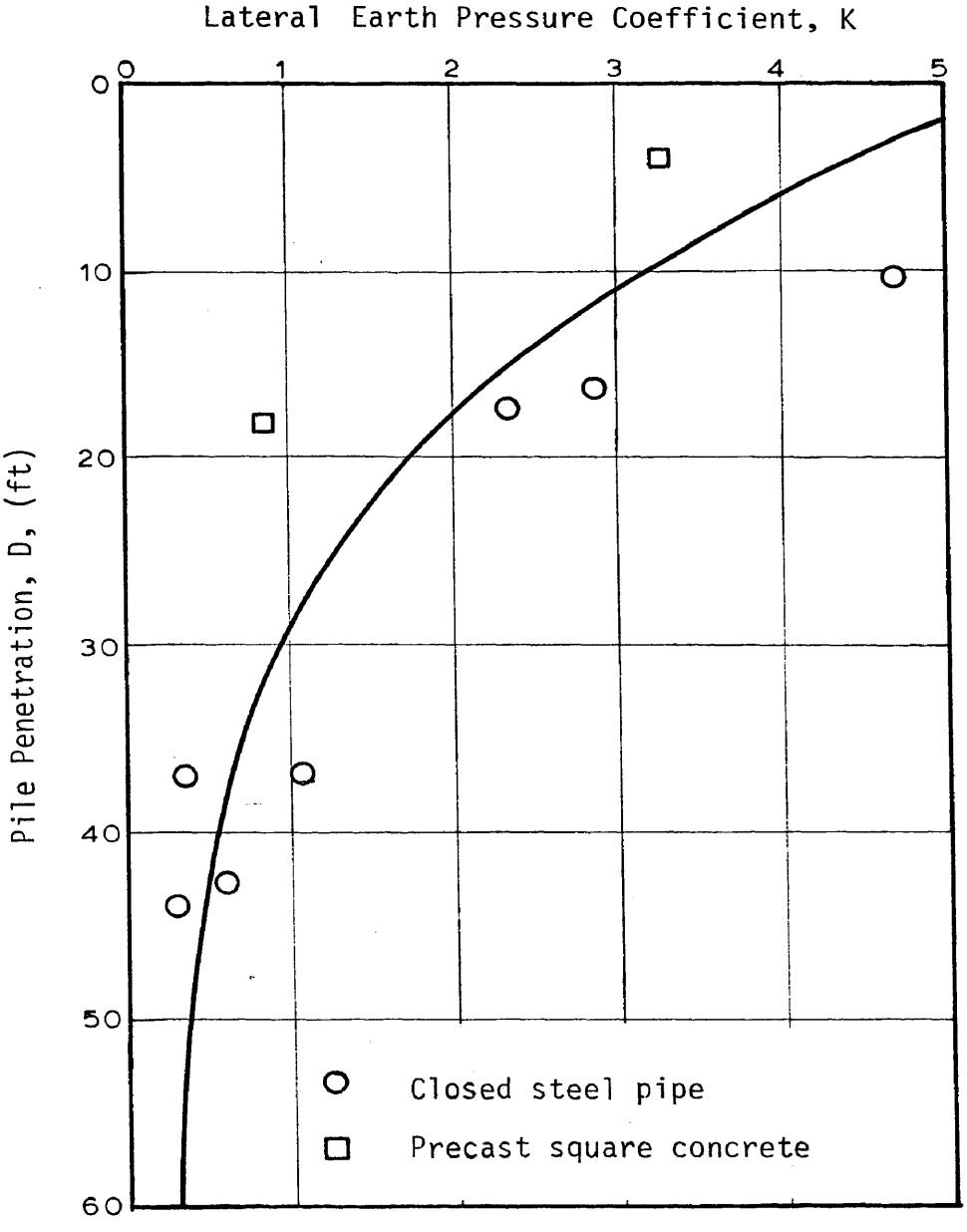

FIG. 14 - K VS PILE PENETRATION (1 ft = 0.305 m); (13)

CORRELATIONS OF BEARING CAPACITY FACTORS

Bearing Capacity Factors and Significant Parameters

Thus far in this study, an effort has been made to identify and discuss the significant parameters that influence the bearing capacity factors used to determine the ultimate capacity of piles in sand. As previously determined, the list of parameters includes:

a) effective overburden pressure (related to depth);

b) soil displacement (related to pile diameter or the diameter of a circle with the same area as the pile cross section); and

c) sand relative density and/or friction angle.

In addition, field load test data have been presented and used to evaluate bearing capacity factors, to establish pile parameters, and to determine the appropriate sand properties. The bearing capacity factors which have been evaluated include:

a) the unit point resistance, q_o;

b) the bearing capacity factor N_q;

c) the unit side resistance, f_s;

d) the combined factor K tan δ; and

e) the lateral earth pressure coefficient, K, determined using δ equal to both the residual friction angle of the sand and equal to 0.8 times the peak friction angle of the sand.

According to the Static Method of determining pile bearing capacity (see Eq. 3a, page 7, and Eq. 10, page 13) the unit resistances, q_o and f_s, are functions of mutually independent factors: N_q, K, tan δ and effective pressure. Consequently, the bearing capacity factors can be

evaluated separately from the overburden pressure or depth. However, experimental investigations have indicated that the bearing capacity factors K and N_q are dependent upon overburden pressure or depth. As a result, there is not a strong justification for the individual determination of N_q or K. Even so, in order to enhance the understanding of pile soil interaction, these factors are also included in the correlations in this study.

The field load test data were used in the development of new correlations which relate the bearing capacity factors to pile geometry parameters and sand properties. A number of different combinations of pile parameters and sand properties were investigated during the development of these correlations. However, the correlations presented are considered the simplest and best for practical usage. A correlation was developed for each method of interpreting pile load tests: unadjusted compression, adjusted compression, and compression/tension.

The parameters which yielded the best correlations were either the depth to diameter ratio, D/B, or a more involved parameter which includes the effective overburden pressure, depth of pile penetration, and the pile diameter squared. The unit weight of water was also included with the sole purpose of making the parameter non-dimensional. As indicated previously, an investigation of the influence of the depth of pile penetration and effective overburden pressure requires the use of surcharges or submerged and nonsubmerged soils. Since for this study the location of the ground water table at all sites dictated the use of submerged soil and no surcharges were present, this type of investigation could not be made. The simpler parameter D/B was used for all

correlations. Identical correlations were developed for the effective pressure dependent parameter and are presented in Appendix I.

As noted by Robinsky, Sagar and Morrison (43) the shape of the curve of unit side resistance is constantly changing with pile penetration. The maximum and minimum values of unit side resistance change positions as the pile penetrates. If the unit side resistance is determined from individual strain-gages, for pile segments, there is considerable scatter with no indication of a well defined trend. This is illustrated in Fig. 15a, for the "Vesic" unadjusted pile tests. On the other hand, if average values of unit side resistance, along the whole pile, are plotted, as in Fig. 15b, a reasonable trend is indicated. For this study all unit side resistances were averaged along the whole pile length.

Unadjusted Compression Tests

The best correlations for the unadjusted compression tests are shown in Figs. 16 through 21. Fig. 16 shows the plot of unit point resistance, q_o, versus relative depth (point depth to diameter ratio). A marked increase in unit point resistance with increasing friction angle (or increasing relative density) is indicated. Despite some scatter, it is possible to develop well defined curves for $\phi' = 30^o$ (very loose sand) and for $\phi' = 34^o$ (medium to dense sand). By extrapolating the rate of increase and the shape of the curves, it is also possible to develop curves for $\phi' = 37^o$ (dense sands) and $\phi' = 39^o$ (very dense sands). The other curves were developed by interpolation. Even though the rate of increase in unit point resistance is sharply

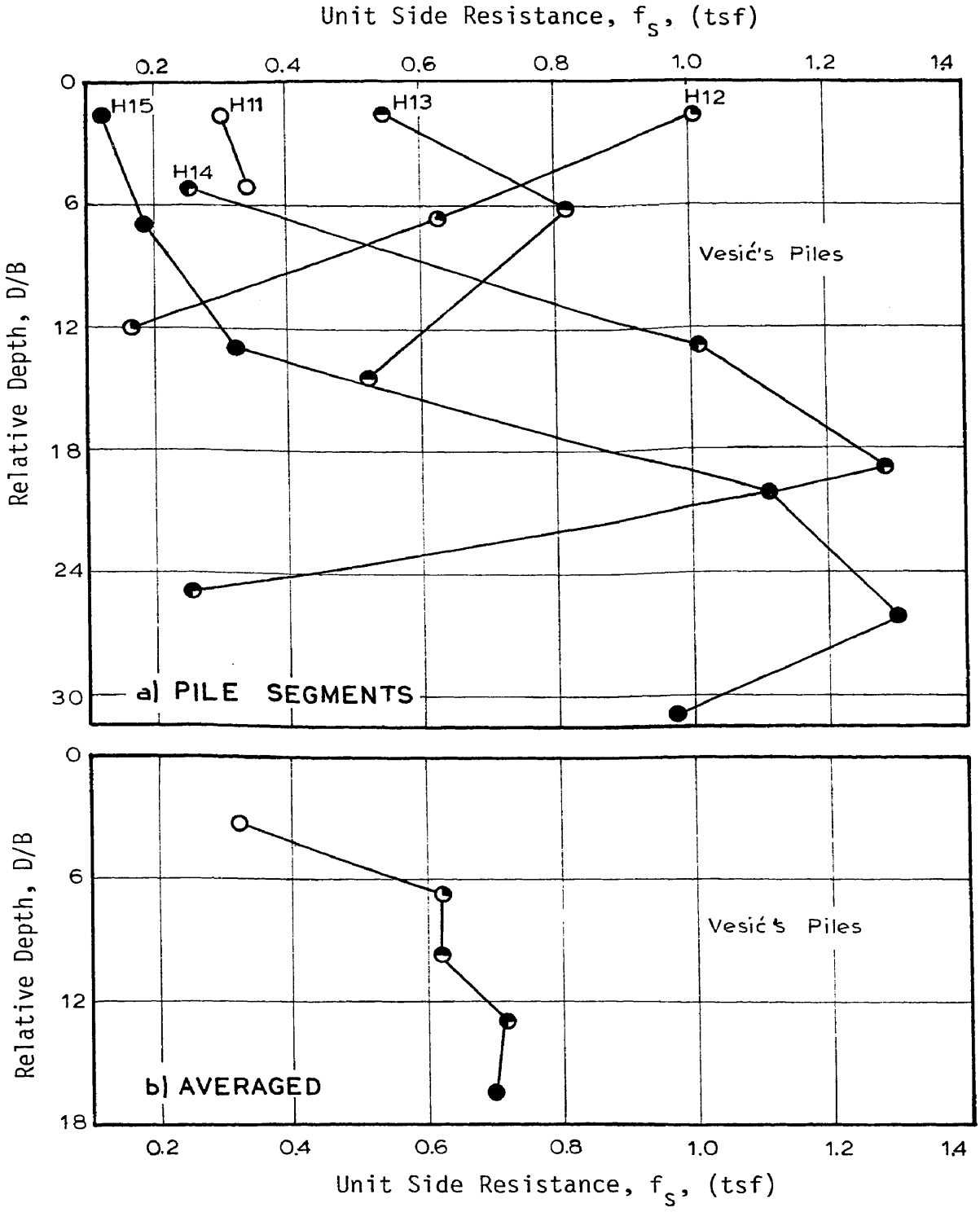

FIG. 15 - DISTRIBUTION OF UNIT SIDE RESISTANCE (1 tsf = 95.76 kN/m^2)

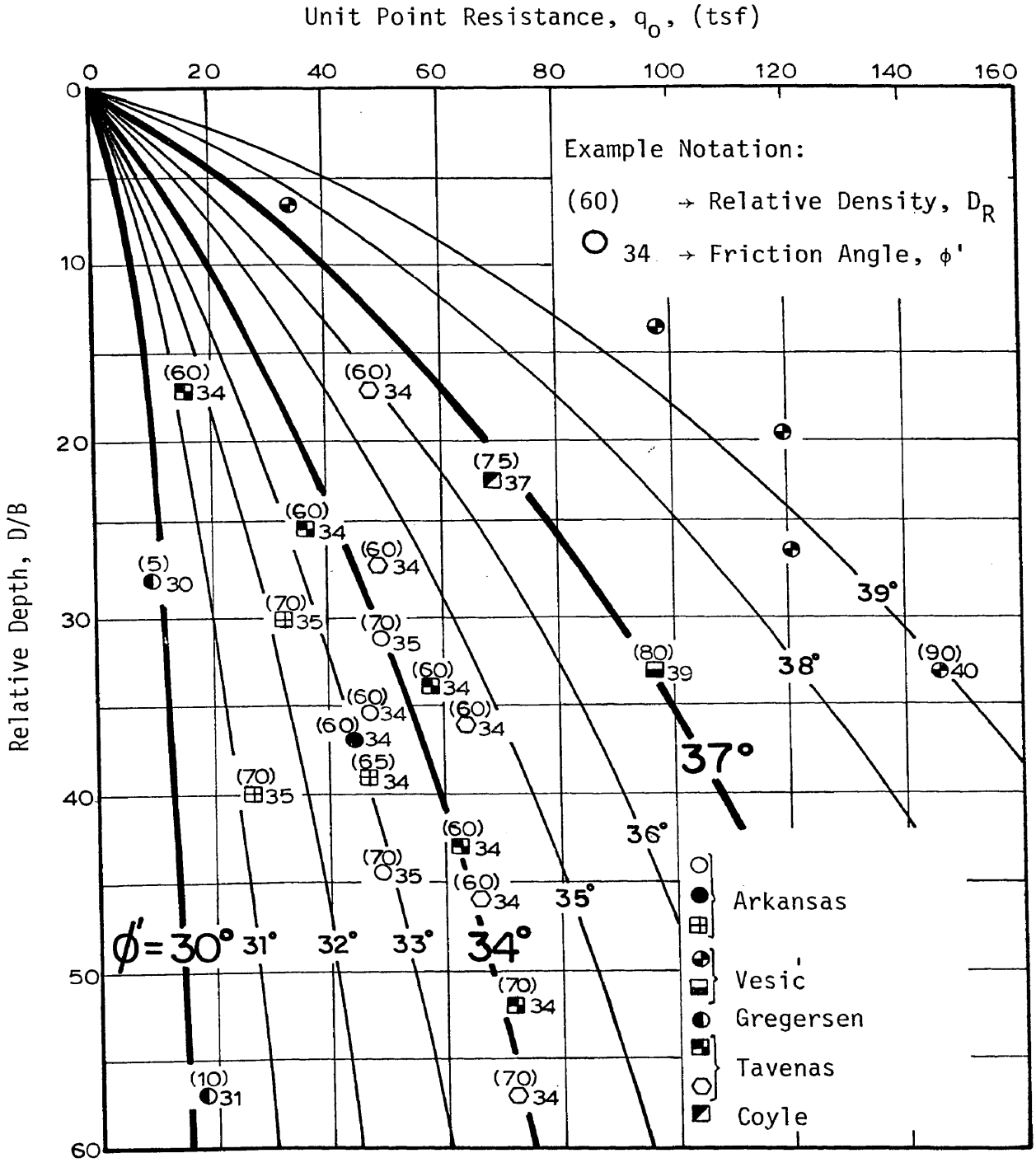

FIG. 16 - q_o VS D/B - UNADJUSTED COMPRESSION (1 tsf = 95.8 kN/m^2)

decreased with increasing relative depth, it can be seen that a constant value of q_o is not achieved even at a depth of about sixty pile diameters. For the looser sands it is observed that at depths below ten to fifteen pile diameters a nearly linear relationship exists between relative depth and unit point resistance. For the denser sands because of lack of data at the greater relative depths, the same observation cannot be made.

Fig. 17 shows a plot of the bearing capacity factor, N_q, (plotted on a log scale), versus relative depth. In general, the N_q values increase with increasing friction angle (and increasing relative density). The data permitted the development of curves for $\phi' = 30^o$ (very loose sand), $\phi' = 34^o$, and $\phi' = 36^o$ (medium to dense sand). The other curves were developed using extrapolation and interpolation. These curves are extended to zero penetration (shallow foundations) in accordance with the shapes of similar curves determined experimentally (37, 58) and the values of N_q for zero penetration were obtained using Terzaghi's theory. It can be seen that the N_q values increase from zero penetration to a maximum value at roughly ten pile diameters for loose sands and twenty-five diameters for dense sands. At deeper penetrations the N_q values seem to decrease linearly with depth.

Fig. 18 presents the plot of the unit side resistance versus relative depth. In this case, the depth was taken as the average depth which is defined by the mid-point of the pile segment being analysed. Even though there is considerable scatter, a definite increase in side resistance occurs for increasing friction angle (or increasing relative density). Three fairly well defined curves are developed: one curve

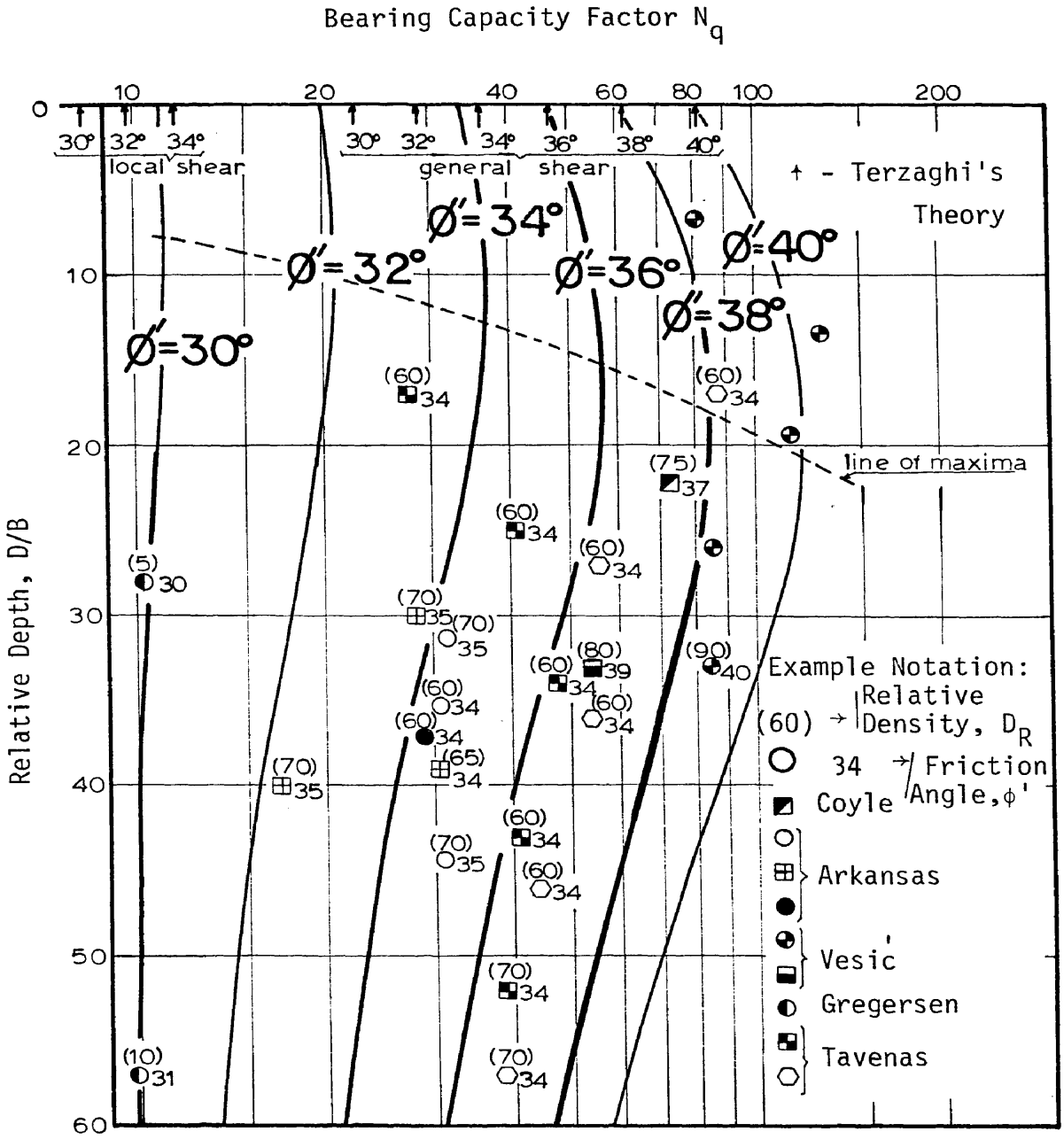

FIG. 17 - N_q VS D/B - UNADJUSTED COMPRESSION

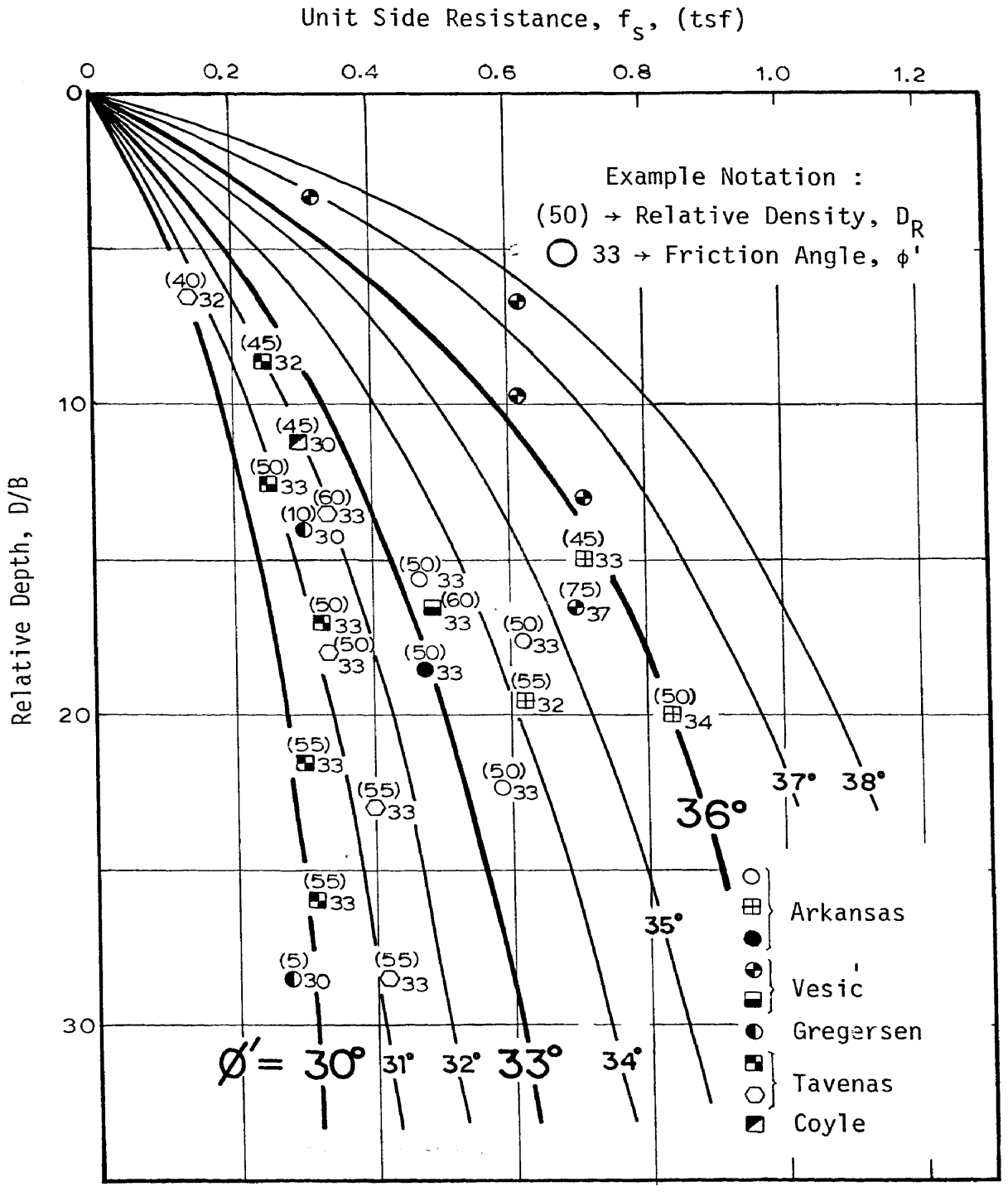

FIG. 18 - f_s VS D/B - UNADJUSTED COMPRESSION (1 tsf = 95.76 kN/m^2)

for $\phi' = 30^{o}$ (very loose sand); another for $\phi' = 33^{o}$ (medium dense sand); and a third for $\phi' = 36^{o}$ (dense sands). The other curves are interpolated. The rate of increase in f_s with depth is reduced considerably below approximately ten pile diameters for loose sands and twenty-five pile diameters for dense sands, and a constant value of f_s is not indicated.

Fig. 19 shows the plot of the combined factor K tan δ (plotted on a log scale) versus the relative depth. Figs. 20 and 21 present the plots of the lateral earth pressure coefficient, K (plotted on a log scale) versus relative depth. In Fig. 20 "δ" was taken as being equal to the residual friction angle of the sand, and in Fig. 21 "δ" was taken as 0.8 times the peak friction angle of the sand. The correlation developed in Fig. 19 was accomplished without having to evaluate "δ". The correlations developed in Figs. 20 and 21 were accomplished in order to investigate any differences resulting from the two methods used to evaluate "δ". It is apparent that the trends are the same for all three correlations. Despite some scatter, a family of straight lines are indicated for increasing friction angle (or increasing relative density). Equations for each basic curve are presented for each correlation. It should be noted that the K values are larger (closer to passive values) at shallow penetrations and tend to decrease (approach active values) as the relative depth increases.

Compression/Tension Tests

The correlations for the compression/tension tests are presented in Figs. 22 through 27. These correlations for the compression/tension tests are presented in the same manner as the unadjusted compression

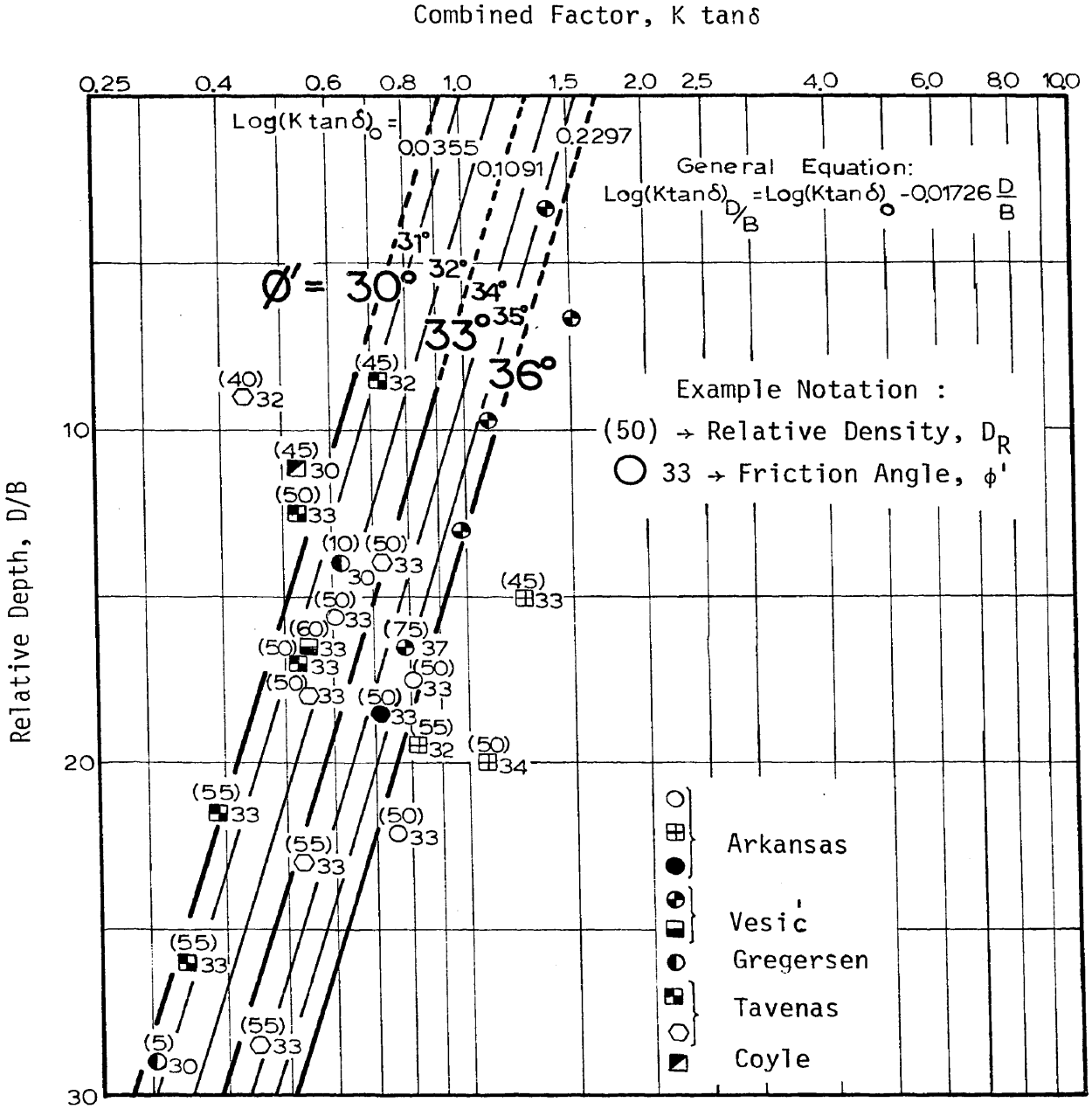

FIG. 19 - K tanδ VS D/B - UNADJUSTED COMPRESSION

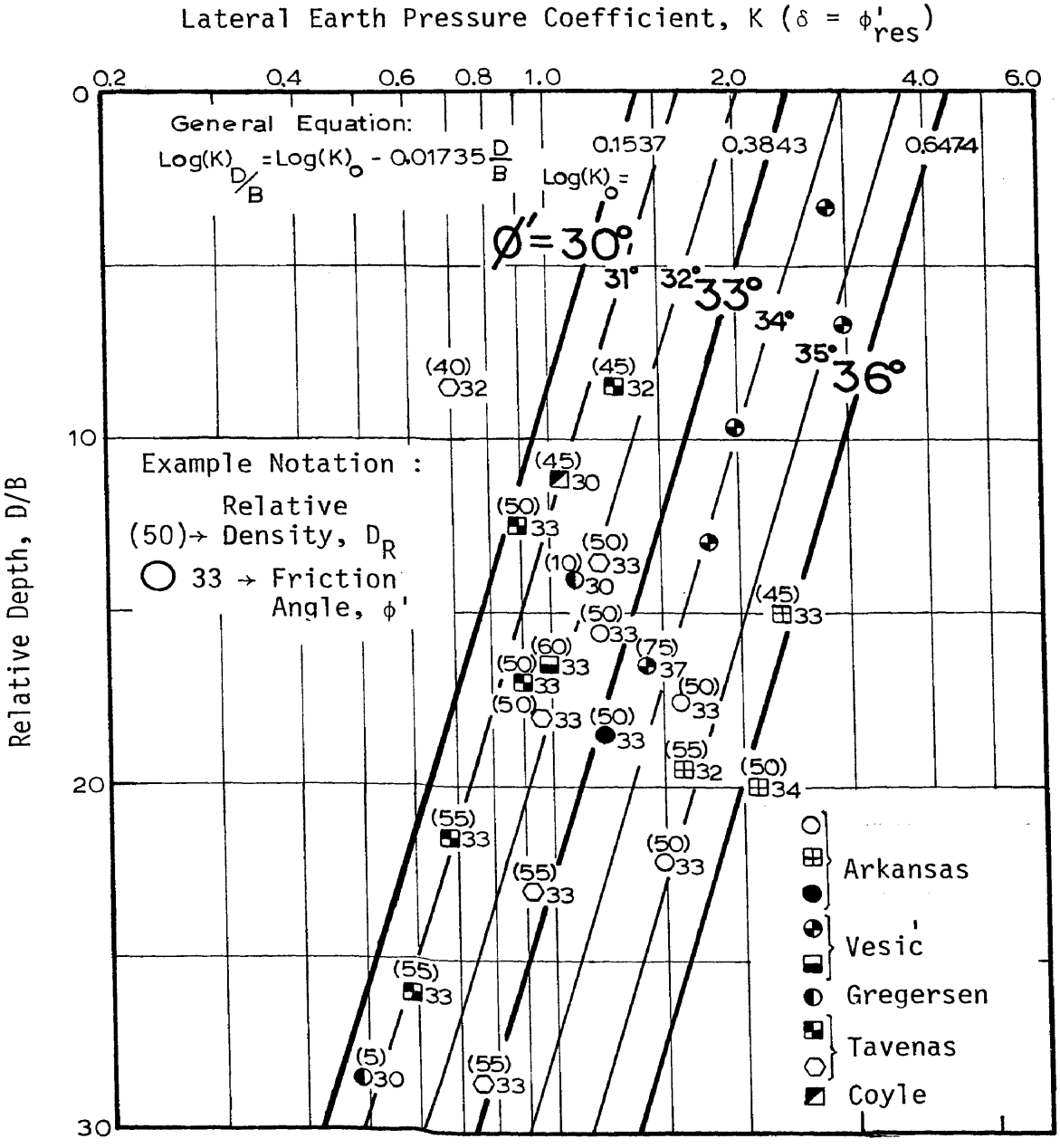

FIG. 20 - K ($\delta = \phi'_{res}$) VS D/B - UNADJUSTED COMPRESSION

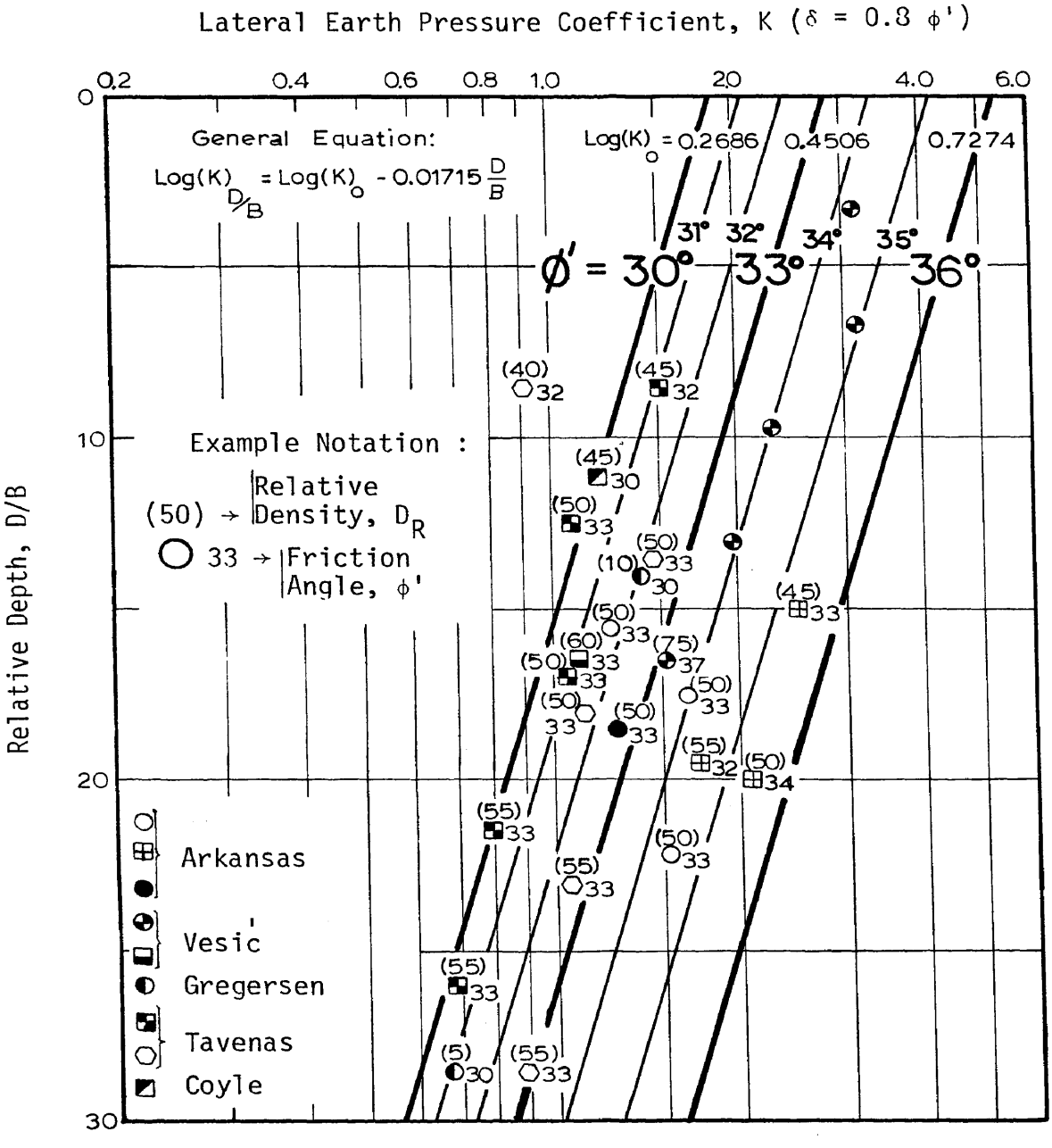

FIG. 21 - K (δ = 0.8 φ') VS D/B - UNADJUSTED COMPRESSION

tests.

Fig. 22 presents the plot of unit point resistance, q_o, versus relative depth. The influence of friction angle (or relative density) is clearly defined in that higher friction angles (or relative densities) indicate higher unit point resistances. In this case the influence of the friction angle, as compared to the relative density, is dominant. With minimal scatter, curves are developed for $\phi' = 30^o$ (very loose sands), $\phi' = 35^o$ (dense sands), and $\phi' = 38^o$ (very dense sands). The other curves were developed by interpolation and extrapolation. At sixty pile diameters of penetration, q_o, has not reached a constant value. A reduced rate of increase is indicated below fifteen pile diameters of penetration for loose sands and below approximately thirty pile diameters for denser sands. Below these critical depths the relationship between q_o and relative depth is nearly linear.

Fig. 23 is a plot of the bearing factor N_q, (plotted on a log scale) versus relative depth. This correlation is similar to the correlation developed for the unadjusted compression tests. The main difference occurs at the extension of the curves for zero penetration using Terzaghi's theory. For the unadjusted tests, the curves fit better at values between the general shear and localized shear cases (principally for the lower friction angles). For the compression/tension tests, agreement with the general shear case seems more appropriate.

Fig. 24 shows the plot of the unit side resistance, f_s, versus relative depth (mid-point depth of pile segment being analysed). The same effect of increasing side resistance with increasing friction angle (or

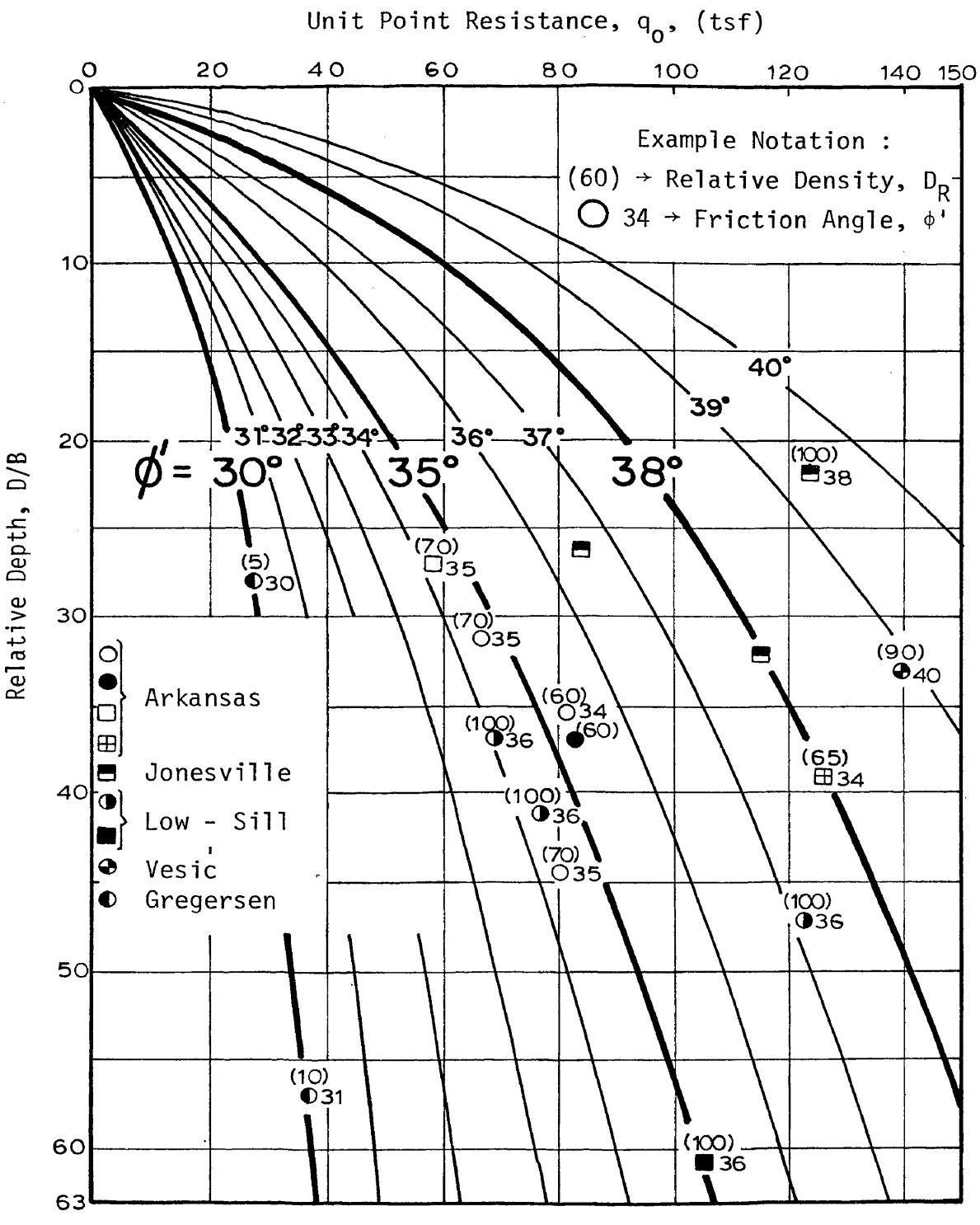

FIG. 22 - q_o VS D/B - COMPRESSION/TENSION (1 tsf = 95.76 kN/m^2)

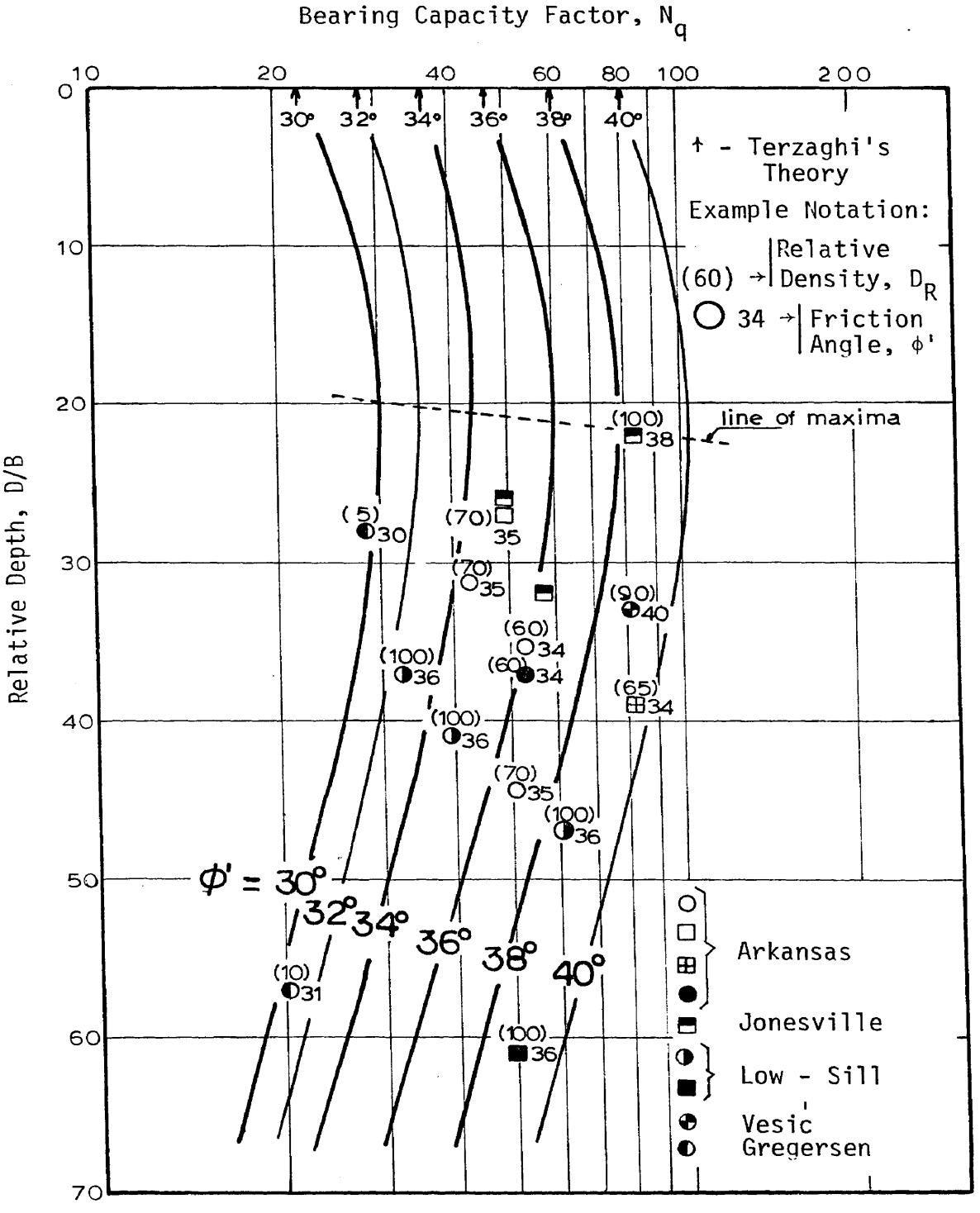

FIG. 23 - N_q VS D/B - COMPRESSION/TENSION

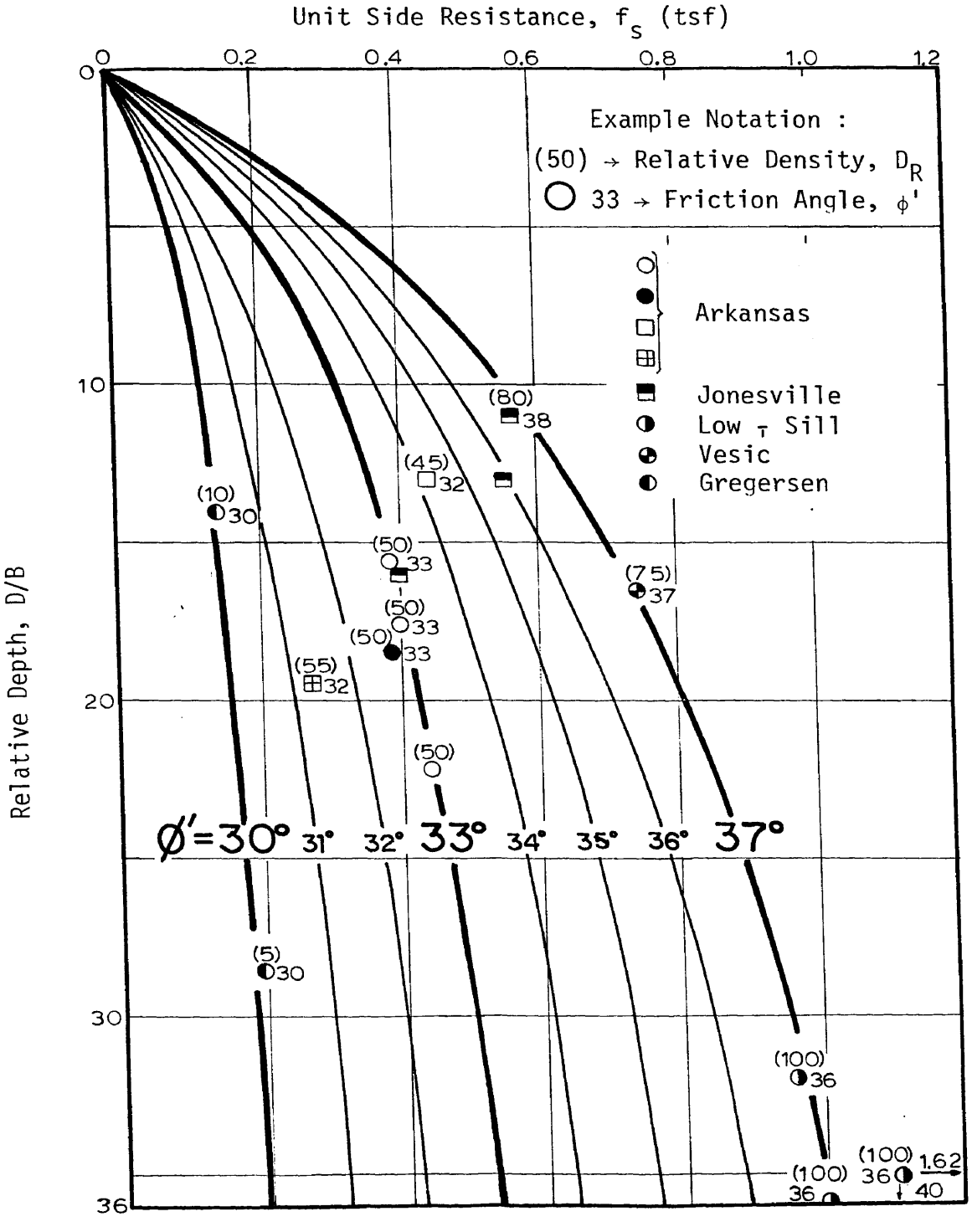

FIG. 24 - f_s VS D/B - COMPRESSION/TENSION (1 tsf = 95.76 kN/m^2)

increasing relative density) is indicated. Three well defined curves are developed: one curve for $\phi' = 30^{o}$ (very loose sand); another for $\phi' = 33^{o}$ (medium dense sand); and a third for $\phi' = 37^{o}$ (dense to very dense sands). Below approximately ten pile diameters of penetration for the loose sands a practically linear relationship between f_s and relative depth is indicated. A similar relationship is suggested for denser sands, at deeper penetrations.

Figs. 25 shows the plot of the combined factor K tan δ (plotted on a log scale) versus the relative depth. Figs. 26 and 27 present the lateral earth pressure coefficient K (plotted on a log scale) versus relative depth. The coefficient K was determined using "δ" equal to the residual friction angle of the sand (in Fig. 26) and using "δ" equal to 0.8 times the peak friction angle (in Fig. 27). A better correlation did not result for any of the three coefficients investigated and general conclusions can be made. Three basic curves based on friction angle (or relative density), are identified and additional curves are obtained by interpolation. For these semi-log plots the relationships are linear and curves with constant slopes are indicated for each factor correlated. The equations for each basic curve are presented for each factor. As in the case of the unadjusted compression test correlations, the K values correspond to a partially developed passive earth pressure coefficient at shallower depths, and decrease to the order of magnitude of active coefficients, as the relative depth increases.

Similar correlations were attempted using data available from adjusted compression tests. The relationships and trends for these

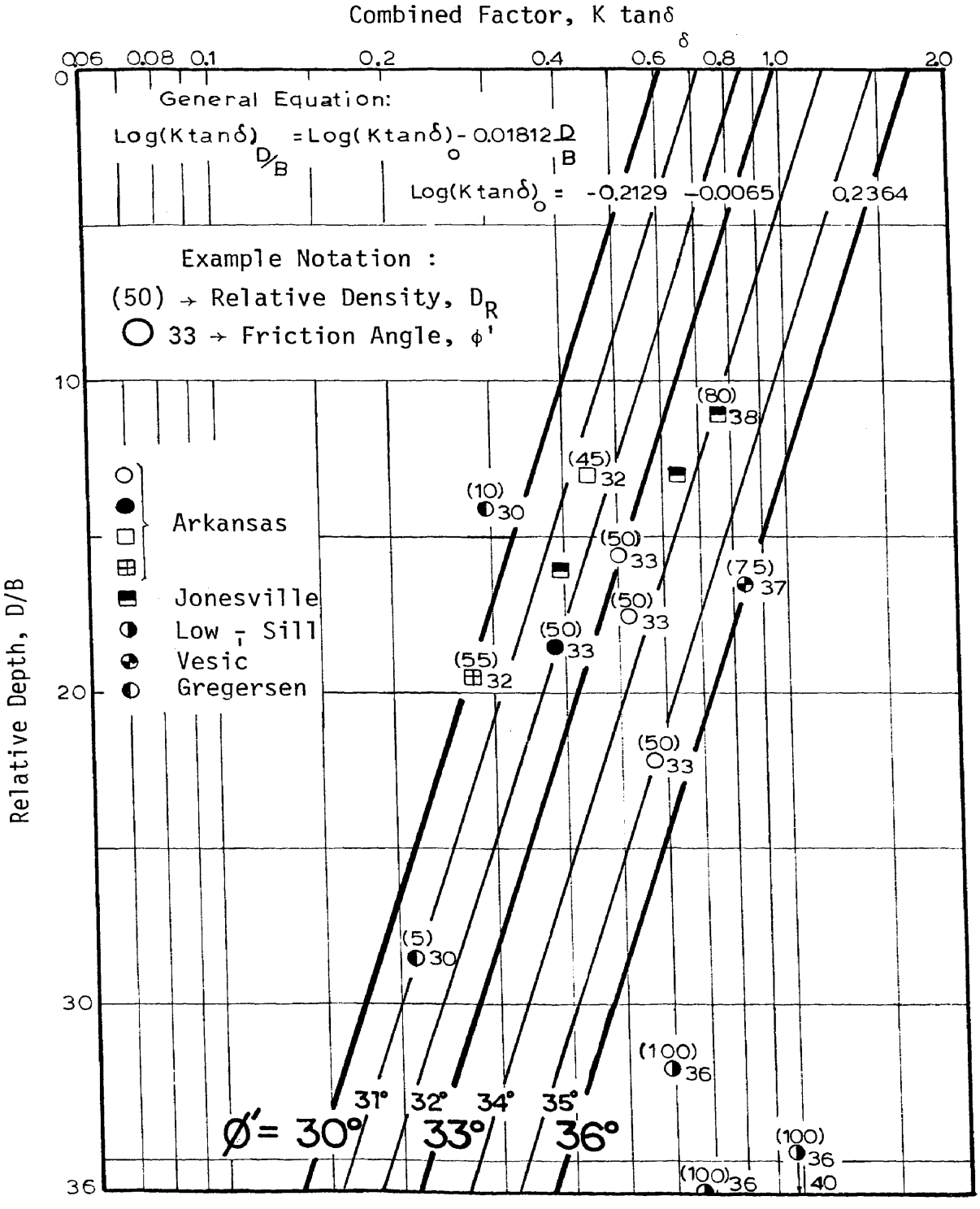

FIG. 25 - K tanδ VS D/B - COMPRESSION/TENSION

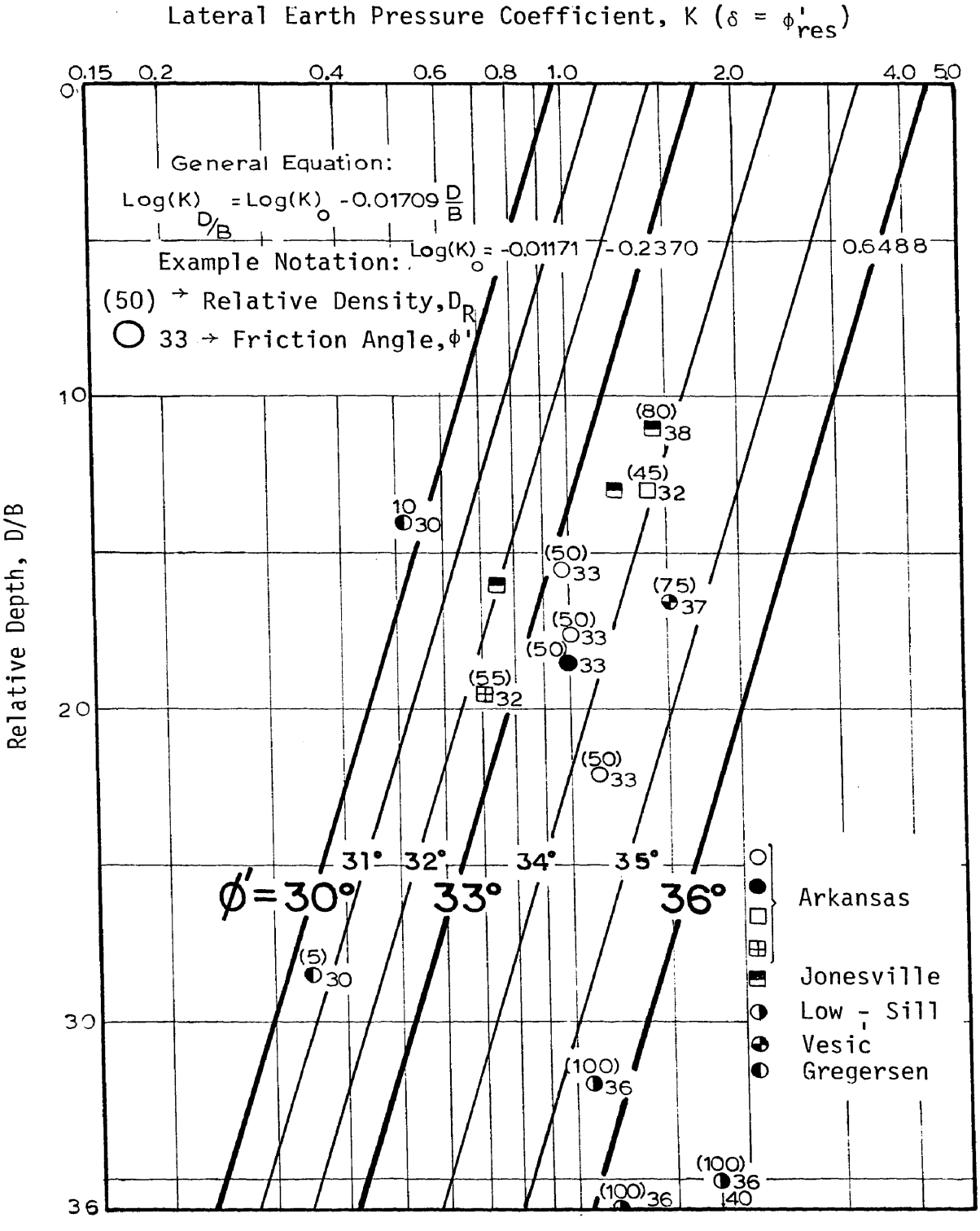

FIG. 26 - K ($\delta = \phi'_{res}$) VS D/B - COMPRESSION/TENSION

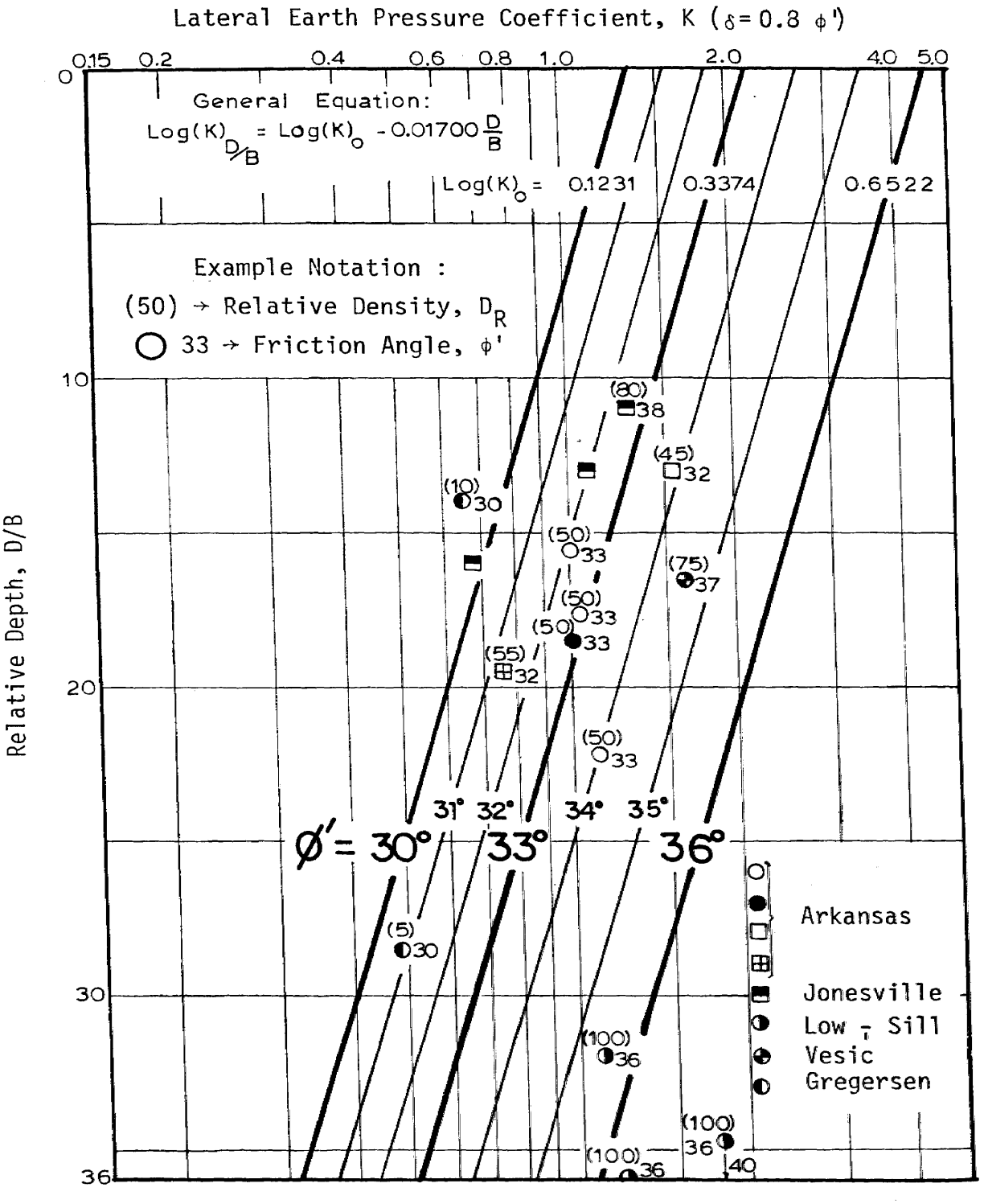

FIG. 27 - K (δ = 0.8 φ') VS D/B - COMPRESSION/TENSION

tests are essentially the same as those developed for unadjusted compression and compression/tension tests. Because of the limited data available, correlations could not be fully developed and the plotted data for the adjusted compression tests are presented in Appendix II.

Errors

New correlations have been developed for use in determining the bearing capacity of piles in sand. In the process of developing these correlations, parameters not considered in previous studies have been added, different methods of obtaining the field load test data have been used, and different bearing capacity factors have been considered. In order to determine the accuracy of the various correlations it is considered necessary to conduct an error analysis. This analysis will permit an evaluation of each correlation separately and also will allow a comparison between different correlations.

The determination of the errors was accomplished by comparing the predicted loads obtained using the new correlations with the measured field loads, as follows:

$$\text{Error } \% = \frac{\text{Predicted Load - Field Load}}{\text{Field Load}} \times 100 \quad \ldots\ldots \quad (11)$$

Errors were determined for side, point, and total loads, and both unadjusted compression and compression/tension tests were analysed. For each type of test the point loads were calculated from correlations developed for q_o and N_q, and the side loads were calculated from correlations developed for f_s, K tan δ and K (assuming both $\delta = \phi'_{res}$

and $\delta = 0.8\ \phi'$). The total load was calculated by the sum of all possible combinations of side and point loads. The two correlated factors used to calculate point load and the four correlated factors used to calculate side load resulted in a total of eight calculated total loads.

In order to evaluate the significance of the errors resulting from the use of the proposed correlations, a formal statistical treatment was considered necessary. The use of a formal statistical treatment will result in a more precise error analysis. The statistical parameters used to analyse the errors were the arithmetic mean and the corresponding standard deviation. The arithmetic mean, $\overline{X}$, is defined as:

$$\overline{X} = \frac{\sum_{i=1}^{n} X_i}{n} \quad \ldots\ldots\ldots\ldots\ldots\ldots\ldots\ldots \quad (12)$$

where: X_i = error (in percent) corresponding to the i^{th} pile test,

n = total number of analysed pile tests.

The mean can be used to provide a measure of error distribution (positive or negative). The best fit of a particular type of curve to the data would result in a zero mean. In the case of this study, if the mean is positive the tendency would be to overpredict bearing capacities, if negative, the tendency would be to underpredict. An example which may help clarify the use of the arithmetic mean is provided in Appendix III.

The standard deviation provides a measure of the error variation. The "Empirical Rule" (23) states that for a statiscally normal

(bell-shaped) distribution, approximately 68 percent of the data will fall within one standard deviation of the mean. The standard deviation, s, is defined as:

$$s = \frac{\sum_{i=1}^{n} (X_i - \bar{X})^2}{n - 1} \quad \ldots\ldots\ldots\ldots\ldots\ldots \quad (13)$$

where the terms have been previously defined.

The standard deviation provides for an analysis of the variation of the individual error for each particular data point. If a particular curve is perfectly fitted to all data, the resulting standard deviation would be zero. The smaller the magnitude of the standard deviation, the better the curve could fit the data. An example which may help clarify the use of the standard deviation is provided in Appendix III.

Before the calculated errors are presented and anlysed some considerations used in the development of the new correlations should be considered. A careful study of the references used to obtain the test data revealed that some data are considered more reliable than others. The authors, in some cases, doubted the accuracy of measurements, and suggested the presence of undetected variations in soil properties or the influence of underlying soil layers. Therefore, in the development of the correlation curves some of the data were considered less significant. Also, the shape of similar correlations developed from laboratory experimentation (25, 37) helped in conforming and adjusting the correlated curve for a given set of data.

Another point to be considered in the analysis of errors is that of checking the accuracy of the proposed correlations by using pile data

not used in the development of a particular correlation. As seen in Table 4 (page 47), only one type of test data (either unadjusted or compression/tension) was used in some cases.

Tables 6 and 7 give the summary of the percent errors obtained when using the new correlations to predict point, side, and total loads which are compared with measured field loads. Each column presents the errors resulting from the use of one particular correlation to predict the loads. In the case of total loads, each column represents one possible combination of correlations.

Table 6 gives the errors resulting from the use of the new correlations obtained from unadjusted compression test data. The means and corresponding standard deviations are shown at the bottom of each column. For example, + 24.6 represents the mean error obtained in the prediction of point load when using the correlation developed for q_0. The corresponding standard deviation is 48.1.

In the case of the total loads mean errors vary from - 12.6 to + 6.6, and the standard deviations vary from 15.5 to 20.5. The consistency in the error of predicted loads, as given by the relatively constant standard deviations, does not indicate that the use of one particular correlation is better than any other correlation. All correlations give predicted loads with about the same level of accuracy. Some idea of the distribution error in the data fit for a particular correlation curve is given by the mean value. Taking into account the "weighted" visual adjustment of data, the error distribution in the data fit for the curves is considered to be relatively small.

For the point loads, the mean errors are + 24.6 and - 8.7, and the

TABLE 6 - ERRORS VS D/B - UNADJUSTED COMPRESSION

Pile Test		D/B	Q_p POINT LOAD		Q_s SIDE LOAD				Q_T TOTAL LOAD							
									from q_o				from N_q			
			from q_o	from N_q	from f_s	from Ktanδ	from K $\delta=\phi'_{res}$	from K $\delta=.8\phi'$	and f_s	and Ktanδ	and K $\delta=\phi'_{res}$	and K $\delta=.8\phi'$	and f_s	and Ktanδ	and K $\delta=\phi'_{res}$	and K $\delta=.8\phi'$
ARKANSAS	# 1	22.2 44.3	+ 64	0	- 10	- 30	- 32	- 24	+ 10	- 4	- 5	+ 1	- 6	- 22	- 23	- 17
	# 2	17.6 35.2	+ 15	- 10	- 21	- 18	- 20	- 10	- 10	- 7	- 10	- 2	- 18	- 15	- 17	+ 11
	# 3	15.6 31.2	+ 31	+ 27	- 16	+ 2	- 1	+ 11	+ 3	+ 14	+ 12	+ 19	+ 1	+ 12	+ 10	+ 17
	# 4	13 27							+ 18	- 5	- 7	- 5	- 19	- 12	- 14	- 11
	# 6	15 30	+ 89	+ 42	- 40	- 43	- 43	- 38	- 8	- 10	- 10	- 6	- 19	- 21	- 22	- 18
	# 7	19.5 39	+ 36	- 7	- 42	- 46	- 50	- 45	- 23	- 26	- 29	- 26	- 34	- 36	- 40	- 36
	# 9	20 40	+176	+ 99	- 28	- 41	- 36	- 27	+ 4	- 8	- 4	+ 4	- 8	- 20	- 15	- 8
	# 10	18.5 37	+ 25	- 7	- 19	- 22	- 25	- 15	- 6	- 8	- 10	- 3	- 16	- 17	- 19	- 12
JONESVILLE # 1		11 22							- 2	- 15	+ 14	+ 35	+ 16	+ 3	+ 31	+ 52

TABLE 6 - Continued

Pile Test		D/B	Q_p POINT LOAD		Q_s SIDE LOAD				Q_T TOTAL LOAD							
									from q_o				from N_q			
			from q_o	from N_q	from f_s	from Ktanδ	from K $\delta=\phi'_{res}$	from K $\delta=.8\phi'$	and f_s	and Ktanδ	and K $\delta=\phi'_{res}$	and K $\delta=.8\phi'$	and f_s	and Ktanδ	and K $\delta=\phi'_{res}$	and K $\delta=.8\phi'$
LOW - SILL	# 2	32 37							+ 17	+ 9	+ 23	+ 31	+ 14	+ 7	+ 20	+ 29
	# 4	40 47							- 26	- 38	- 32	- 27	- 37	- 49	- 43	- 39
	# 6	36 41							+ 12	0	+ 9	+ 14	+ 2	- 10	- 1	+ 4
VESIC	H-15	16.5 33	- 16	- 14	- 21	- 7	+ 10	+ 15	- 18	- 13	- 6	- 4	- 17	- 11	- 5	- 3
	H-2	16.5 33	- 1	+ 11	- 7	+ 21	+ 27	+ 32	- 4	+ 9	+ 11	+ 14	+ 3	+ 15	+ 17	+ 20
GREGERSEN	# A	14 28	+ 20	+ 5	- 28	- 15	- 26	- 23	+ 20	- 7	- 6	- 14	- 21	- 11	- 19	- 17
	#D/A	28.5 57	+ 58	+ 19	+ 12	- 2	- 7	- 11	+ 22	+ 11	+ 8	+ 4	+ 14	+ 3	- 1	- 5
TAVENAS	H-1	8.5 17	+100	+ 35	+ 34	+ 2	- 4	+ 4	+ 64	+ 46	+ 48	+ 47	+ 34	+ 17	+ 18	+ 18
	H-2	12.5 25	+ 14	- 21	+ 34	+ 26	+ 44	+ 38	+ 23	+ 19	+ 27	+ 24	+ 3	0	+ 7	+ 4

TABLE 6 - Continued

Pile Test		D/B	Q_p POINT LOAD		Q_s SIDE LOAD				Q_T TOTAL LOAD							
									from q_o				from N_q			
			from q_o	from N_q	from f_s	from Ktanδ	from K $\delta=\phi'_{res}$	from K $\delta=.8\phi'$	and f_s	and Ktanδ	and K $\delta=\phi'_{res}$	and K $\delta=.8\phi'$	and f_s	and Ktanδ	and K $\delta=\phi'_{res}$	and K $\delta=.8\phi'$
TAVENAS	H-3	17 34	- 9	- 42	+ 22	+ 8	+ 19	+ 18	+ 5	- 1	+ 4	+ 4	- 13	- 19	- 13	- 13
	H-4	21.5 43	- 2	- 40	+ 51	+ 24	+ 35	+ 35	+ 24	+ 10	+ 16	+ 1	+ 4	- 9	- 4	- 4
	H-5	26 52	- 4	- 42	+ 61	+ 19	+ 29	+ 29	+ 29	+ 7	+ 13	+ 13	+ 10	- 11	- 6	- 6
	J-1	8.5 17	- 35	- 58	+ 65	+ 79	+101	+ 81	- 17	- 14	- 10	- 14	- 36	- 33	- 30	- 33
	J-2	13.5 27	- 8	- 44	+ 17	0	+ 9	+ 9	+ 4	- 4	0	0	- 17	- 25	- 21	- 21
	J-3	18 36	- 14	- 50	+ 34	+ 7	+ 17	+ 18	+ 8	- 5	0	0	- 12	- 25	- 20	- 20
	J-4	23 46	- 3	- 46	+ 28	- 8	+ 2	+ 2	+ 14	- 6	- 1	- 1	- 6	- 26	- 20	- 20
	J-5	28.5 57	+ 1	- 44	+ 36	- 12	- 2	- 2	+ 22	- 8	- 1	- 1	+ 3	- 25	- 19	- 19
COYLE C.Christi		11.2 22.3	+ 4	- 5	- 32	+ 10	- 13	- 1	- 6	+ 6	0	+ 3	- 12	- 1	- 7	- 4
Mean Error, $\bar{X}$ Std.Deviation, s			+24.6 48.1	- 8.7 37.9	+ 5.9 33.7	- 2.1 27.8	+ 1.5 34.0	+ 4.4 28.9	+ 6.6 19.1	- 1.8 15.5	+ 2.0 16.3	+ 4.1 16.9	- 6.9 16.9	-12.6 16.0	- 9.5 18.0	- 5.6 20.5

standard deviations are 48.1 and 37.9. For the side loads, the mean errors vary from + 5.9 to - 21, and standard deviations vary from 27.8 to 34. It can be seen that for the component loads, point and side, the accuracy of predictions is not as good as for the total load. Also it can be seen that the assumption of "$\delta = 0.8\ \phi'$" yielded slightly better results for the prediction of side loads. On the other hand, the assumption of "$\delta = \phi'_{res}$" yielded slightly better results for the prediction of total loads.

A careful examination of all test pile data shows that those piles which consistently show errors above 20% are "Arkansas" #7, "Low-Sill" #4 and "Tavenas" H-1 and J-1. For the "Arkansas" pile #7 no probable justification for the larger error could be found. The authors (29) of the "Low-Sill" #4 test report noted the greater capacity of this pile and tentatively explained it as being due to "the presence of a dense pocket of sand, or possibley a gravel pocket". The "Tavenas" piles H-1 and J-1 are 17 ft (5.2 m) long piles driven through 16 ft (4.9 m) of loose crushed stone to penetrate 1 ft (0.3 m) in the sand. The influence of the layer of crushed stone could be significant and the effects of layering transition could be dominant. In the case of the precast concrete pile, J-1, pushing crushed stones into sand could explain why the measured point and total loads are higher than predicted. In the case of the "H" pile, H-1, the crushed stone could have prevented the formation of a soil "plug" in the zone between the flanges and prevented the development of the full pile point area. This reduced area would explain why the measured loads are lower than the predicted loads.

Table 7 summarizes the errors resulting from the use of the new

TABLE 7 - ERRORS VS D/B - COMPRESSION/TENSION

Pile Test		D/B	Q_p POINT LOAD		Q_s SIDE LOAD				Q_T TOTAL LOAD							
									from q_o				from N_q			
			from q_o	from N_q	from f_s	from Ktanδ	from K $\delta=\phi'_{res}$	from K $\delta=.8\phi'$	and f_s	and Ktanδ	and K $\delta=\phi'_{res}$	and K $\delta=.8\phi'$	and f_s	and Ktanδ	and K $\delta=\phi'_{res}$	and K $\delta=.8\phi'$
ARKANSAS	# 1	22.2 44.3	+ 8	- 24	+ 1	- 31	- 36	- 22	+ 4	- 13	- 15	- 8	- 10	- 28	- 30	- 23
	# 2	17.6 35.2	- 18	- 28	+ 2	+ 8	- 15	+ 3	- 9	- 13	- 17	- 8	- 15	- 19	- 22	- 14
	# 3	15.6 31.2	+ 6	+ 15	- 1	+ 3	- 5	+ 16	+ 3	+ 5	+ 1	+ 10	+ 8	+ 10	+ 6	+ 15
	# 4	13 27	+ 9	0	- 41	- 34	- 40	- 30	- 15	- 12	- 15	- 10	- 20	- 16	- 19	- 15
	# 6	15 30							- 8	- 16	- 17	- 12	- 16	- 24	- 25	- 20
	# 7	19.5 39	- 44	- 56	+ 22	+ 5	- 7	+ 47	- 26	- 30	- 34	- 19	- 34	- 13	- 42	- 27
	# 9	20 40							- 1	- 13	- 10	- 4	- 9	- 22	- 19	- 13
	# 10	18.5 37	- 19	- 31	+ 8	- 7	- 14	+ 4	- 7	- 14	- 17	- 9	- 14	- 21	- 24	- 16
JONESVILLE # 1		11 22	- 23	- 5	+ 2	+ 41	+101	+125	- 15	- 3	+ 16	+ 24	- 3	+ 10	+ 31	+ 32

TABLE 7 - Continued

Pile Test		$\frac{D}{B}$	Q_p POINT LOAD		Q_s SIDE LOAD				Q_T TOTAL LOAD							
									from q_o				from N_q			
			from q_o	from N_q	from f_s	from Ktanδ	from K $\delta=\phi'_{res}$	from K $\delta=.8\phi'$	and f_s	and Ktanδ	and K $\delta=\phi'_{res}$	and K $\delta=.8\phi'$	and f_s	and Ktanδ	and K $\delta=\phi'_{res}$	and K $\delta=.8\phi'$
LOW - SILL	# 2	32 37	+ 35	+ 48	- 12	- 25	+ 18	+ 20	+ 19	+ 14	+ 29	+ 30	+ 27	+ 22	+ 38	+ 38
	# 3	53 61	+ 13	- 32												
	# 4	40 47	- 16	- 32	- 43	- 68	- 48	- 47	- 27	- 37	-29	- 28	- 36	- 46	- 38	- 38
	# 6	36 41	+ 28	+ 23	- 17	- 44	- 8	- 8	+ 12	+ 3	+ 15	+ 16	+ 9	0	+ 12	+ 13
VESIĆ	H-15	16.5 33	- 17	- 12	- 35	- 28	- 17	- 13	- 24	- 22	- 17	- 15	- 22	- 19	- 14	- 13
	H-2	16.5 33							- 6	- 1	- 1	+ 4	0	+ 5	+ 5	+ 10
GREGERSEN	# A	14 28	- 1	+ 2	- 7	+ 15	+ 7	+ 16	- 4	+ 5	+ 2	+ 5	- 2	+ 6	+ 3	+ 7
	#D/A	28.5 57	+ 28	+ 3	- 5	- 13	- 9	- 10	+ 10	+ 5	+ 8	+ 7	- 1	- 6	- 3	- 4
TAVENAS	H-1	8.5 17							+ 57	+ 57	+ 56	+ 59	+ 14	+ 15	+ 13	+ 16
	H-2	12.5 25							+ 35	+ 24	+ 28	+ 29	+ 10	0	+ 3	+ 4
	H-3	17 34							+ 9	- 3	- 1	+ 2	- 8	- 19	- 17	- 14

TABLE 7 - Continued

Pile Test		D/B	Q_p POINT LOAD		Q_s SIDE LOAD				Q_T TOTAL LOAD							
									from q_o				from N_q			
			from q_o	from N_q	from f_s	from Ktanδ	from K $\delta=\phi'_{res}$	from K $\delta=.8\phi'$	and f_s	and Ktanδ	and K $\delta=\phi'_{res}$	and K $\delta=.8\phi'$	and f_s	and Ktanδ	and K $\delta=\phi'_{res}$	and K $\delta=.8\phi'$
TAVENAS	H-4	21.5 43							+ 23	+ 6	+ 8	+ 11	+ 4	- 14	- 1	- 8
	H-5	26 52							+ 24	+ 1	+ 4	+ 7	+ 5	- 19	- 16	- 13
	J-1	8.5 17							- 8	- 8	- 2	- 8	- 36	- 36	- 30	- 36
	J-2	13.5 27							+ 11	- 2	+ 1	+ 2	- 13	- 26	- 23	- 22
	J-3	18 36							+ 10	- 5	- 14	- 1	- 11	- 26	- 24	- 22
	J-4	23 46							+ 12	- 9	- 7	- 4	- 9	- 30	- 28	- 25
	J-5	28.5 57							+ 17	- 12	- 9	- 7	- 4	- 33	- 30	- 27
COYLE C.Christi		11.2 22.3							0	+ 7	+ 4	+ 7	- 20	- 12	- 16	- 12
Mean Error, $\bar{X}$			- 0.8	- 9.2	- 9.7	-13.7	- 5.6	+ 7.8	+ 3.6	- 3.2	- 1.2	+ 3.0	- 7.6	-13.4	-11.9	- 8.2
Std.Deviation, s			22.9	27.1	19.6	28.7	36.8	42.7	19.0	17.7	19.0	17.8	15.2	16.9	19.9	19.7

correlations obtained from compression/tension test data. Again the resulting means and corresponding standard deviations are presented at the bottom of each column.

For the total loads, mean errors vary from - 13.4 to + 3.6, and the corresponding standard deviations vary from 15.2 to 19.9. These standard deviations for total loads are almost the same as the results obtained with the unadjusted compression test correlations, in that, all correlations give predicted loads with about the same level of accuracy. In this case the means show that there is no significant tendency to overpredict or underpredict when q_o is used in the determination of total load. However, if N_q is used there is a tendency to underpredict total load.

For point loads, the means are - 0.8 and - 9.2, and the standard deviations are 22.9 and 27.1. These standard deviations show that, for compression/tension tests, the predictions of point loads are almost as good as the predictions of total loads. The means show that there is a slight tendency for underprediction with the use of N_q correlations. For side loads, the means resulting from the use of f_s and K tan δ are - 9.7 and - 13.7, with corresponding standard deviations of 19.6 and 28.7. If the side loads are calculated using K (by both methods) a more significant variation in error occurs. Using $\delta = \phi'_{res}$ the resulting errors have a standard deviation of 36.8, and using $\delta = 0.8\ \phi'$ the standard deviation is 42.7.

Another careful check of all test results shows that those piles which consistently present errors above 20% are "Arkansas" #7, "Low-Sill" #4 and "Tavenas" H-1 and J-1. The peculiarities for each of these

piles which could explain the probable causes of deviation were presented previously, when discussing the results for the unadjusted compression tests.

In summary, it has been shown that the correlations which individually yielded the best predicted values were q_o for point loads and f_s for side loads, both derived from compression/tension test data. Consequently, when using these same correlations (q_o and f_s) from compression/tension test data, predictions of total load agree well with field measurements. Finally, it has been shown that the use of the combination of any pair of correlations (one for side load and the other for point load) from either unadjusted compression or compression/tension test data gives predicted total loads which agree well with measured field loads.

CONCLUSIONS AND RECOMMENDATIONS

Conclusions

A rather thorough investigation has been made of existing bearing capacity theories and of experimental studies for piles in sand. The most significant parameters which influence the bearing capacity of piles in sand have been identified. Using twenty-eight instrumented field pile load tests in sand, it was possible to check the accuracy of existing theories and demonstrate the need for improvement in the state-of-the-art of bearing capacity prediction. This improvement was achieved through the development of new correlation curves which can be used to predict point load, side load, and total load. The correlations were developed from both unadjusted compression and compression/tension test data.

A comparison of the errors resulting in predicting total ultimate load when using the correlations from both unadjusted compression and compression/tension test data shows that a good level of accuracy is achieved. However, if the component loads (point and side loads) are analysed separately, the compression/tension test correlations give better predicted loads. This result seems to confirm the hypothesis that compression/tension tests more consistently represent the real point and side loads in a system free of residual stresses.

If the bearing capacity factor correlations are analysed separately when used to predict total load, the conclusion is that all (both unadjusted compression and compression/tension) yield compatible results. On the other hand, only the compression/tension test correlations

provided about the same level of precision when predicting the component loads. For point loads, the q_o correlation, and for side loads, the f_s correlation, give best results. The use of the correlations for N_q and K tan δ yields slightly less accurate predictions. The least accurate predictions are obtained when using the K factor correlations.

As a result of this study it has been shown that the parameters which provided the best correlations are the relative depth (depth to diameter ratio) and the sand friction angle. The relative depth is probably related to the effective overburden pressure of the soil surrounding the pile, and the volume of displaced and deformed soil. All soils investigated in this study have the same quartzose composition and most have fine gradation. Consequently, the sand friction angle in addition to reflecting the shear strength may be related to relative density (compressibility).

For the unit point resistance, q_o, constant values were not indicated at penetrations of sixty diameters. And for the unit side resistance, f_s, constant values were not indicated at penetrations of thirty diameters. The unit resistances showed pronounced increase with increase in relative depth for shallow penetration. However, the rate of increase in average unit resistance with relative depth becomes smaller, and relatively constant, at greater penetration (roughly between ten and thirty pile diameters).

The use of the correlations for q_o and f_s from compression/tension tests as given in Figs. 22 (page 73) and 24 (page 75) is recommended for design purposes. Besides requiring less calculation for determination of ultimate load, smaller percent errors should result. Figs. 28

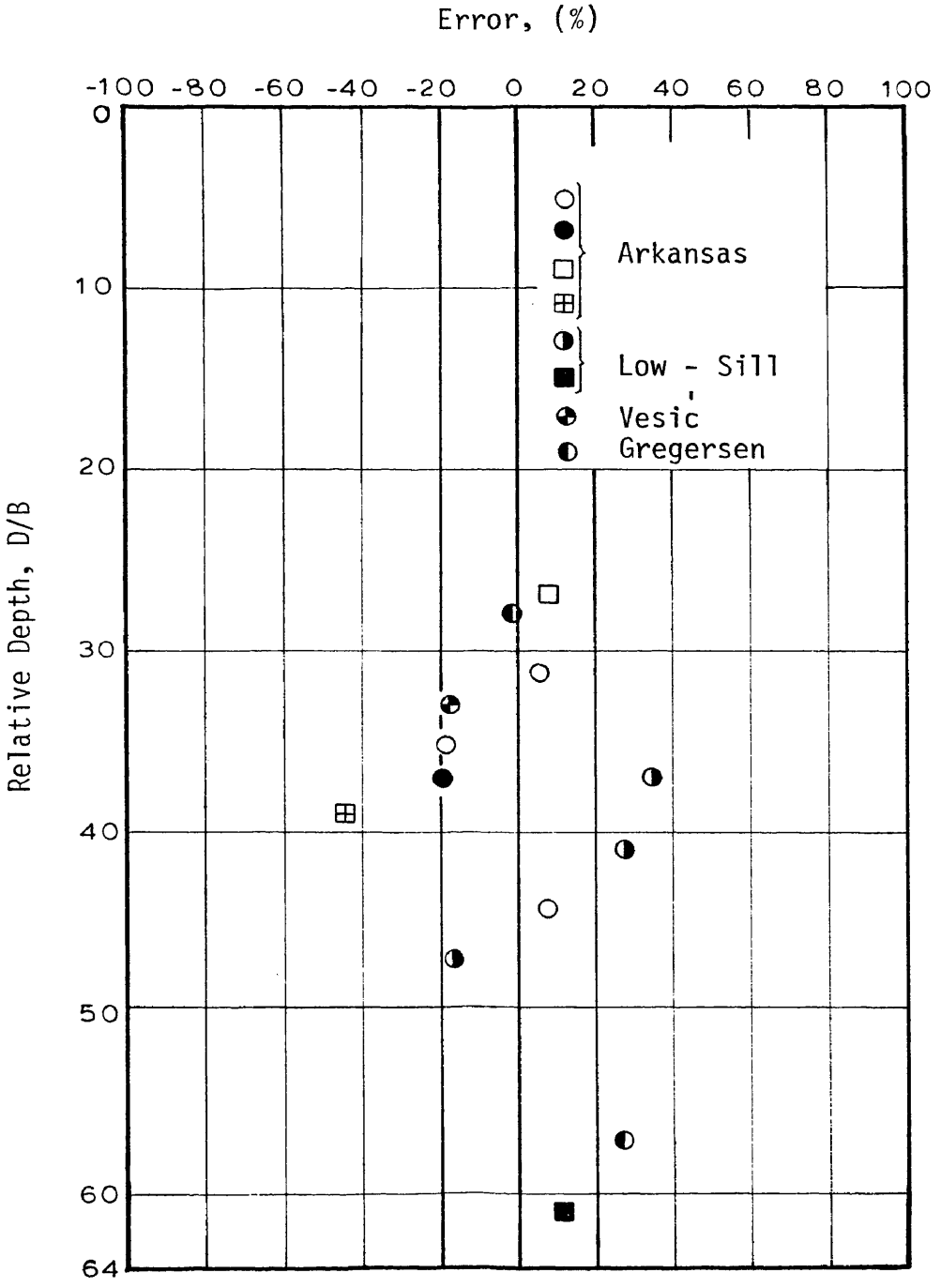

FIG. 28 - ERROR OF Q_p (FROM q_o) VS D/B - COMPRESSION/TENSION

through 30 show graphically the error distribution versus relative depth resulting from using these correlations. Fig. 28 shows the error distribution when calculating Q_p from q_o, Fig. 29 the error distribution when calculating Q_s from f_s, and Fig. 30 the error distribution if Q_u is calculated from the same correlations. For the side load, Q_s, the depth used is that of the mid point of the segment analysed. For point load, Q_p, and total ultimate load, Q_u, the depth is defined as that at the pile point. It is seen, in Figs. 28 and 29, that the maximum error resulting in the prediction of component loads, with the exception of "Arkansas" pile #7, is less than 40%. Also the vast majority of the predicted loads are within an error band of $\pm$ 20%. Fig. 30 shows that the maximum error, with the exception of the two shorter "Tavenas" H-piles (driven through crushed stones), is less than 30%. Also, the vast majority of the predicted loads are within an error band of $\pm$ 20%.

Recommendations

Because of the limitation of the available data for this study, it was not possible to investigate the influence of the location of the water table and to separate the influence of relative density from that of the friction angle. In all cases, the ground water level was very close to the ground surface which means that all test piles were penetrated into submerged sands. It is recommended that the case of "dry" soils be investigated. At the same relative depth the pressures for a "dry" soil would be larger than those for a submerged soil.

In order to differentiate between the influences of friction angle and relative density it is recommended that sands of very different

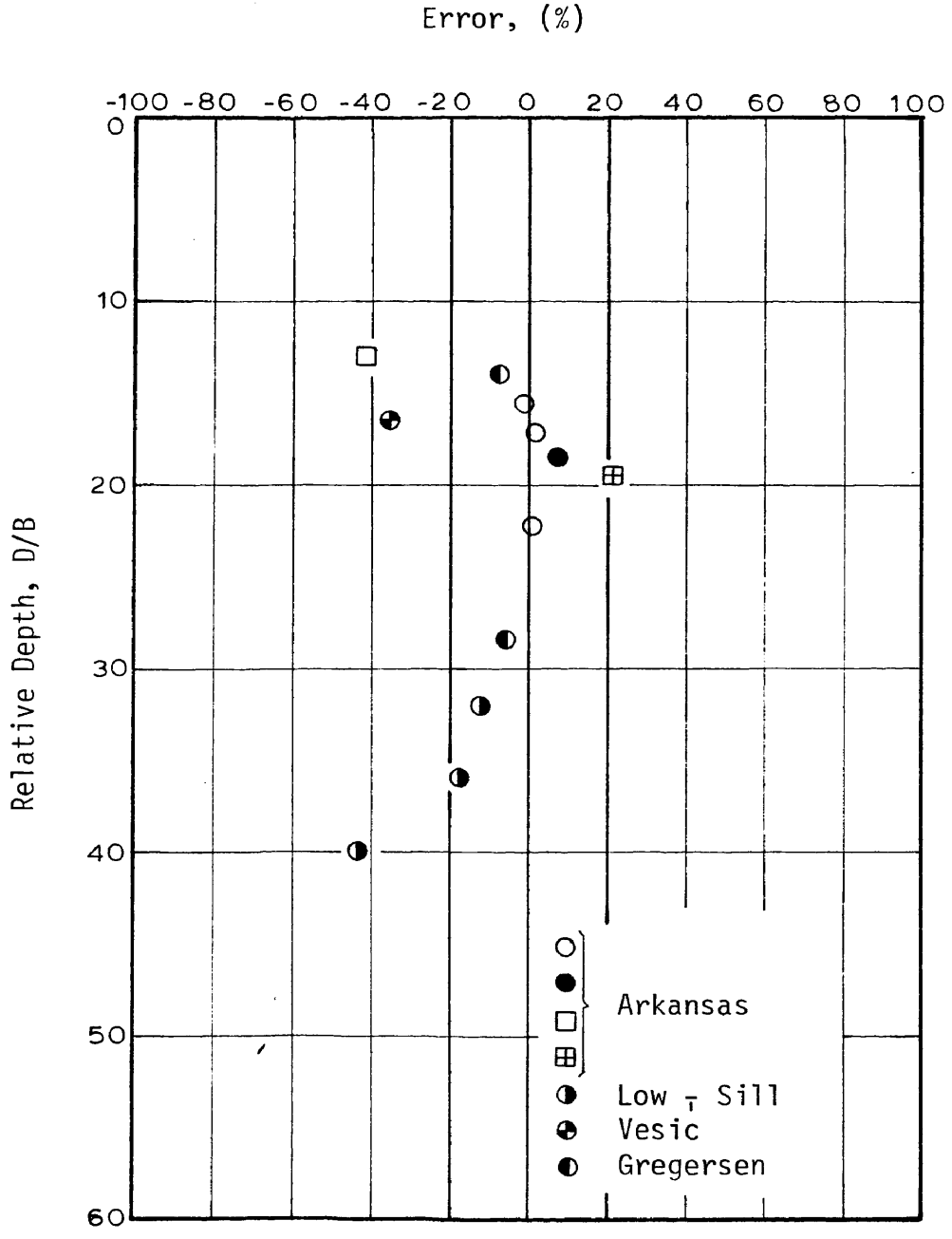

FIG. 29 - ERROR OF Q_s (FROM f_s) VS D/B - COMPRESSION/TENSION

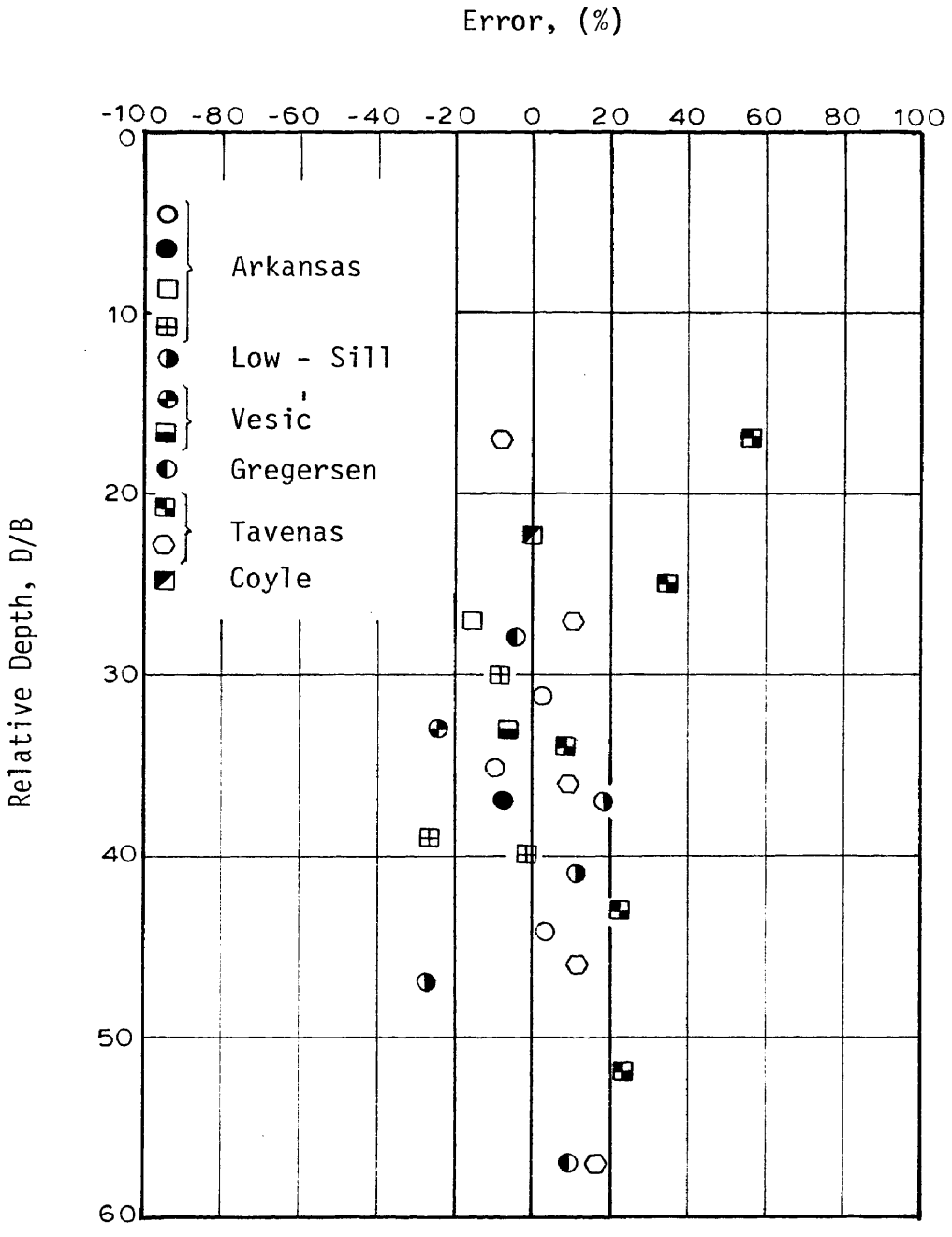

FIG. 30 - ERROR OF Q_u (FROM q_o AND f_s) VS D/B - COMPRESSION/TENSION

gradation, grain shape, mineral composition, and degree of particle roundness be investigated.

APPENDIX I

EFFECTIVE OVERBURDEN AS A CORRELATION PARAMETER

Another correlation parameter which was investigated during this study is the effective overburden pressure parameter. This parameter is defined as the product of the effective overburden pressure times the pile penetration depth divided by the product of the pile diameter squared times the unit weight of water ($pD/\gamma_w B^2$). Since the accuracy of bearing capacity predictions is compatible with those obtained using the relative depth (depth over diameter ratio) parameter, the relative depth was chosen for its simplicity. However, there are cases where the use of the more complicated parameter may be more appropriate, such as the case of surcharges or "dry" sands.

The explanation of the use of the effective overburden pressure has been given. The pile penetration depth, D, is a measure of the distance from the stress free ground surface. In the case of shallow penetrations, this parameter would define the type of failure: general shear, localized shear, or some intermediate type. The pile diameter, B, is representative of the volume of displaced soil during pile penetration. The diameter is squared and the unit weight of water is used in order to develop a nondimensional parameter. It is interesting to note that the ratio of overburden pressure to unit weight of water represents a fictious depth.

The bearing capacity factors for which correlations were developed are: the unit point resistance, q_o; the bearing capacity factor, N_q; the unit side resistance, f_s; the combined factor K tan δ; and the

lateral earth pressure coefficient K (with $\delta = \phi'_{res}$ and $\delta = 0.8\ \phi'$). For the unit point resistance, q_o, and its related factor, N_q, the pile penetration depth is the depth to the point, and the effective overburden pressure is also determined at point level. For the unit side resistance, f_s, and its related factors, K tan δ and K, the pile depth is taken as half of total penetration, and the effective overburden pressure is taken as the average pressure along the pile shaft. Correlations were developed using both unadjusted compression tests and compression/tension test data.

The correlation curves for the unadjusted compression test data are shown in Figs. 31 through 36, presenting the log of the effective overburden pressure parameter versus, respectively: the unit point resistance, q_o; the log of the bearing capacity factor, N_q; the unit side resistance, f_s; the log of the combined factor K tan δ; and the log of the lateral earth pressure coefficient K, for $\delta = \phi'_{res}$ and $\delta = 0.8\ \phi'$. The same procedure and conclusions drawn from the relative depth parameter are repeated for these correlations. One exception is that due to scale effects the shape of curves of unit resistances are different. In the case of the effective overburden pressure parameter the indication of increasing resistance with increasing depth is more definitive.

The correlation curves for compression/tension test data are shown in Figs. 37 through 42, presenting the log of the effective overburden pressure parameter versus respectively: the unit point resistance, q_o; the log of the bearing capacity factor, N_q; the unit side resistance, f_s; the log of the combined factor, K tan δ; and the log of

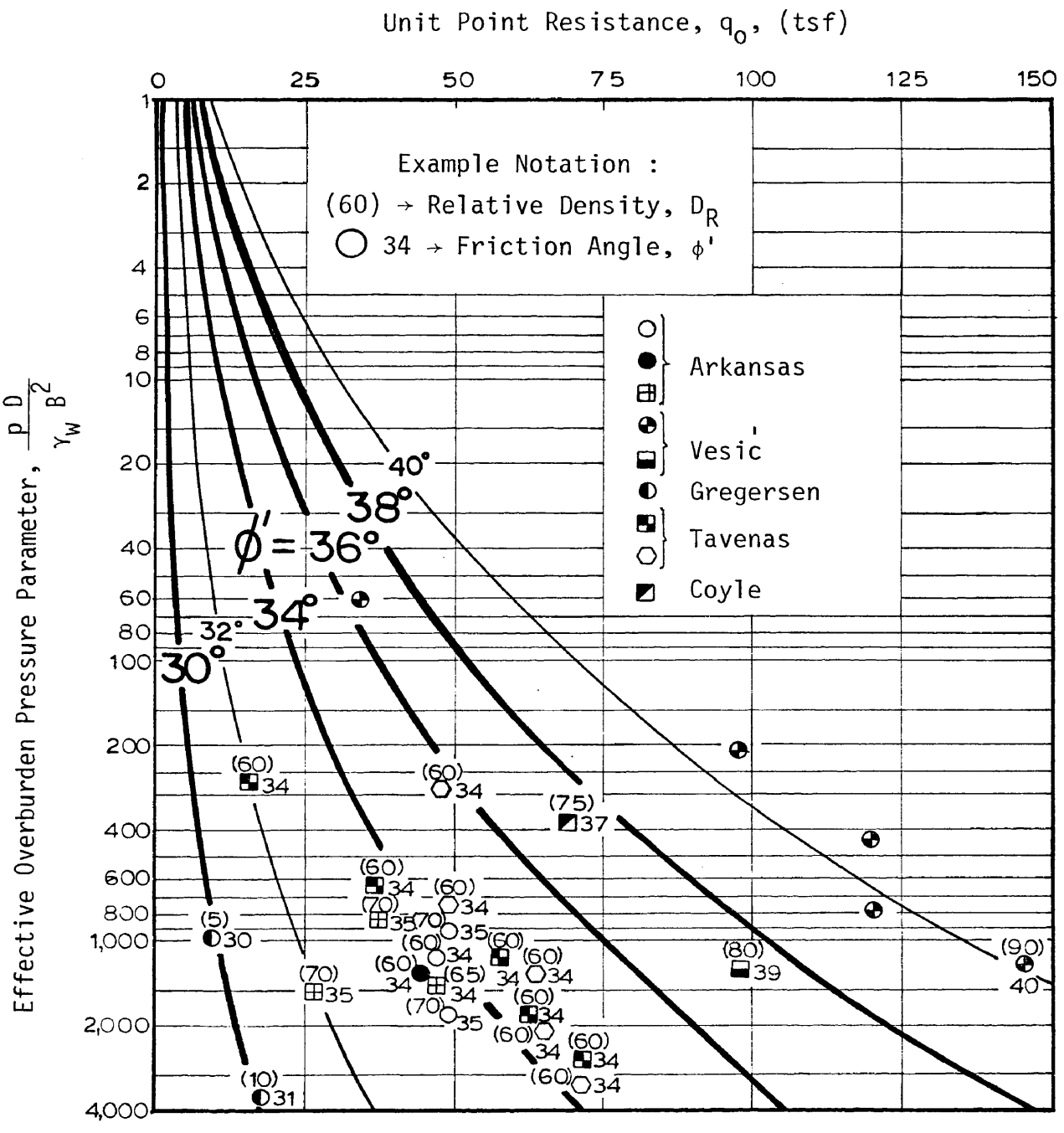

FIG. 31 - q_o VS $\frac{p\ D}{\gamma_w\ B^2}$ - UNADJUSTED COMPRESSION (1 tsf = 95.76 kN/m^2)

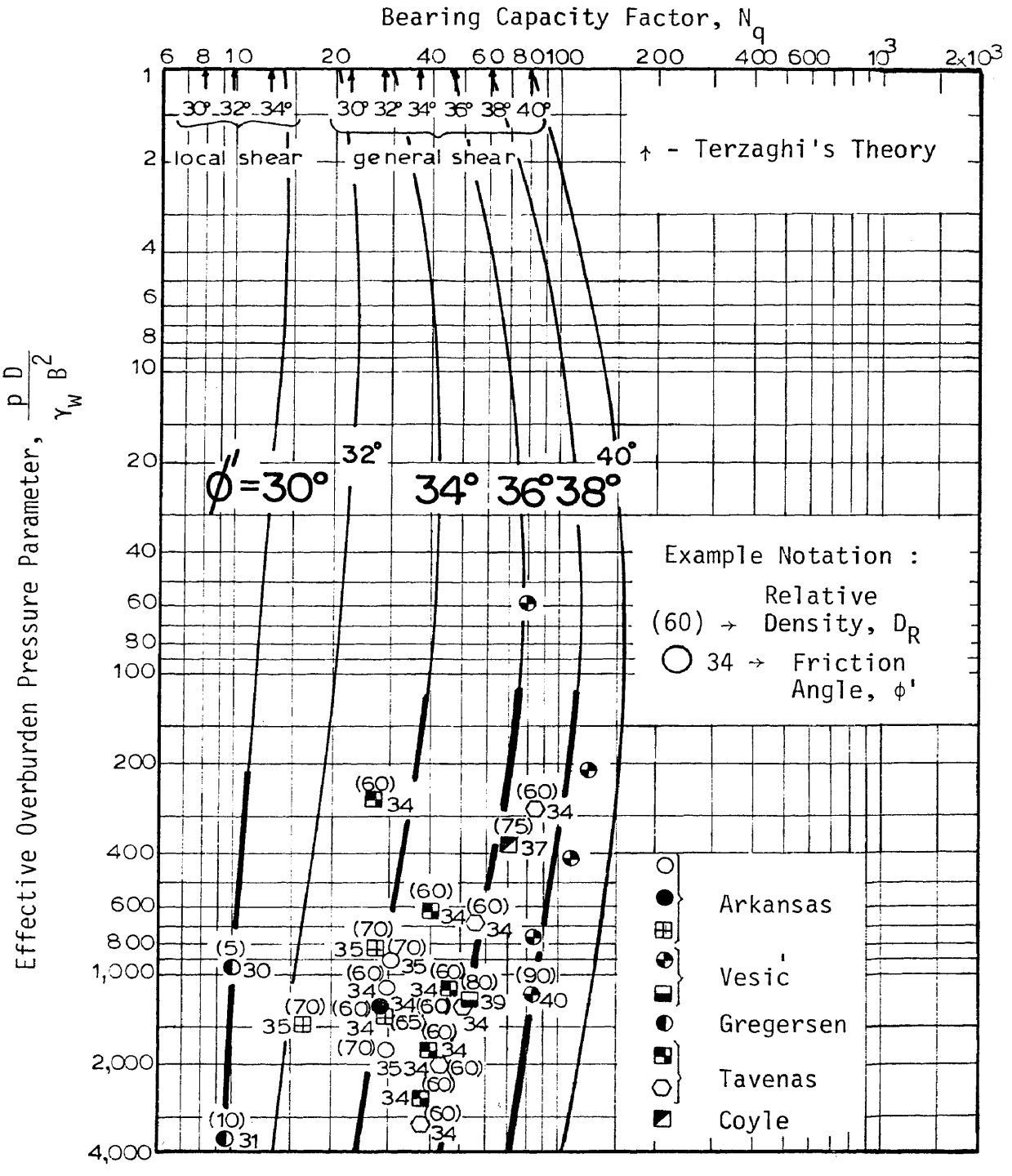

FIG. 32 - N_q VS $\frac{p\,D}{\gamma_w\,B^2}$ - UNADJUSTED COMPRESSION

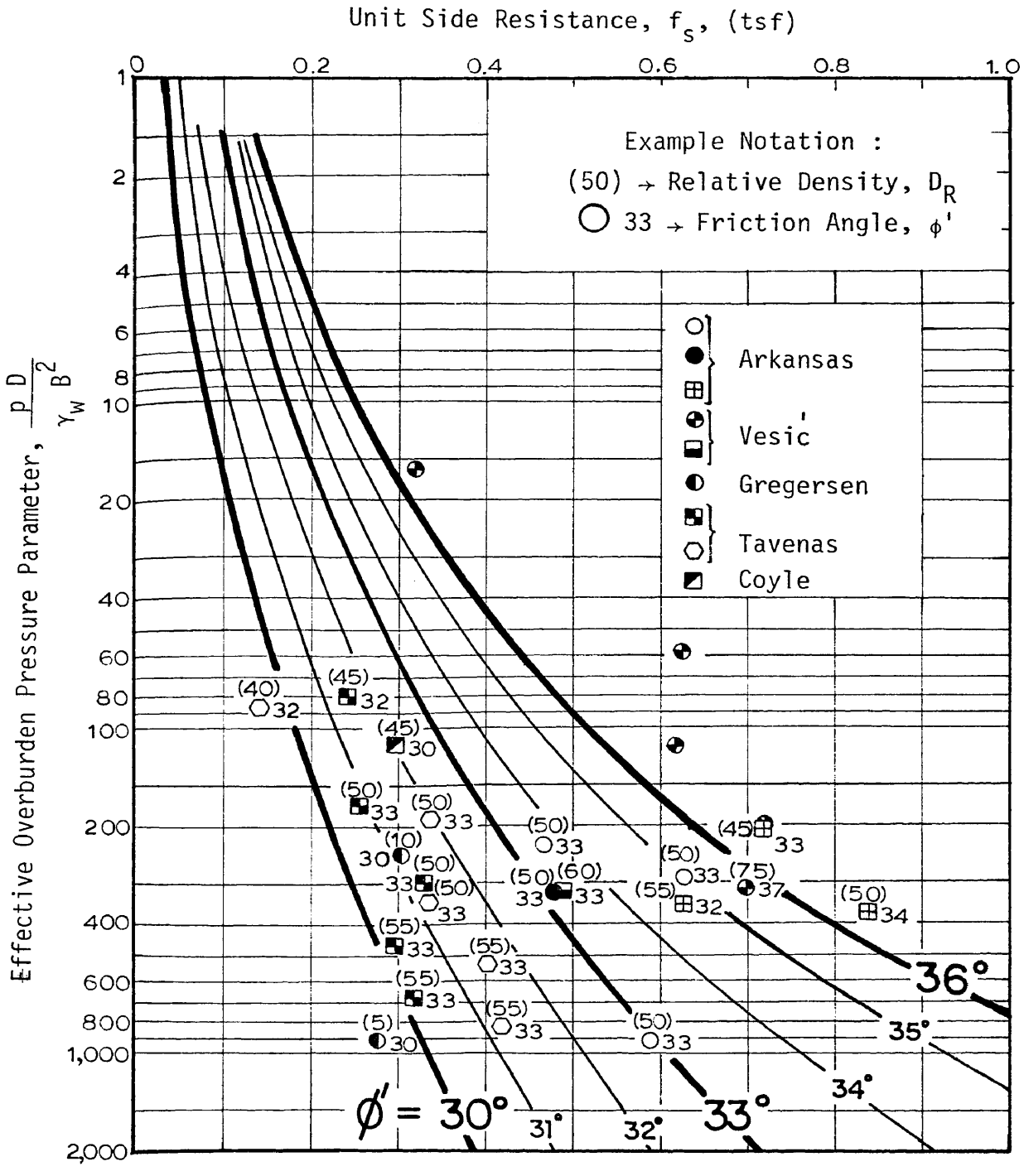

FIG. 33 - f_s VS $\frac{p\ D}{\gamma_w\ B^2}$ - UNADJUSTED COMPRESSION (1 tsf = 95.76 kN/m^2)

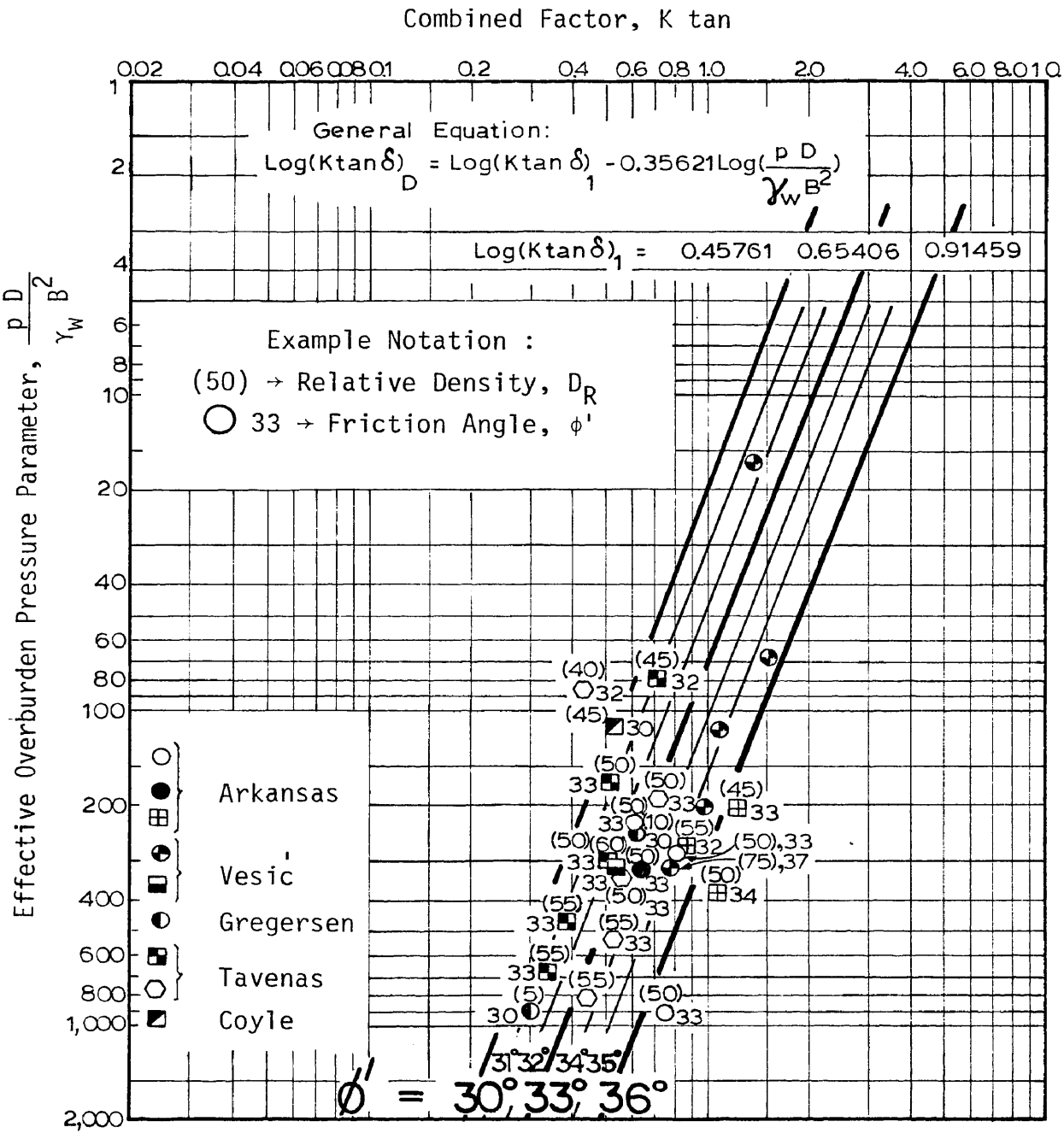

FIG. 34 - K tan VS $\frac{p\ D}{\gamma_w\ B^2}$ - UNADJUSTED COMPRESSION

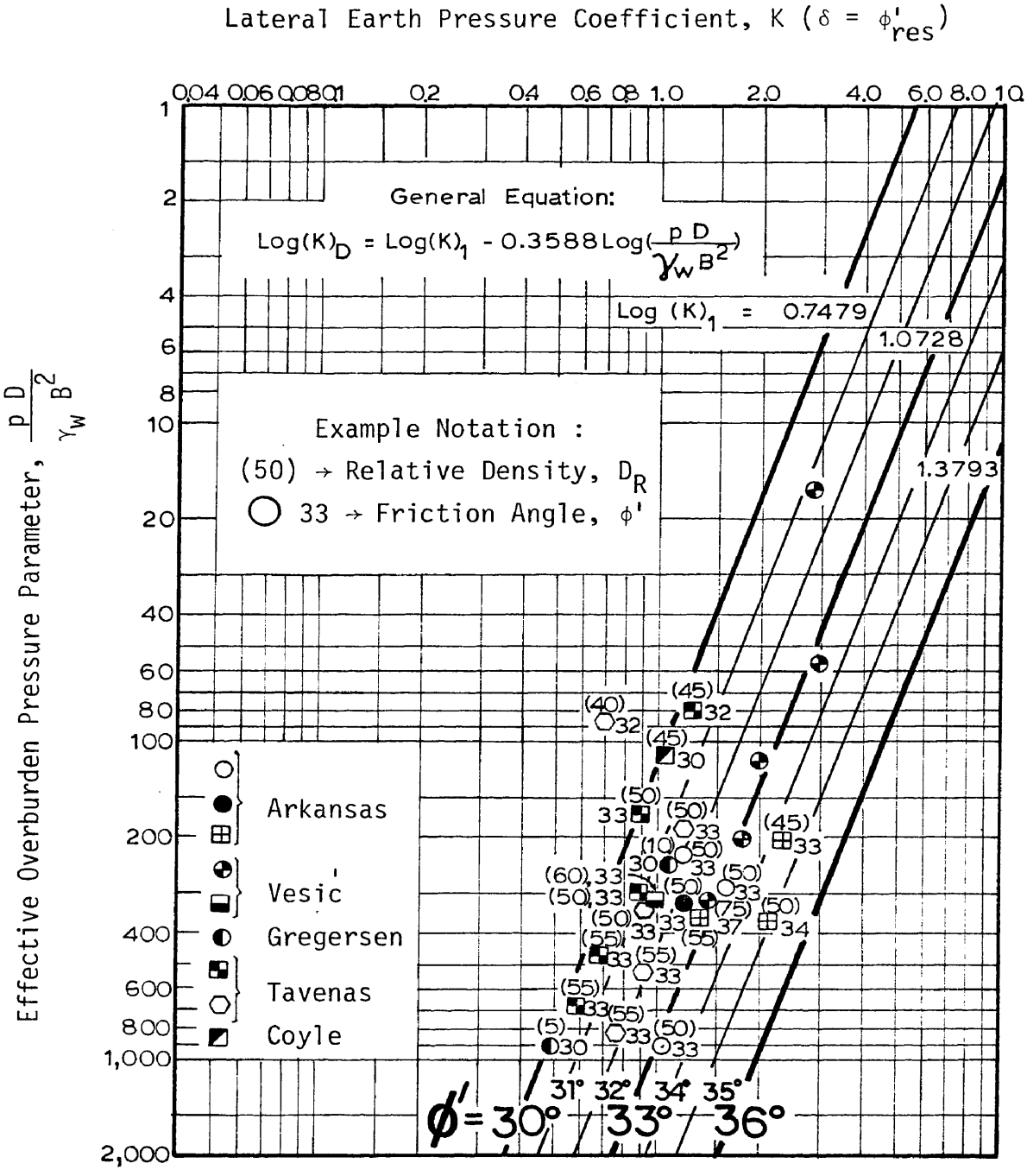

FIG. 35 - K ($\delta = \phi'_{res}$) VS $\frac{p\,D}{\gamma_w B^2}$ - UNADJUSTED COMPRESSION

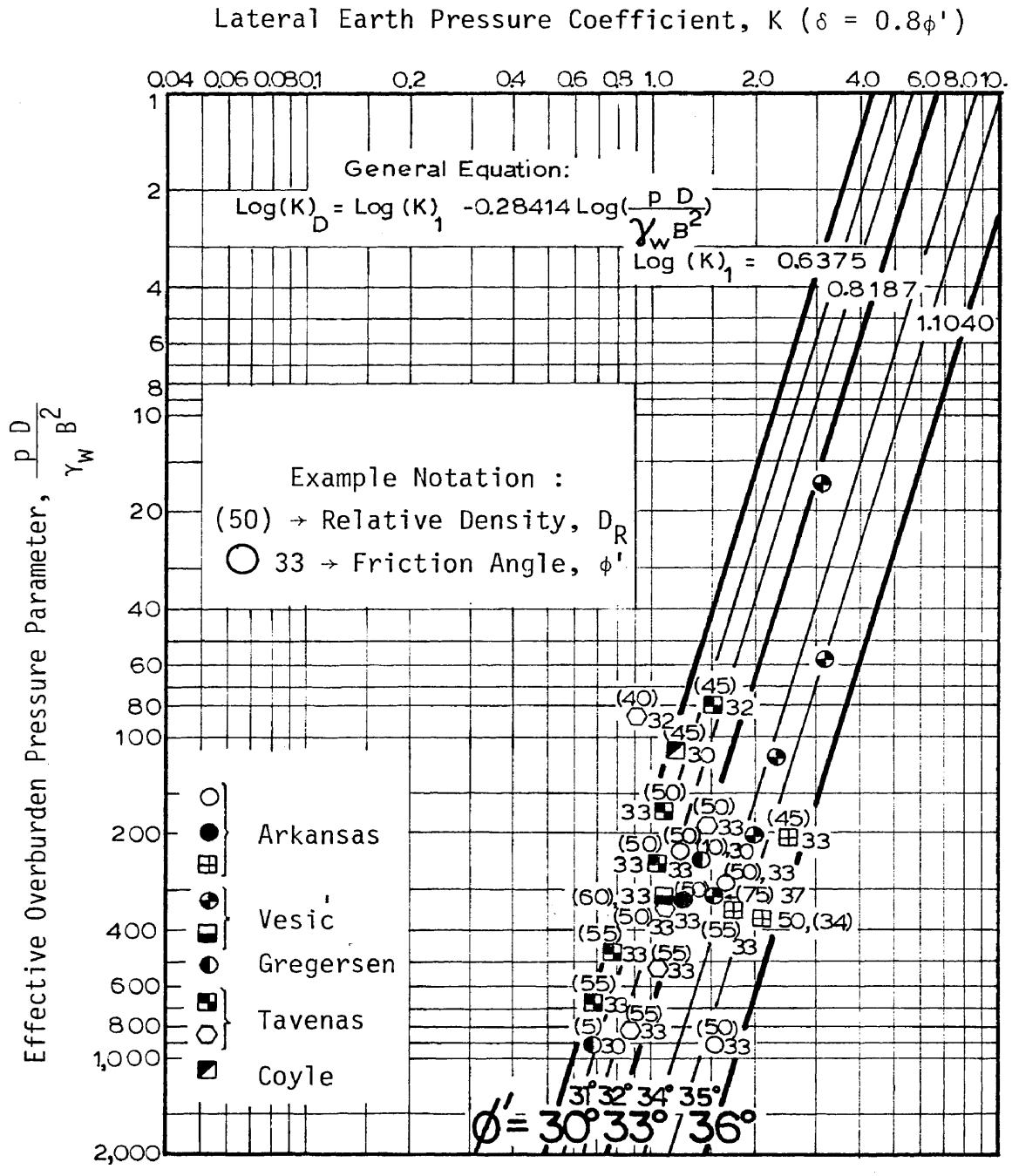

FIG. 36 - K ($\delta = 0.8\phi'$) VS $\frac{p\ D}{\gamma_w\ B^2}$ - UNADJUSTED COMPRESSION

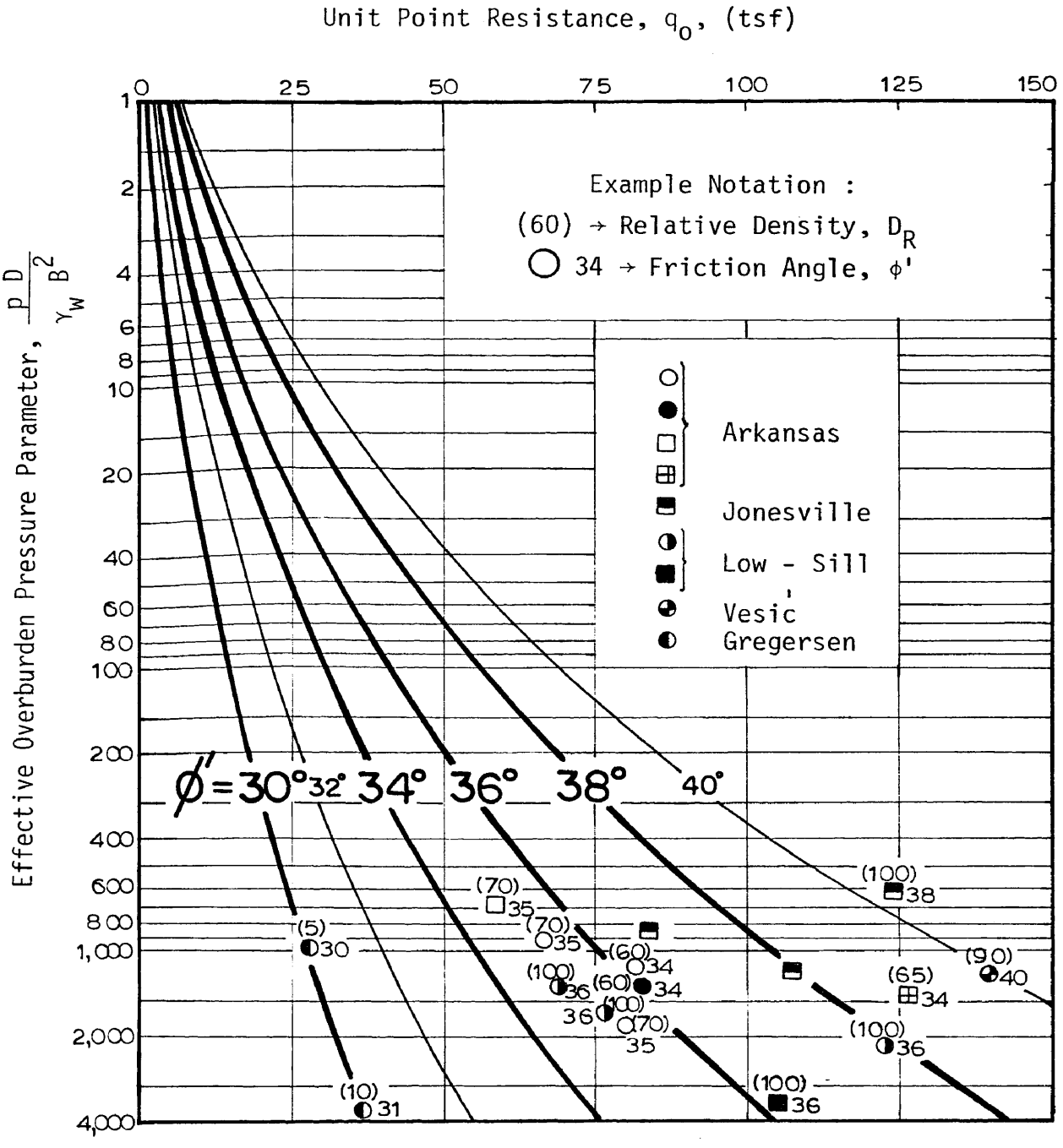

FIG. 37 - q_o VS $\frac{p\ D}{\gamma_w\ B^2}$ - COMPRESSION/TENSION (1 tsf = 95.76 kN/m^2)

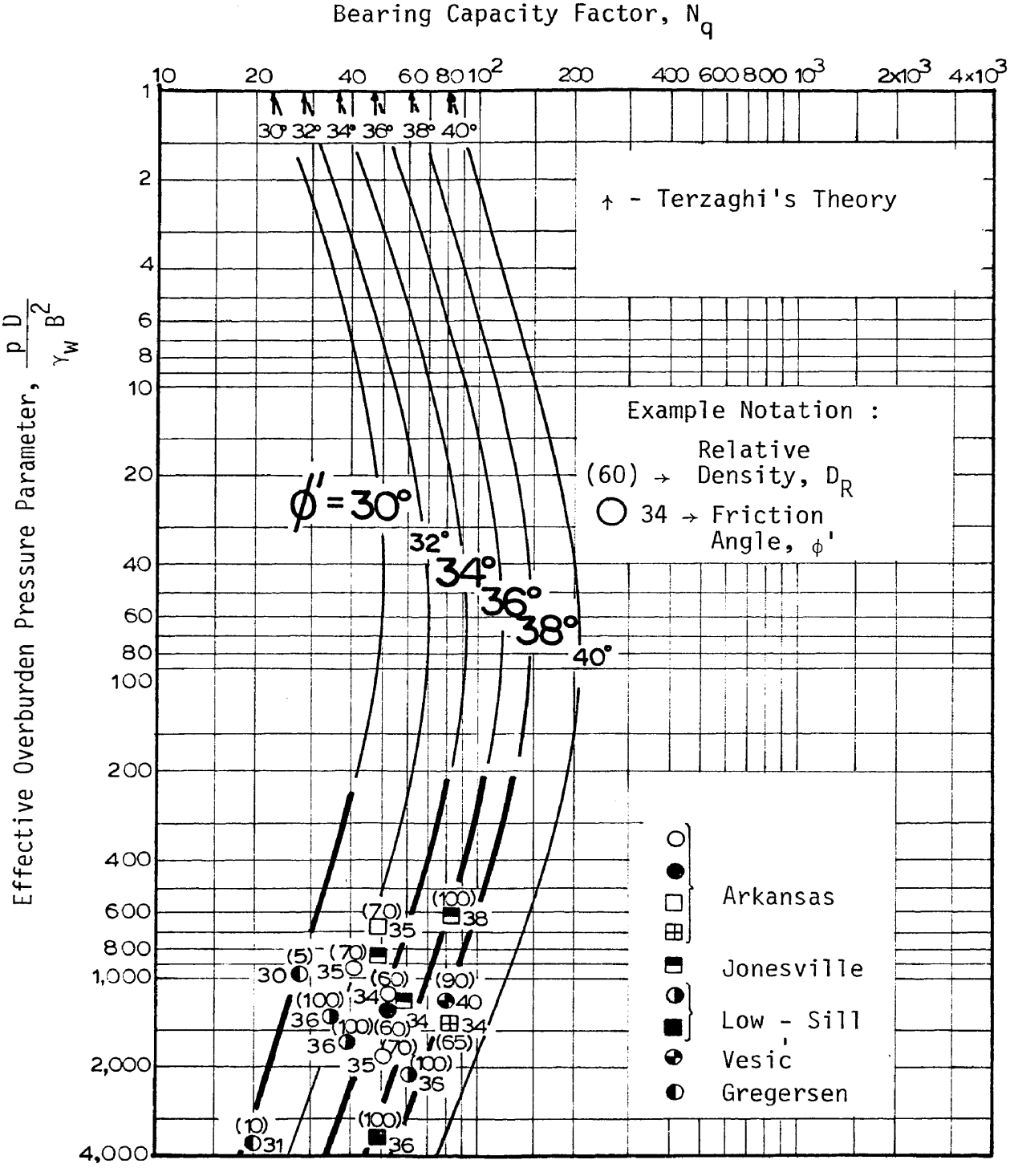

FIG. 38 - N_q VS $\frac{p\ D}{\gamma_w\ B^2}$ - COMPRESSION/TENSION

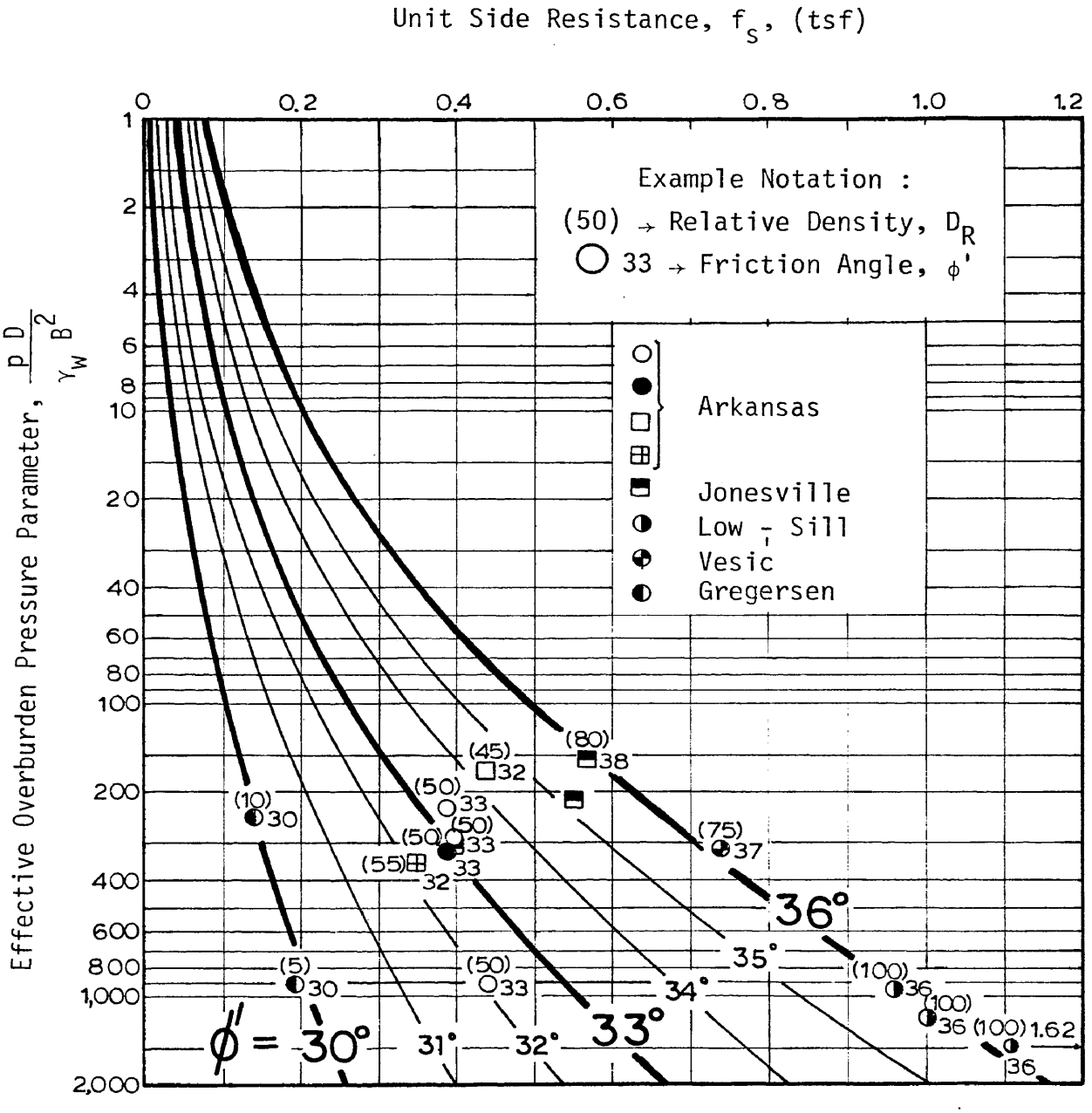

FIG. 39 - f_s VS $\frac{p\ D}{\gamma_w\ B^2}$ - COMPRESSION/TENSION (1 tsf = 95.76 kN/m^2)

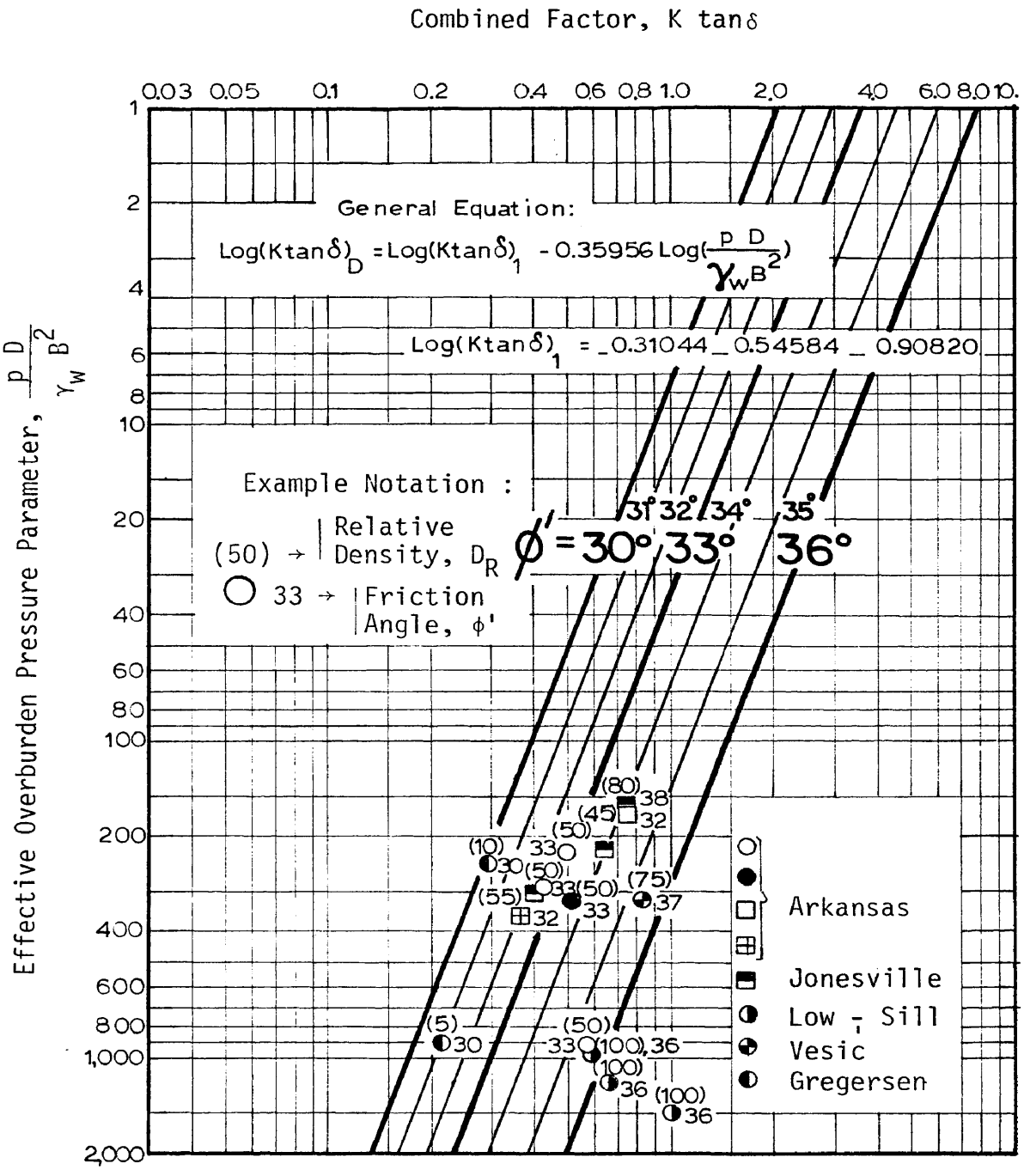

FIG. 40 - K tanδ VS $\frac{p\ D}{\gamma_w\ B^2}$ - COMPRESSION/TENSION

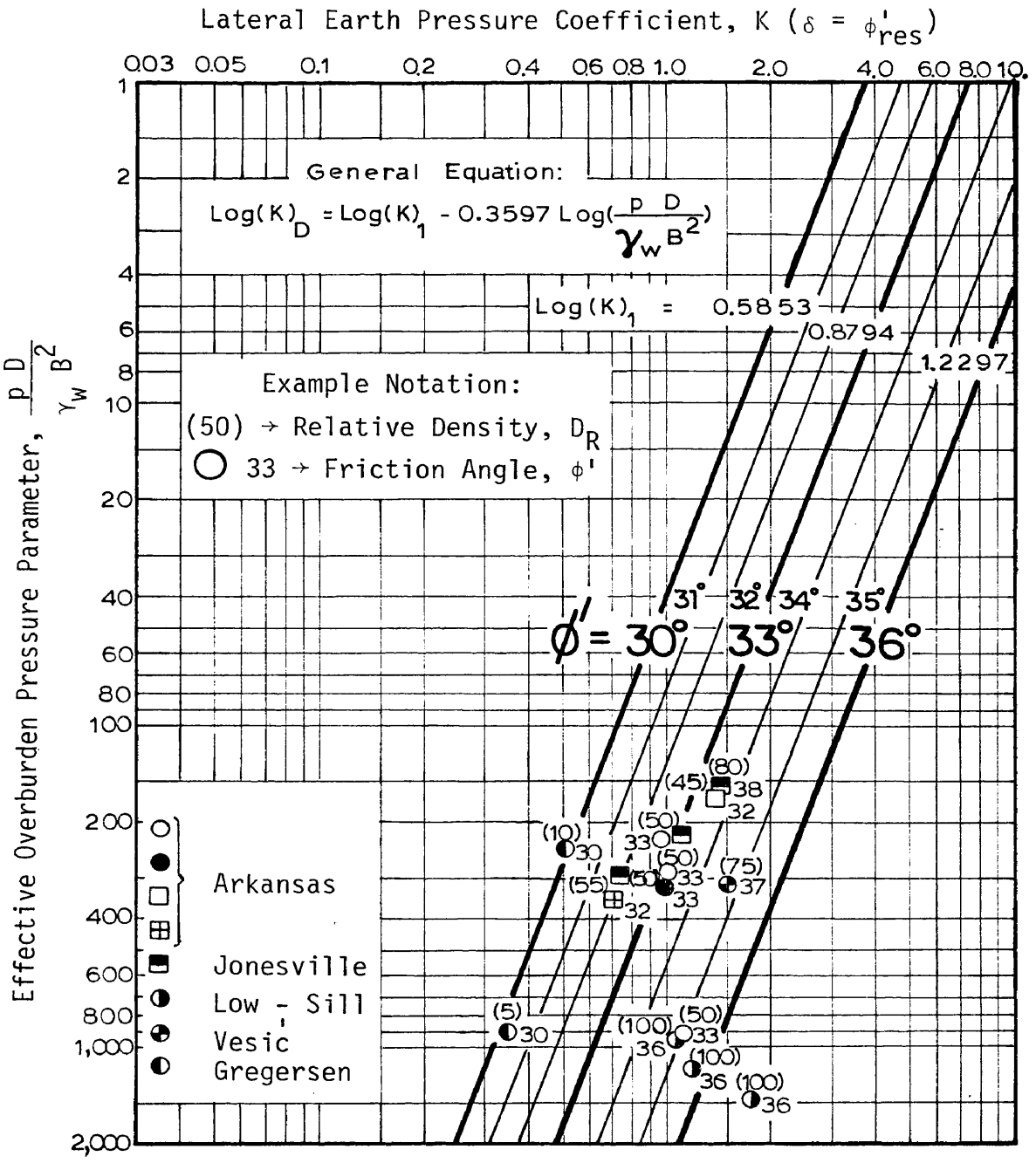

FIG. 41 - K ($\delta = \phi'_{res}$) VS $\frac{p\ D}{\gamma_w\ B^2}$ - COMPRESSION/TENSION

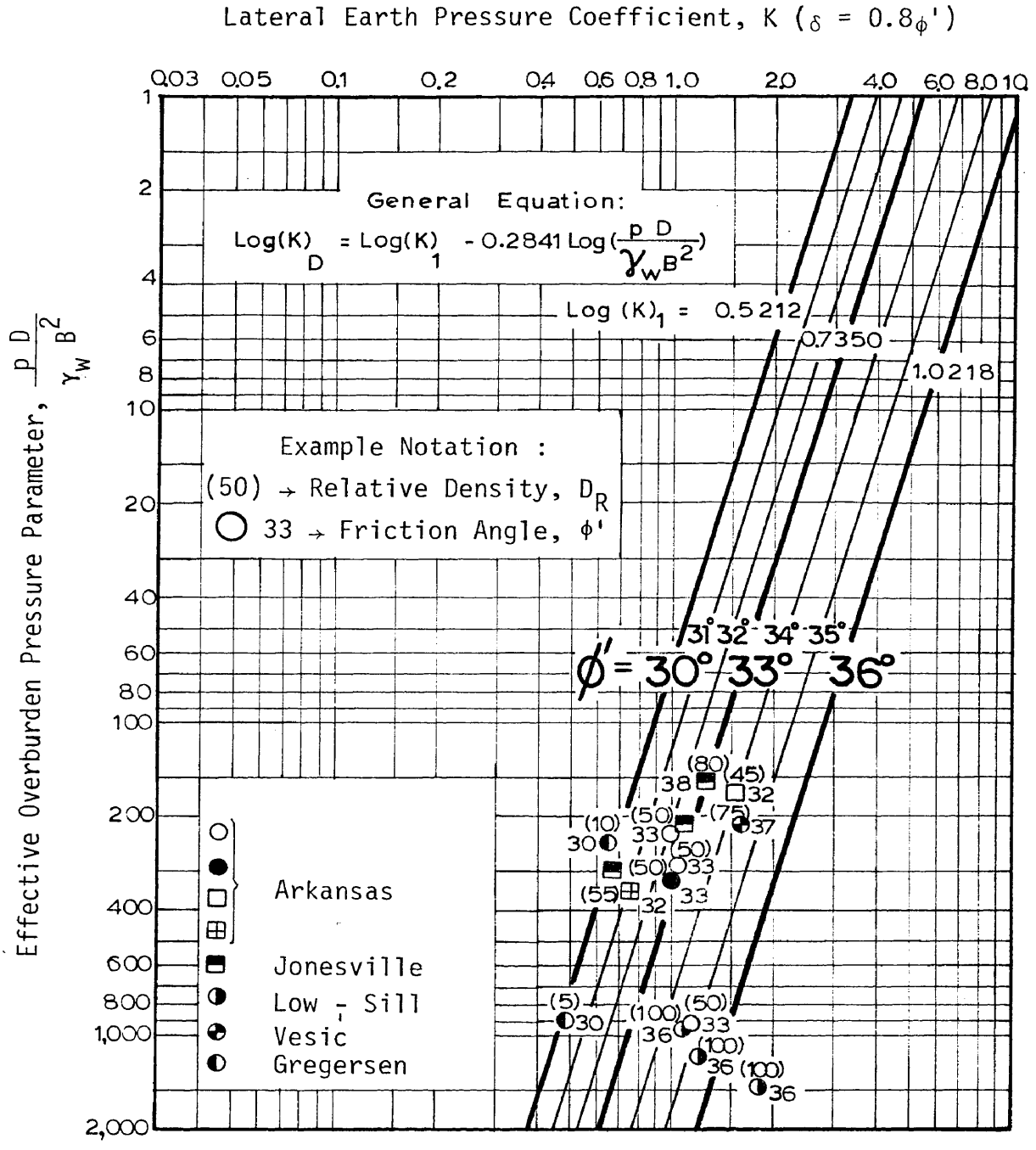

FIG. 42 - K ($\delta = 0.8\phi'$) VS $\frac{p\ D}{\gamma_w\ B^2}$ - COMPRESSION/TENSION

the lateral earth pressure coefficient, K, for $\delta = \phi'_{res}$ and $\delta = 0.8\ \phi'$. It is obvious that these results are similar to those obtained for unadjusted compression tests.

It should be noted that each correlation should be analysed individually, without regard to previous correlations. In some cases it is possible that different decisions were made for different correlations. That is the case for the q_o correlations versus the relative depth and versus the effective overburden pressure parameter. In the first correlation (relative depth) the maximum friction angle curve is for 39^o, and in the second (effective overburden pressure) it is for $\phi' = 40^o$, using the same data.

Tables 8 and 9 present the errors resulting from the predicted values as compared with field measurements. Table 8 refers to unadjusted compression test data and Table 9 to compression/tension test data. The same procedure and conclusions obtained using the relative depth parameter are repeated. The same piles ("Arkansas" #7, "Low-Sill" #4, and "Tavenas" H-1 and J-1) yielded larger deviations from the predicted values. Both pile testing methods present good agreement between the total predicted and measured loads. But only the compression/tension test data present good agreement for the component loads, especially if calculated from the unit resistances, q_o and f_s, correlations.

TABLE 8 - ERRORS VS $\frac{pD}{\gamma_w B^2}$ - UNADJUSTED COMPRESSION

Pile Test		$\frac{p\,D}{\gamma_w B^2}$	Q_p POINT LOAD		Q_s SIDE LOAD				Q_T TOTAL LOAD							
									from q_o				from N_q			
			from q_o	from N_q	from f_s	from Ktanδ	from K $\delta=\phi'_{res}$	from K $\delta=.8\phi'$	and f_s	and Ktanδ	and K $\delta=\phi'_{res}$	and K $\delta=.8\phi'$	and f_s	and Ktanδ	and K $\delta=\phi'_{res}$	and K $\delta=.8\phi'$
ARKANSAS	# 1	915 1,867	+ 48	+ 19	0	- 43	- 32	- 38	+ 13	- 18	- 10	- 14	+ 5	- 26	- 18	- 23
	# 2	288 1,158	+ 4	- 2	- 24	- 17	+ 1	- 16	- 16	- 10	+ 2	- 10	- 17	- 12	+ 1	- 12
	# 3	228 926	+ 24	+ 37	- 19	+ 3	+ 26	+ 3	- 1	+ 11	+ 25	+ 11	+ 4	+ 17	+ 31	+ 17
	# 4	170 678							- 15	- 9	- 2	- 10	- 18	- 12	- 6	- 14
	# 6	206 835	+ 77	+ 51	- 42	- 42	- 26	- 43	- 13	- 12	0	- 13	- 19	- 18	+ 7	- 19
	# 7	352 1,425	+ 24	+ 4	- 46	- 48	- 43	- 47	- 29	- 31	- 26	- 30	- 34	- 36	- 31	- 35
	# 9	370 1,509	+154	+125	- 32	- 39	- 16	- 24	- 3	- 10	+ 10	+ 3	- 8	- 14	+ 6	- 1
	# 10	322 1,300	+ 17	0	- 24	- 22	- 5	- 20	- 12	- 10	+ 2	- 9	- 17	- 15	- 3	- 14
JONESVILLE		157 625							- 18	+ 2	+ 36	+ 35	+ 8	+ 28	+ 62	+ 61

TABLE 8 - Continued

Pile Test		$\frac{p\ D}{\gamma_w B^2}$	Q_p POINT LOAD		Q_s SIDE LOAD				Q_T TOTAL LOAD							
									from q_o				from N_q			
			from q_o	from N_q	from f_s	from Ktanδ	from K $\delta=\phi'_{res}$	from K $\delta=.8\phi'$	and f_s	and Ktanδ	and K $\delta=\phi'_{res}$	and K $\delta=.8\phi'$	and f_s	and Ktanδ	and K $\delta=\phi'_{res}$	and K $\delta=.8\phi'$
LOW - SILL	# 2	955 1,347							+ 17	+ 15	+ 44	+ 37	+ 41	+ 39	+ 68	+ 60
	# 4	1,479 2,112							- 33	- 41	- 25	- 28	- 22	- 30	-13	- 17
	# 6	1,189 1,643							- 2	- 9	+ 15	+ 10	+ 23	+ 16	+ 40	+ 35
VESIC	H-15	313 1,203	- 27	- 1	- 22	- 12	+ 33	+ 8	- 25	- 21	- 4	- 13	- 9	- 5	+ 13	+ 3
	H-2	317 1,269	- 3	+ 27	- 6	+ 13	+ 50	+ 15	- 4	+ 4	+ 20	+ 5	+ 13	+ 21	+ 37	+ 22
GREGERSEN	# A	244 975	+ 11	+ 3	- 21	- 34	- 29	- 35	- 15	- 24	- 20	- 25	- 16	- 26	- 22	- 27
	#D/A	906 3,622	+ 42	+ 14	+ 19	- 15	0	- 9	+ 24	- 2	+ 10	+ 3	+ 18	- 9	+ 3	- 4
TAVENAS	H-1	80 272	+106	+ 35	- 2	+ 6	+ 32	- 2	+ 48	+ 52	+ 66	+ 47	+ 15	+ 19	+ 33	+ 15
	H-2	171 640	+ 14	- 22	+ 34	+ 25	+ 81	+ 22	+ 22	+ 18	+ 43	+ 17	+ 2	- 2	+ 23	- 3

TABLE 8 - Continued

Pile Test		$\frac{p\ D}{\gamma_w\ B^2}$	Q_p POINT LOAD		Q_s SIDE LOAD				Q_T TOTAL LOAD							
									from q_o				from N_q			
			from q_o	from N_q	from f_s	from Ktanδ	from K $\delta=\phi'_{res}$	from K $\delta=.8\phi'$	and f_s	and Ktanδ	and K $\delta=\phi'_{res}$	and K $\delta=.8\phi'$	and f_s	and Ktanδ	and K $\delta=\phi'_{res}$	and K $\delta=.8\phi'$
TAVENAS	H-3	300 1,162	- 16	- 38	+ 14	+ 6	+ 45	+ 7	- 2	- 6	+ 12	- 6	- 14	- 18	+ 1	- 17
	H-4	468 1,838	- 10	- 34	+ 47	+ 23	+ 69	+ 28	+ 18	+ 6	+ 28	+ 9	+ 5	- 6	+ 15	- 4
	H-5	675 2,669	- 11	- 34	- 42	- 54	+ 24	+ 69	+ 22	+ 7	+ 30	+ 11	+ 11	- 4	+ 18	- 1
	J-1	86 288	- 33	- 58	+216	+ 81	+148	+ 67	+ 13	- 12	+ 1	- 14	- 9	- 34	- 21	- 36
	J-2	188 703	- 12	- 43	+ 16	- 1	+ 43	- 2	0	- 7	+ 12	- 8	- 17	- 24	- 5	- 25
	J-3	336 1,300	- 19	- 47	+ 30	+ 5	+ 44	+ 6	+ 4	- 16	+ 10	- 7	- 12	- 24	- 6	- 23
	J-4	530 2,079	- 11	- 38	+ 23	- 6	+ 29	- 1	+ 8	- 8	+ 11	- 6	- 5	- 21	- 2	- 18
	J-5	823 3,253	- 6	- 35	+ 31	- 3	+ 31	+ 3	+ 15	- 5	+ 15	- 1	+ 3	- 17	+ 3	- 13
COYLE C.Christi		112 382	- 2	+ 14	- 36	+ 1	- 2	- 6	- 11	- 1	- 2	- 3	+ 1	+ 11	+ 10	+ 9
Mean Error, $\bar{X}$			+16.9	- 1.0	+ 5.2	- 3.0	+22.9	- 0.7	+ 0.2	- 5.1	+11.2	- 0.3	- 2.5	- 7.5	+ 9.0	- 3.1
Std.Deviation, s			45.5	41.8	54.8	31.2	43.6	30.1	18.8	17.5	21.2	18.7	16.5	20.0	24.2	25.1

TABLE 9 - ERRORS VS $\frac{pD}{\gamma_w B^2}$ - COMPRESSION/TENSION

Pile Test		$\frac{pD}{\gamma_w B^2}$	Q_p POINT LOAD		Q_s SIDE LOAD				Q_T TOTAL LOAD							
									from q_o				from N_q			
			from q_o	from N_q	from f_s	from $K\tan\delta$	from K $\delta=\phi'_{res}$	from K $\delta=.8\phi'$	and f_s	and $K\tan\delta$	and K $\delta=\phi'_{res}$	and K $\delta=.8\phi'$	and f_s	and $K\tan\delta$	and K $\delta=\phi'_{res}$	and K $\delta=.8\phi'$
ARKANSAS	# 1	915 1,867	- 9	- 4	+ 23	- 45	- 42	- 32	+ 8	- 28	- 27	- 22	+ 10	- 26	- 25	- 19
	# 2	288 1,158	- 30	- 6	- 1	- 9	- 4	+ 4	- 19	- 20	- 18	- 15	- 6	- 8	- 5	- 2
	# 3	228 926	- 6	+ 41	- 9	+ 2	+ 8	+ 15	- 7	- 2	0	+ 3	+ 19	+ 24	+ 27	+ 30
	# 4	170 678	+ 1	+ 30	- 42	- 37	- 34	- 32	- 20	- 17	- 16	- 15	- 5	- 2	- 1	0
	# 6	206 835							- 17	- 21	- 17	- 17	- 10	- 14	- 10	- 10
	# 7	352 1,425	- 52	- 42	+ 19	+ 2	+ 1	+ 15	- 32	- 37	- 37	- 33	- 25	- 30	- 30	- 26
	# 9	370 1,509							- 8	- 17	- 13	- 10	- 1	- 10	- 6	- 2
	# 10	322 1,300	- 31	- 11	+ 3	- 8	- 3	+ 5	- 16	- 21	- 18	- 15	- 5	- 10	- 8	- 4
JONESVILLE # 1		157 625	- 26	+ 19	+ 2	+ 65	+ 93	+ 93	- 17	+ 3	+ 12	+ 25	+ 14	+ 34	+ 43	+ 43

TABLE 9 - Continued

Pile Test		$\frac{p\ D}{\gamma_w B^2}$	Q_p POINT LOAD		Q_s SIDE LOAD				Q_T TOTAL LOAD							
									from q_o				from N_q			
			from q_o	from N_q	from f_s	from Ktanδ	from K $\delta=\phi'_{res}$	from K $\delta=.8\phi'$	and f_s	and Ktanδ	and K $\delta=\phi'_{res}$	and K $\delta=.8\phi'$	and f_s	and Ktanδ	and K $\delta=\phi'_{res}$	and K $\delta=.8\phi'$
LOW - SILL	# 2	955 1,347	+ 18	+ 78	0	+ 9	+ 35	+ 39	+ 11	+ 14	+ 24	+ 25	+ 51	+ 54	+ 63	+ 65
	# 3	2,405 3,474	- 3	- 3												
	# 4	1,479 2,112	- 27	- 11	- 33	- 44	- 31	- 26	- 29	- 34	- 29	- 27	- 20	- 24	- 19	- 17
	# 6	1,189 1,643	+ 11	+ 52	- 5	- 10	+ 12	+ 17	+ 6	+ 4	+ 12	+ 13	+ 32	+ 30	+ 38	+ 40
VESIC	H-15	313 1,203	- 23	- 2	- 33	- 31	- 16	+ 14	- 27	- 26	- 20	- 8	- 15	- 14	- 8	+ 5
	H-2	317 1,269							- 10	- 9	- 3	- 3	+ 10	+ 12	+ 17	+ 17
GREGERSEN	# A	244 975	- 3	- 6	- 2	- 3	+ 2	+ 5	- 3	- 3	- 1	0	- 5	- 5	- 4	- 3
	#D/A	906 3,622	+22	+ 14	+ 6	- 16	- 4	- 2	+ 13	+ 1	+ 8	+ 9	+ 10	- 3	+ 4	+ 5
TAVENAS	H-1	80 272							+ 59	+ 62	+ 67	+ 63	+ 70	+ 73	+ 78	+ 74
	H-2	171 640							+ 24	+ 17	+ 27	+ 21	+ 30	+ 23	+ 33	+ 27

TABLE 9 - Continued

Pile Test		$\frac{p\ D}{\gamma_w\ B^2}$	Q_p POINT LOAD		Q_s SIDE LOAD				Q_T TOTAL LOAD							
									from q_o				from N_q			
			from q_o	from N_q	from f_s	from Ktanδ	from K $\delta=\phi'_{res}$	from K $\delta=.8\phi'$	and f_s	and Ktanδ	and K $\delta=\phi'_{res}$	and K $\delta=.8\phi'$	and f_s	and Ktanδ	and K $\delta=\phi'_{res}$	and K $\delta=.8\phi'$
TAVENAS	H-3	300 1,162							- 5	- 12	- 4	- 6	+ 3	- 8	- 1	- 3
	H-4	468 1,838							+ 15	- 4	+ 4	+ 4	+ 17	- 2	+ 7	+ 6
	H-5	675 2,669							+ 17	- 7	+ 2	+ 3	+ 19	- 5	+ 4	+ 4
	J-1	86 288							- 6	- 6	- 1	- 6	- 4	- 4	+ 1	- 4
	J-2	188 703							+ 1	- 9	- 1	- 6	- 1	- 11	- 3	- 7
	J-3	336 1,300							+ 1	- 15	- 8	- 9	- 1	- 17	- 10	- 11
	J-4	530 2,079							+ 5	- 17	- 10	- 10	+ 3	- 20	- 12	- 12
	J-5	823 3,253							+ 12	- 18	- 10	- 8	+ 10	- 20	- 12	- 10
COYLE C.Christi		112 382							- 15	- 6	- 7	- 6	+ 14	+ 23	+ 22	+ 23
Mean Error, $\bar{X}$			-11.3	+ 9.3	- 5.5	- 9.6	+ 1.3	+ 8.8	- 2.2	- 8.4	- 3.1	- 2.3	+ 7.9	+ 1.5	+ 6.8	+ 7.7
Std.Deviation, s			21.1	33.4	19.6	28.7	34.5	32.8	19.3	19.2	20.5	18.8	20.6	24.9	25.8	24.8

APPENDIX II

ADJUSTED COMPRESSION TESTS

The test pile data collected for this study have only four piles, tested at the same site, which included corrections for residual stresses. Consequently, it was not possible to develop significant correlations for adjusted compression test data. For comparison purposes only, these data were plotted in the same manner as the unadjusted compression and compression/tension test data. All factors plotted versus relative depth, are shown in Figs. 43 through 48. Also shown on these plots are the correlation curves which were developed using the unadjusted compression and compression/tension test data.

Figs. 43 and 44 show that the correlation curves for q_o and N_q, developed from compression/tension test data fit the adjusted compression test data better. This better fit should be expected, because the adjusted compression loads are considered equivalent to the compression/tension loads.

Figs. 45 through 48 present the data for unit side resistance and related coefficients. It can be seen that for these factors the adjusted compression test data does not favor either the unadjusted or the compression/tension curves.

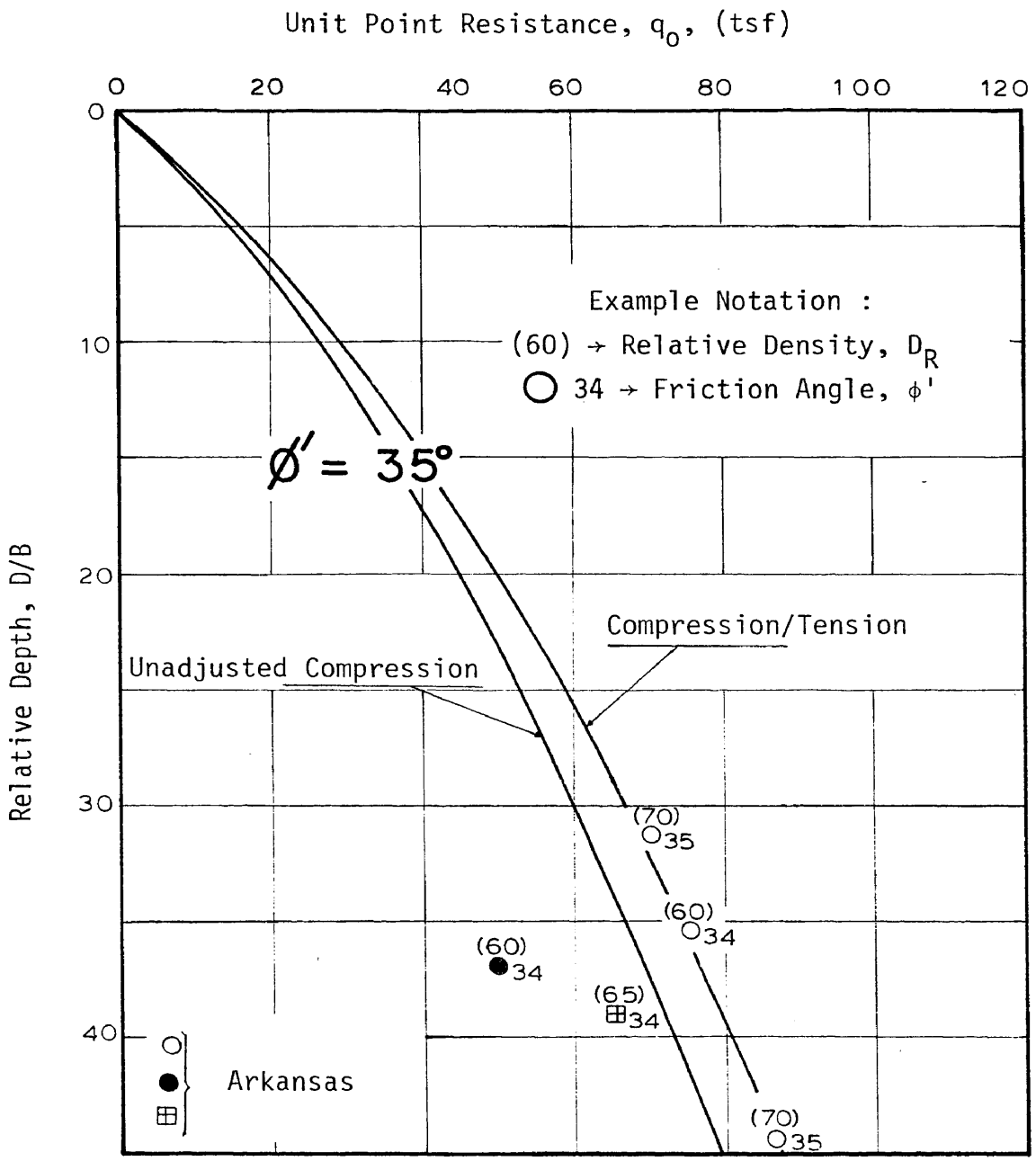

FIG. 43 - q_0 VS D/B - ADJUSTED COMPRESSION (1 tsf = 95.76 kN/m^2)

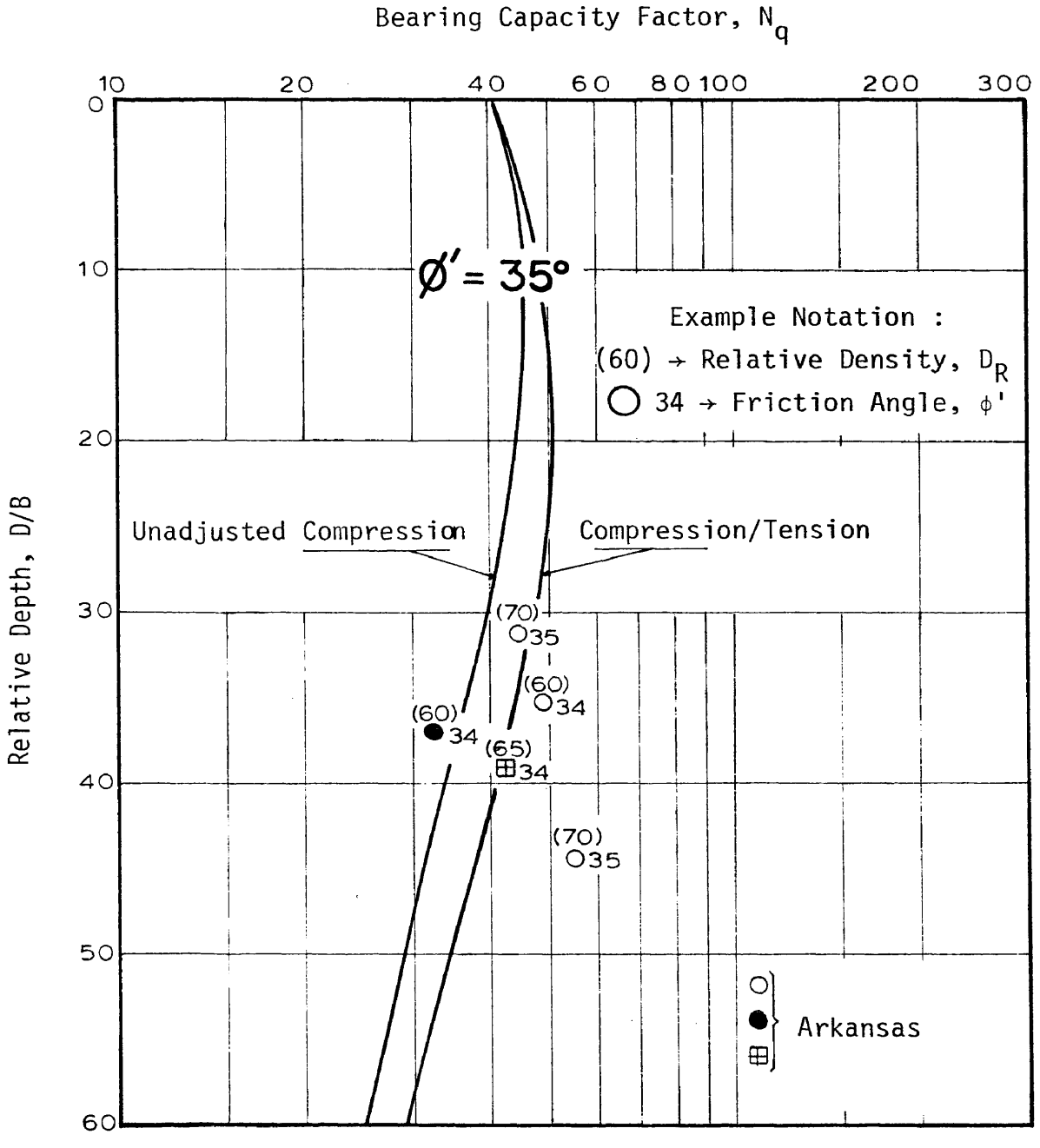

FIG. 44 - N_q VS D/B - ADJUSTED COMPRESSION

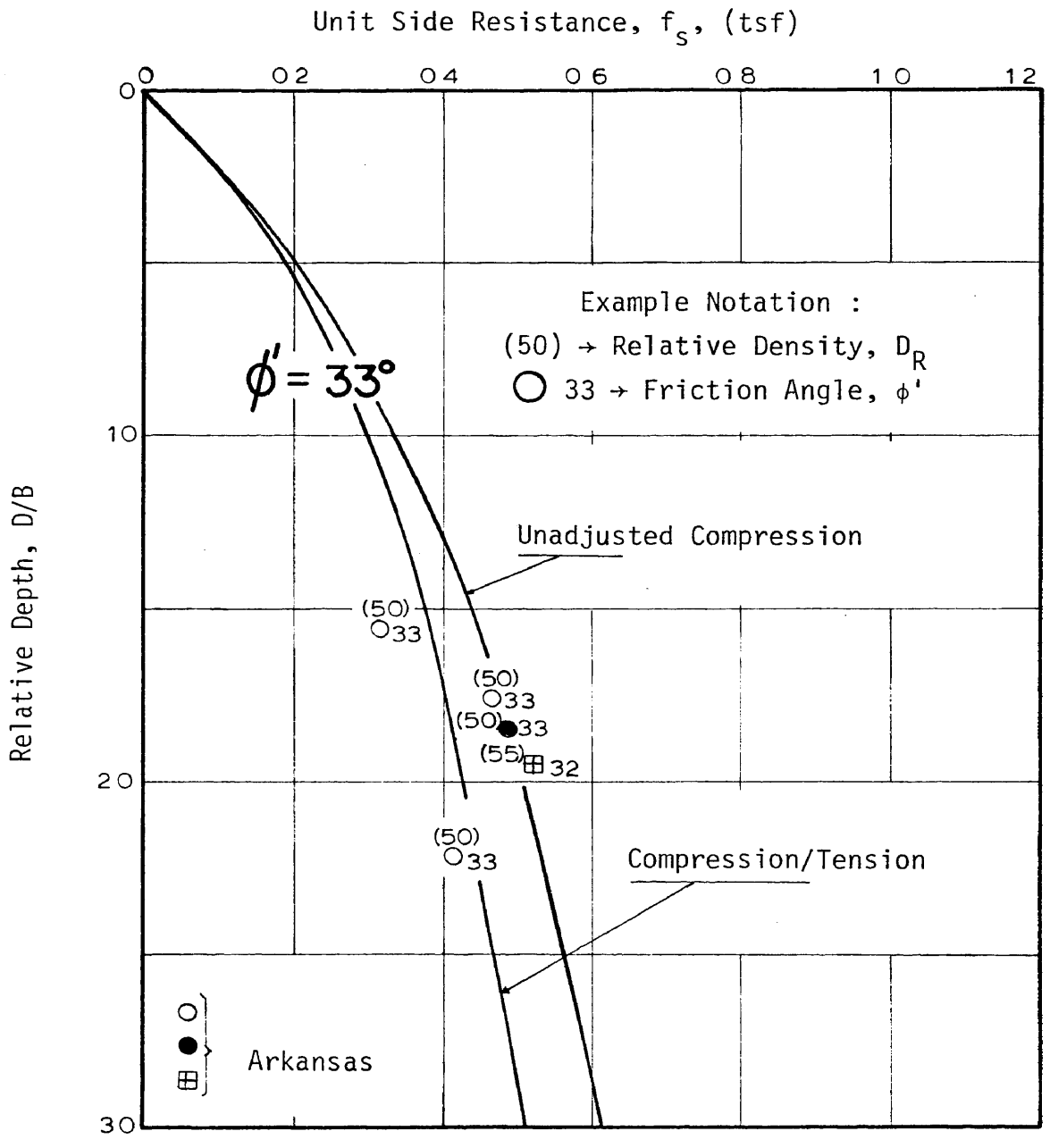

FIG. 45 - f_s VS D/B - ADJUSTED COMPRESSION (1 tsf = 95.76 kN/m^2)

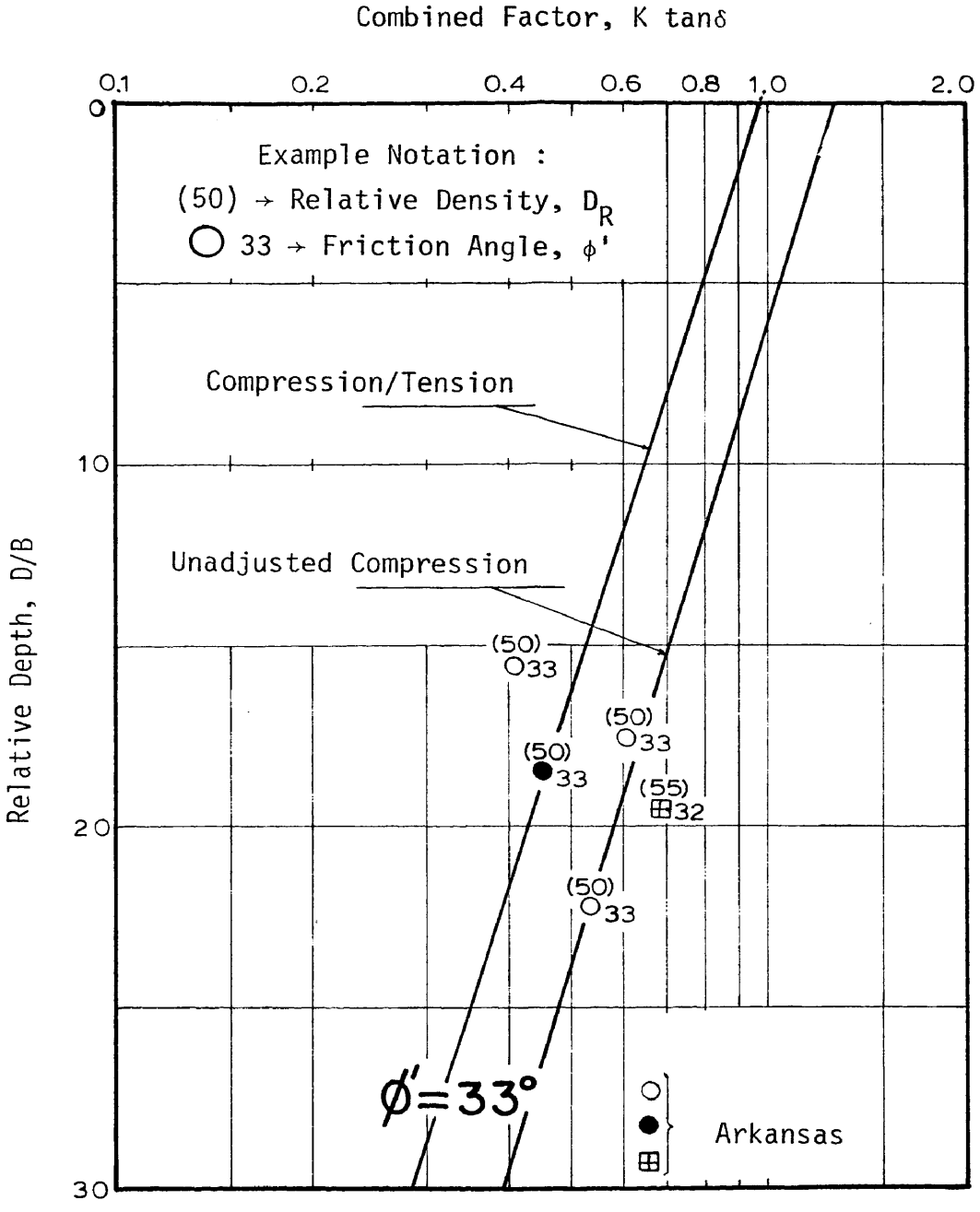

FIG. 46 - K tanδ VS D/B - ADJUSTED COMPRESSION

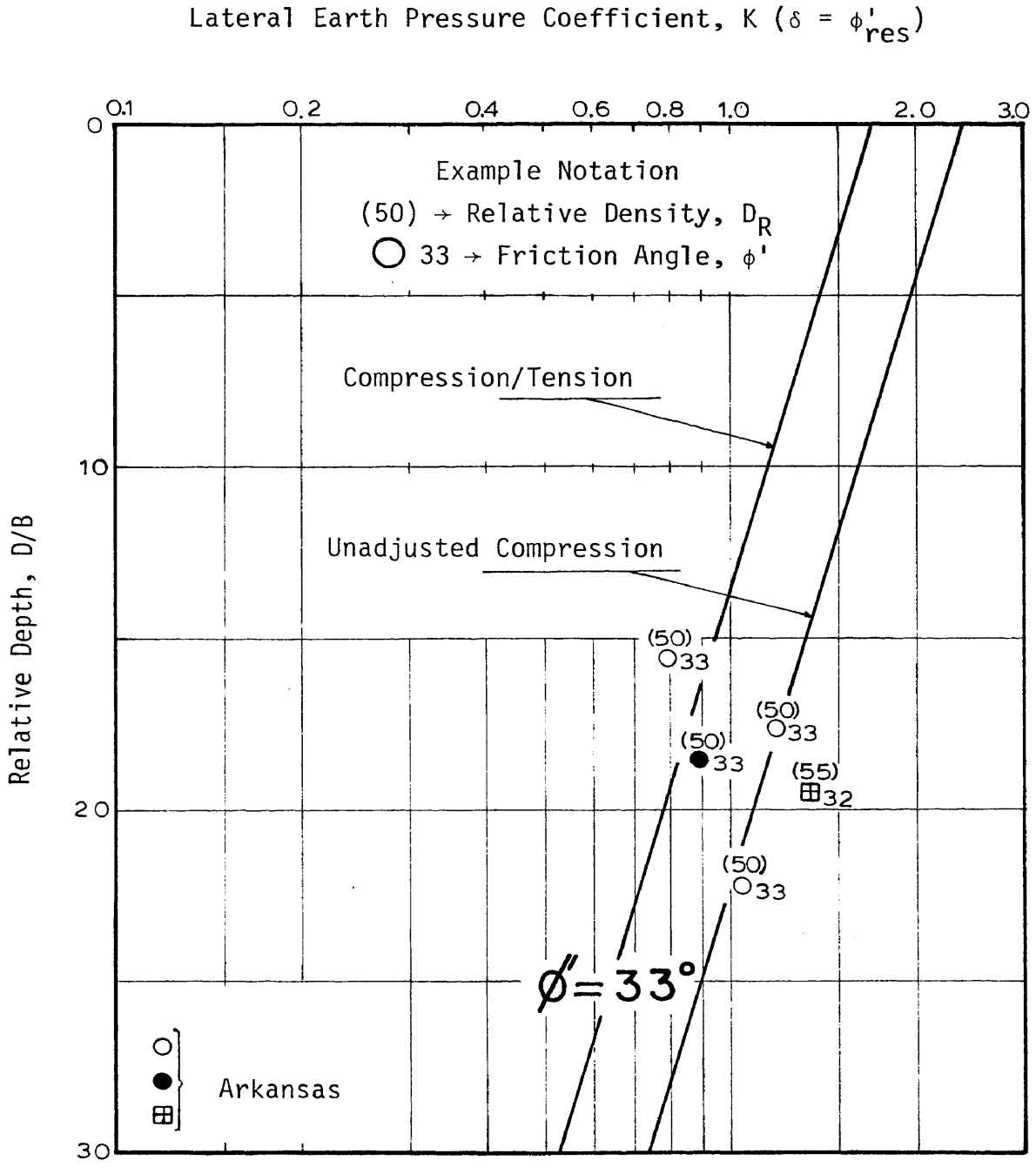

FIG. 47 - K ($\delta = \phi'_{res}$) VS D/B - ADJUSTED COMPRESSION

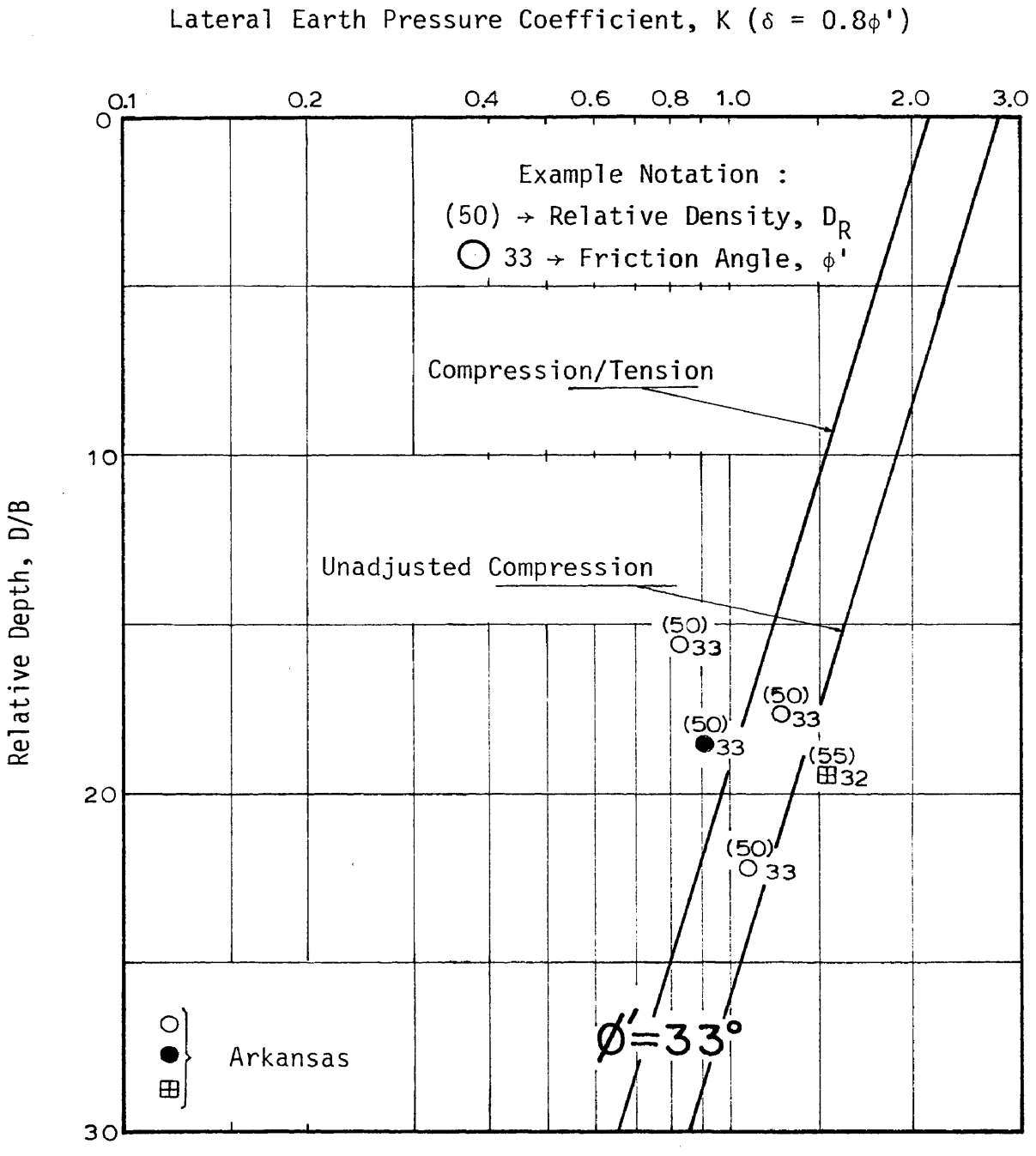

FIG. 48 - K (δ = 0.8φ') VS D/B - ADJUSTED COMPRESSION

APPENDIX III

ARITHMETIC MEAN AND STANDARD DEVIATION

The example illustrated in Fig. 49 is used for clarification of the use of the arithmetic mean of errors and the corresponding standard deviation. Straight lines are to be adjusted to the points (x_1, y_1) and (x_2, y_2). The curves to be analysed, in Fig. 49a, are the curves "a" and "b". The curve "c" which fits the points perfectly is used for comparison purposes.

In this example the analysis of each curve is performed with the use of errors defined as the difference between the ordinate of one point and the ordiante of a proposed line, of the same abscissa. For instance "ε_b" is the vertical distance between line "b" and point (x_1, y_1). The other errors are defined in the same manner.

If the means are plotted on a line, as in Fig. 49b, it is seen that curves "a" and "c" yield zero mean error and curve "b" a finite value. On the other hand, if the standard deviations of the errors are calculated, curves "b" and "c" would yield a zero value and curve "a" a finite value. So for this example, the standard deviation indicates that curve "b" (when compared to curve "a") is the one which best correlates the variables "x" and "y". The mean defines the amount that curve "b" should be translated in the "y" direction to match the points better (in this case perfectly).

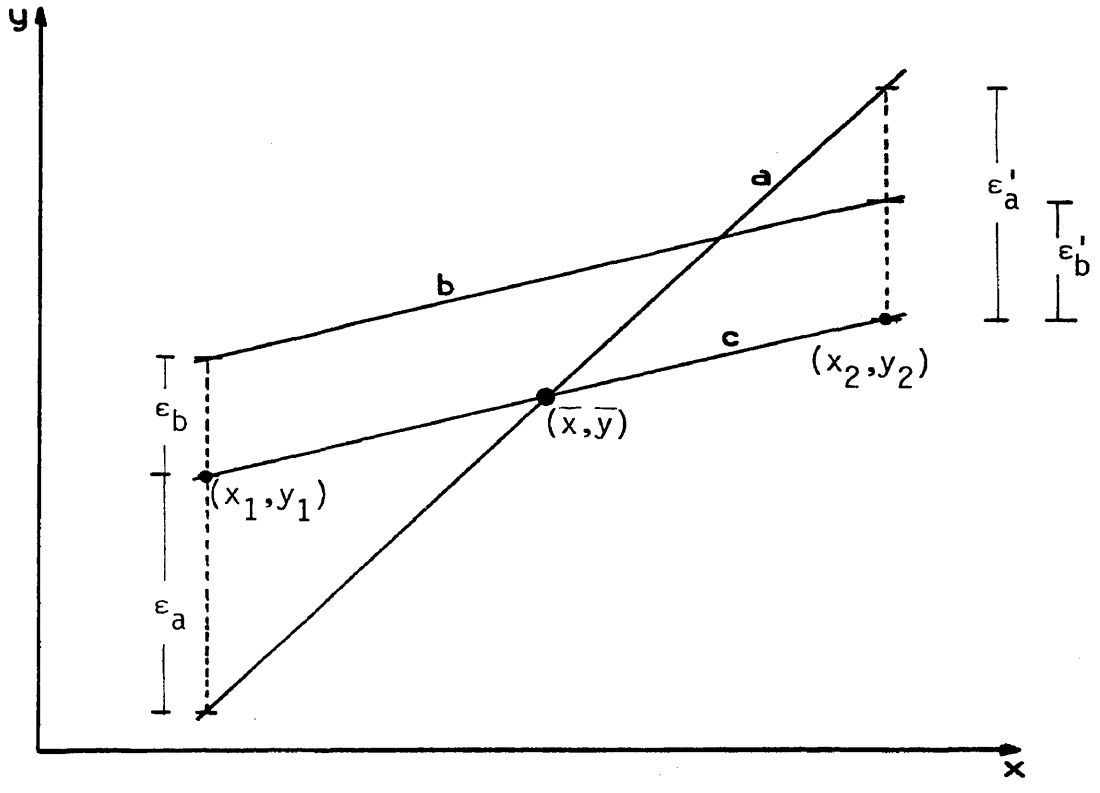

a) Adjustment of Curves

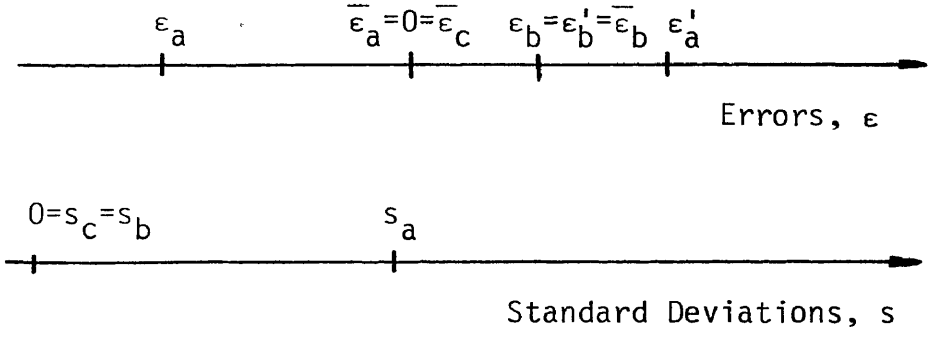

b) Mean of Errors and Standard Deviation

FIG. 49 - THE MEAN AND THE STANDARD DEVIATION

APPENDIX IV

REFERENCES

1. Aihart, T. P., Coyle, H. M., Hirsch, T. J., and S. J. Buchanan, "Pile Soil System Response in a Cohesive Soil", Performance of Deep Foundations, ASTM, STP 444, 1969, pp. 264-294.

2. Berezantzev, V. G., Khristoforov, V. S., and Golubkov, V. N., "Load Bearing Capacity and Deformation of Pile Foundations", Proceedings of the V International Conference on Soil Mechanics and Foundation Engineering, Paris, Vol. 2, 1961, pp. 11-15.

3. Biarez, J., and Gresillon, J. M., "Essais et Suggestions pour le Calcul de la Force Portante des Pieux en Milieu Pulverulent", Geotechnique, Vol. XXII, No. 3, September 1972, pp. 433-450.

4. Bishop, A. W., Collingridge, V. H., and O'Sullivan, T. P., "Driving and Loading Tests on Six Precast Concrete Piles in Gravel", Geotechnique, Vol. I, No. 1, June 1948, pp. 49-58.

5. Bjerrum, L., and Johannssen,I., "Pore Pressures Resulting from Driving Piles in Soft Clay", Conference on Pore Pressure and Suction in Soils, London, 1960, pp. 108-111.

6. Bowles, J. E., Foundation Analysis and Design, McGraw-Hill Book Company, New York, 1968.

7. Bowles, J. E., Foundation Analysis and Design, 2nd. ed., McGraw-Hill Book Company, New York, 1977.

8. Broms, B. B., "Methods of Calculating the Ultimate Bearing Capacity of Piles: A Summary", Sol-Soils, France, Vol. V, Nos. 18-19, 1966, pp. 21-31.

9. Coyle, H. M., and Reese, L. C., "Load Transfer to Axially Loaded Piles in Clay", Journal of the Soil Mechanics and Foundation Division, ASCE, Vol. 92, No. SM2, Proc. Paper 4072, March 1966, pp. 1-26.

10. Coyle, H. M., and Sulaiman, I. H., "Skin Friction for Steel Piles in Sand", Journal of the Soil Mechanics and Foundation Division, ASCE, Vol. 93, No. SM6, Proc. Paper 5590, November 1967, pp. 261-278.

11. Coyle, H. M., and Sulaiman, I. H., "Bearing Capacity of Foundation Piles: State of the Art", Highway Research Record No. 333, 1970, p. 87.

12. Coyle, H. M., Bartoskewitz, R. E., and Berger, W. J., "Bearing Capacity Prediction by Wave Equation Analysis - State of the Art", Research Report No. 125-8, Texas Transportation Institute, Texas A&M University, August 1973.

13. Coyle, H. M., "Marine Foundation Engineering", Unpublished Class Notes, Texas A&M University, 1977.

14. DeBeer, E. E., "The Scale Effect in the Transposition of the Results of Deep-Sounding Tests on the Ultimate Bearing Capacity of Piles and Caisson Foundations", Geotechnique, Vol. XIII, No. 1, March 1963, pp. 39-75.

15. Fruco and Associates, "Pile Driving and Loading Tests", Report for Corps of Engineers, Little Rock, Arkansas, September 1964.

16. Furlow, C. R., "Pile Tests, Jonesville Lock and Dam, Ouachita and Black Rivers, Arkansas and Louisiana", Technical Report S-68-10, U. S. Army Engineer Waterways Experiment Station, December 1968.

17. Gibbs, H. J., and Holtz, W. G., "Research on Determining the Density of Sands by Spoon Penetration Testing", Proceedings of the IV International Conference on Soil Mechanics and Foundation Engineering, London, Vol. 1, 1957, pp. 35-39.

18. Gregersen, O. S., Aas, G., and DiBiagio, E., "Load Tests on Friction Piles in Loose Sand", Proceedings of the VIII International Conference on Soil Mechanics and Foundation Engineering, Moscow, Vol. 2.1, 1973, pp. 19-27.

19. Hanna, T. H., and Tan, R. H. S., "The Behavior of Long Piles Under Compressive Loads in Sand", Canadian Geotechnical Journal, Vol. 10, No. 3, August 1973, pp. 311-340.

20. Holloway, D. M., Clough, G. W., and Vesic, A. S., "The Mechanics of Pile-Soil Interaction in Cohesionless Soils", Contract Report S-75-5 (Final Report), U. S. Army Engineer Waterways Experiment Station, December 1975.

21. Hunter, A. H., and Davisson, M. T., "Measurement of Pile Load Transfer", Performance of Deep Foundation, ASTM, STP 444, 1969, pp. 106-117.

22. Ireland, H. O., "Pulling Tests on Piles in Sand", Proceedings of the IV International Conference on Soil Mechanics and Foundation Engineering, London, Vol. 2, 1957, pp. 43-45.

23. Johnson, R. R., Elementary Statistics, 2nd. ed., Duxbury Press, North Scituate, Massachusetts, 1976.

24. Kerisel, J., "Fondations Profondes en Milieux Sableux: Variation de la Force Portante Limite en Fonction de la Densite, de la Profondeur, du Diametre et de la Vitesse d'Enfoncement", Proceedings of the V International Conference on Soil Mechanics and Foundation Engineering, Paris, Vol. 2, 1961, pp. 73-83.

25. Kerisel, J. L'Herminier, R., and Tcheng, Y., "Resistance de Pointe

en Millieux Pulverulents de Serrages Divers", Proceedings of the VI International Conference on Soil Mechanics and Foundation Engineering, Montreal, Canada, Vol. 4, 1965, pp. 265-269.

26. Kezdi, A., "Pile Foundations", Foundation Engineering Handbook, edited by H. F. Winterkorn and H. Y. Fang, Van Nostrand Reinhold, Co., New York, 1975, pp. 556-600.

27. Klos, J., and Tejchman, A., "Analysis of Behavior of Tubular Piles in Subsoil", Proceedings of the IX International Conference on Soil Mechanics and Foundation Engineering, Tokyo, Vol. 1, 1977, pp. 605-608.

28. Lambe, T. W., and Whitman, R. V., Soil Mechanics, John Wiley & Sons, Inc., New York, 1969.

29. Mansur, C. I., and Kaufman, R. I., "Pile Tests, Low-Sill Structure, Old River, Louisiana", Transactions of ASCE, Vol. 123, 1958, pp. 715-748.

30. Mansur, C. I., and Hunter, A. H., "Pile Tests - Arkansas River Project", Journal of the Soil Mechanics and Foundation Division, ASCE, Vol. 96, No. SM5, September 1970, pp. 1545-1582.

31. Mayer, A., and L'Herminier, R., "Le Pouvoir Portant des Pieux en Milieu Coherent", Proceedings of the III International Conference on Soil Mechanics and Foundation Engineering, Switzerland, Vol. 2, 1953, pp. 60-65.

32. McClelland, B., Focht, Jr., J. A., and Emrich, W. J., "Problems in Design and Installation of Heavily Loaded Pipe Piles", Journal of the Soil Mechanics and Foundation Division, ASCE, Vol. 95, No. SM6, November 1969.

33. McClelland, B., "Design and Performance of Deep Foundations", ASCE Specialty Conference on Performance of Earth and Earth-Supported Structures, Purdue University, Lafayette, Indiana, June 1972.

34. Meyerhof, G. G., "The Ultimate Bearing Capacity of Foundations", Geotechnique, Vol. 2, No. 4, December 1951, p. 301.

35. Meyerhof, G. G., "Compaction of Sands and Bearing Capacity of Piles", Journal of the Soil Mechanics and Foundation Division, ASCE, Vol. 85, No. SM6, Proc. Paper 2292, December 1959, pp. 1-29.

36. Meyerhof, G. G., "Bearing Capacity and Settlement of Pile Foundations", Journal of the Geotechnical Engineering Division, ASCE, Vol. 102, No. GT3, March 1976, pp. 197-228.

37. Meyerhof, G. G., and Valsangkar, "Bearing Capacity of Piles in Layered Soils", Proceedings of the IX International Conference on Soil Mechanics and Foundation Engineering, Tokyo, Vol. 1, 1977, pp. 645-650.

38. Milovic, D. M., "Comparison Between the Calculated and Experimental Values of the Ultimate Bearing Capacity", Proceedings of the VI International Conference on Soil Mechanics and Foundation Engineering, Montreal, Canada, Vol. 2, 1965, pp. 142-144.

39. Morgan, J., Introduction to University Physics, Vol. 1, 2nd. ed., Allyn and Bacon, Boston, 1963.

40. Nordlund, R. L., "Bearing Capacity of Piles in Cohesionless Soils", Journal of the Soil Mechanics and Foundation Division, ASCE, Vol. 89, No. SM3, Proc. Paper 3506, May 1963, pp. 1-35.

41. Potyondy, J. G., "Skin Friction Between Various Soils and Construction Materials", Geotechnique, Vol. II, No. 4, December 1961, pp. 339-353.

42. Robinsky, E. I., and Morrison, C. F., "Sand Displacement and Compaction Around Model Friction Piles", Canadian Geotechnical Journal, Vol. 1, No. 2, March 1964, pp. 81-93.

43. Robinsky, E. I., Sagar, W. L., and Morrison, C. F., "Effect of Shape and Volume on the Capacity of Model Piles in Sand", Canadian Geotechnical Journal, Vol. 1, No. 4, November 1964, pp. 189-204.

44. Schultze, E., and Menzenbach, E., "SPT and Compressibility of Soils", Proceedings of the V International Conference on Soil Mechanics and Foundation Engineering, Paris, Vol. 1, 1961, pp. 527-532.

45. Sherman, Jr., W. C., Holloway, D. M., and Trahan, C. C., "Analysis of Pile Tests", Technical Report S-74-3, U. S. Army Engineer Waterways Experiment Station, April 1974.

46. Sowers, G. B., and Sowers, G. F., Introductory Soil Mechanics and Foundations, 3rd. ed., MacMillan Publishing Co., Inc., New York, 1970, p. 446.

47. Szechy, C., "The Effects of Vibration and Driving Upon the Voids in Granular Soils Surrounding a Pile", Proceedings of the V International Conference on Soil Mechanics and Foundation Engineering, Paris, Vol. 2, 1961, pp. 161-164.

48. Tavenas, F. A., "Load Tests on Friction Piles in Sand", Canadian Geotechnical Journal, Vol. 8, No. 7, 1971, pp. 7-22.

49. Terzaghi, K., Theoretical Soil Mechanics, John Wiley and Sons, Inc. New York, 1943.

50. Terzaghi, K., and Peck, R. B., Soil Mechanics in Engineering Practice, 2nd. ed., John Wiley & Sons, Inc., New York, 1967.

51. Tomlinson, J. J., "The Adhesion of Piles Driven in Clay Soils", Proceedings of the IV International Conference on Soil Mechanics

and Foundation Engineering, London, Vol. 2, 1957, pp. 66-71.

52. Tomlinson, M. J., Pile Design and Construction Practice, Viewpoint Publications by Cement and Concrete Association, London, 1977.

53. Vesić, A. S., "A Study of Bearing Capacity of Deep Foundations", Project B-189 (Final Report), Georgia Institute of Technology, August 1966.

54. Vesić, A. S., "Ultimate Loads and Settlement of Deep Foundations in Sand", Proceedings of the Symposium on Bearing Capacity and Settlement of Foundations, Duke University, April 1967.

55. Vesić, A. S., "Load Transfer, Lateral Loads, and Group Action of Deep Foundations", Performance of Deep Foundations, ASTM, STP 444, June 1968, pp. 5-14.

56. Vesić, A. S., "Expansion of Cavities in Infinite Soil Mass", Journal of the Soil Mechanics and Foundation Division, ASCE, Vol. 98, No. SM3, Proc. Paper 8790, March 1972, pp. 265-290.

57. Vesić, A. S., "Tests on Instrumented Piles, Ogeechee River Site", Journal of the Soil Mechanics and Foundation Division, ASCE, Vol. 96, No. SM2, March 1970, pp. 561-583.

58. Vesić, A. S., "Design of Pile Foundations", NCHRP Synthesis of Highway Practice No. 42, Transportation Research Board, 1977.

59. Vesić, A. S., "On Significance of Residual Loads for Load Response of Piles", Contribution presented at Main Session 2: "Behavior of Foundations and Structures", Proceedings of the IX International Conference on Soil Mechanics and Foundation Engineering, Tokyo, Vol. 3, 1977, pp. 374-379.

APPENDIX V

NOTATION

The following symbols are used in this dissertation:

A_p = area of the pile point;

A_s = area of the pile shaft;

b = smallest foundation dimension;

B = pile diameter (or, for non-circular piles, the diameter of a circle with the same area as the pile cross section);

c = cohesion of the soil;

D = depth of pile penetration;

$\overline{D}$ = average deviation of K values;

D_i = deviation of K values;

D_R = relative density of the sand;

D/B = relative depth;

E = modulus of deformation of the soil;

f_s = ultimate unit side resistance;

I_r = rigidity index;

K = lateral earth-pressure coefficient;

K_o = coefficient of lateral earth-pressure at-rest;

$K_{0.7}$ = back calculated value of K, from unadjusted compression test, multiplied by 0.7;

n = total number of pile test data in a statistical analysis;

N_q = combined bearing capacity factor for circular and squared piles (includes the shape factor);

N_γ^*, N_q^*, N_c^* = bearing capacity factors in terms of vertical overburden pressure;

N_σ = bearing capacity factor in terms of average confining pressure;

p = effective overburden pressure;

$\overline{p}$ = average vertical effective overburden pressure along pile segment;

p_o = effective vertical overburden pressure at the pile point level;

$\frac{pD}{\gamma_w B^2}$ = effective overburden pressure parameter;

q_o = ultimate unit point resistance;

Q_p = ultimate load carried by the pile point;

Q_s = ultimate load carried by the pile shaft;

Q_T = total axial load on the pile;

Q_u = ultimate total axial load on the pile;

s = standard deviation of the mean error;

s_γ, s_c, s_q = shape factors;

x = a variable;

$\overline{X}$ = arithmetic mean of errors;

X_i = error corresponding to the i^{th} pile test;

y = a variable

γ = effective unit weight of the soil;

γ_w = unit weight of the water;

ΔV = soil volume variation;

δ = angle of friction between the pile and the soil;

ε = error between prediction and measurement;

ν = Poisson's ratio of the soil;

$\overline{\sigma}$ = average effective confining pressure at pile point;

ϕ' = peak friction angle of the soil based on effective stresses; and

ϕ'_{res} = residual friction angle of the soil, based on effective stresses.